THE ABSORPTION OF ULTRASOUND IN AQUEOUS SOLUTIONS OF BIOLOGICAL POLYMERS

BY

WILLIAM DANIEL O'BRIEN, JR.
B.S., University of Illinois, 1966
M.S., University of Illinois, 1968

THESIS

Submitted in partial fulfillment of the requirements
for the degree of Doctor of Philosophy in Electrical Engineering
in the Graduate College of the
University of Illinois at Urbana-Champaign, 1970

Urbana, Illinois

THE ABSORPTION OF ULTRASOUND IN AQUEOUS SOLUTIONS OF BIOLOGICAL POLYMERS

William Daniel O'Brien, Jr., Ph. D.
Department of Electrical Engineering
University of Illinois at Urbana-Champaign, 1970

The ultrasonic absorption and velocity were measured in aqueous solutions of four biologically important molecules, viz., hemoglobin, ovalbumin, serum albumin and deoxyribose nucleic acid, so that the principle mechanisms responsible for the ultrasonic absorption in biological media could be further investigated. The majority of the data were taken at 10.0°C over the frequency range 1.6-50 MHz. A distribution of relaxation processes was necessary to characterize the absorption spectra for all the biological solutions investigated. No correlation can be suggested relative to the absorption magnitude and speciman purity, i.e., uncrystallized, twice crystallized, etc. Also, molecular weight differences appear to be unimportant (ovalbumin - M = 46,000 and bovine serum albumin - M = 68,000). Ultrasonic absorption mechanisms of dynamic shear viscosity, mode conversion, electroviscous effects and particulate relaxation have been shown to be unimportant as the primary processes responsible for the absorption of acoustic energy in aqueous protein solutions at their isoelectric point. Since all of the aqueous solutions at their isoelectric point in this study possess approximately the same frequency dependence and magnitude within the frequency range investigated, the absorption mechanism is considered the same. It is felt that the mechanism is the interaction of the acoustic wave with the hydration layer of the macromolecule and is not directly associated with the macromolecular configuration since the DNA structure

is worm-like while the globular protein structure is a rigid, compact ellipsoid.

Hemoglobin and ovalbumin solutions were examined as a function of pH over the range 1.5-13.5 at 10.0°C, the former over the frequency range 2.390-50.50 MHz while the latter only at 14.80 MHz. These ultrasonic absorption titration curves exhibited maxima around pH 2-4 and 11-13 in addition to the hemoglobin curves possessing a bow shape within the pH range 4-9. The shape of these curves closely resemble those for bovine serum albumin (J. Phys. Chem., 73, 4256, 1969). The peaks in the absorption titration curves for these three globular proteins are attributed to the proton transfer reaction occuring between particular amino acid side chain groups and the solvent. The bow shape resulting in the hemoglobin titration curves is attributed to the proton transfer reaction resulting from the imidazolium function of the histidine amino acid.

The ultrasonic absorption of aqueous deoxyribose nucleic acid (salmon sperm, $M \simeq 10^6$) solutions were measured in the acid pH range over the frequency range 5.690-19.30 MHz at 10.0°C and 25.0°C. The alkaline pH range was investigated by Lang and Cerf (J. Chim. Phys., 66, 81, 1969). The ultrasonic absorption titration curves for deoxyribose nucleic acid shows peaks around pH 2.6 and 12 which are attributed to the transfer of hydrogen bonds from base-base to base-solvent. Proton transfer is considered unimportant as the pK values of the nucleotide bases do not occur within the appropriate pH range.

Aqueous hemoglobin solutions were investigated as a function of guanidine hydrochloride (GuHCl) concentration up to almost 7 molar, at

10.0°C, over the frequency range 8.870-50.50 MHz. The absorption, at constant frequency, increased with increasing GuHCl concentration to around 2 molar and then decreased, leveling off for GuHCl concentration greater than 4-5 molar. No correlation between the acoustic absorption and known conformational changes (Biochemistry, 4, 1203, 1965) results. The maximum around 2 molar GuHCl is attributed to the proton transfer reaction which can result when the guanidinium ion (GuH^+) partakes in a proton exchange reaction with water when a second solute (hemoglobin) forms strong hydrogen bonds with either water or GuH^+ (J. Phys. Chem., 73, 2853, 1969).

This investigation was supported by the Institute of General Medical Sciences, National Institute of Health (Contract No. GM 12281).

ACKNOWLEDGMENT

The author wishes to express his grateful appreciation to his advisor, Professor Floyd Dunn, for his encouragement and guidance throughout this investigation. The assistance in data analysis by Mr. Wayne Alexander and Mr. Jim Lohnes is also appreciated. To his typist, Mrs. Marilena Stone, and draftsman, Mr. George Morris, a special thanks. Finally, the author must acknowledge the support, encouragement and patience from his wife, Wilma, throughout this difficult period.

TABLE OF CONTENTS

LIST OF TABLES

LIST OF FIGURES

FIGURE Page

FIGURE Page

FIGURE Page

CHAPTER 1 INTRODUCTION

The mechanisms by which biological media absorb energy from a propagating acoustic wave are poorly understood. Further, the principle mechanisms acting on the biological system can be quite different depending upon the chemical and physical state of the system. It is the intent of this study to examine the physical and chemical mechanisms contributing to this absorption by correlating the ultrasonic absorption spectra of aqueous solutions of biological macromolecules with the physico-chemical properties of the molecule. These solutions will be examined over the ultrasonic frequency range 1.680-50.50 MHz, mostly at 10.0°C. Initially the absorption spectra at the solutions' isoelectric point will be examined and then the biopolymers will be subjected to varying degrees of denaturation such as the addition of an acid or base or the strong electrolytic guanidine hydrochloride.

When intense acoustic waves are propagated through biological systems, changes in structure and function can result. When the energy level exceeds a "threshold" condition in a liquid medium, the growth and collapse of cavities occurs. This phenomenon, termed cavitation, results in extreme hydrodynamic shearing forces in the neighborhood of the collapsed cavity (Fry and Dunn, 1962). Thus it is easily seen that cavitation can disrupt biological structure (Fry et al., 1970). However, by performing the experiment under conditions in which cavitation is inhibited, Fry et al. (1951) demonstrated that tissue modification can still result, thus demonstrating that it is not an essential mechanism in lesion production. In addition, histologically, it is easily determinable whether or not the lesion is produced as a result of cavitation (Fry et al., 1970).

The work of Fry and coworkers (Fry et al., 1950; Fry et al., 1951; Fry, 1953; Fry and Fry, 1953; Fry and Dunn, 1956; Fry, 1958; Dunn, 1958) showed that thermal processes resulting from intense noncavitating ultrasonic energy (in the range of 20 to 1000 w/cm^2) were not the fundamental reason by which biological structure is damaged. By irradiating the spinal cord of cooled frogs and day old mice, damage was assessed by monitoring whether or not limb paralysis resulted. At the same time, the temperature rise resulting from the ultrasound was monitored, making sure the local temperature never reached damaging levels. This work assumed, via theoretical considerations, that microscopic "hot spots" did not exist.

Intense noncavitating ultrsound has been utilized to produce biological structural changes (lesions) in nervous tissue (Fry, 1958), in the brain (Fry et al., 1958; Fry, 1970), in skeletal muscle (Welkowitz and Fry, 1956) and in liver tissue (Curtis, 1965). Welkowitz (1955) proposed a mechanical mechanism by wich unidirectional forces resulted in elastic failure of structural components. But it was shown that this mechanism did not support more accurate experimental results (Dunn, 1957). However, it is believed that the mechanism is mechanical in nature (Fry, 1958; Dunn, 1958). As hydrodynamic shearing forces have been shown to degrade DNA (Levinthal and Davison, 1961), Hawley et al. (1963) proposed a mechanism in which the shearing forces resulting from the relative motion between DNA and solvent molecules produced DNA degradation by intense noncavitating ultrasonic energy. Wells (1968) suggests that the cause of the non-thermal damage to water flea Daphnia magna is fundamentally similar to the mechanism proposed by Hawley et al. (1963), although there is an extreme difference in scale. Dyson et al. (1968) attribute tissue regeneration by intense noncavitating ultrasound also to a mechanical and not a thermal mechanism.

When ultrasonic lesions induce functional changes, such as limb paralysis, the physiological changes are observed almost immediately. However, histological evidence of the lesion does not result until approximately 10-15 minutes later, suggesting that the primary site of the energy exchange process may occur at the macromolecular level (Dunn, 1958; Fry, 1958). Irradiation of five enzyme molecules in solution with intense non-cavitating ultrasound resulted in no permanent changes in their normal enzymatic function (Macleod, 1966; Macleod and Dunn, 1968), in which case interaction with molecular processes may be ruled out as an important mechanism if the assumption is made that in vitro studies accurately duplicate in vivo studies. Coble and Dunn (1970) have proposed that the action by which the acoustic energy produces destruction may be interaction with membraneous structure.

The above method, that of determining the levels of structure at which the ultrasonic energy results in tissue destruction, is one approach. Another approach, that attempted in this study, is to identify these physical mechanisms responsible by using very low intensity ultrasonic energy ($\simeq 10^{-3}$ w/cm^2) to examine possible absorption mechanisms in aqueous solutions of biologically important macromolecules. It is hoped that from this information the mechanisms responsible for lesion production with high intensity ultrasound may be inferred. In any case the mechanisms responsible for the energy exchange processes at low intensities could possibly help elucidate rapid biological processes such as highly specific enzymatic processes (Pancholy and Saksena, 1968).

Although ultrasonic spectroscopy has been available, in principle, for at least two decades, to date, only a few biological macromolecules have been examined. Probably the most extensively studied macromolecule

is the protein hemoglobin, the oxygen carrier in the red blood cells of vertebrates (Dunn et al., 1969; Schneider et al., 1969; Edmonds et al., 1970). The earliest work of importance is that by Carstensen et al. (1953), who investigated the ultrasonic absorption and velocity in blood, plasma and solutions of albumin and hemoglobin, and concluded that the acoustical properties of blood are largely a result of the protein concentration. In addition they determined that the absorption coefficient of hemoglobin is approximately the same as that of serum albumin within the frequency range 0.8-3 MHz over the temperature range 10-40°C.

Within the neutral pH region, aqueous solutions of hemoglobin have now been examined over the extended frequency range 35 KHz to 1000 MHz (Dunn et al., 1969; Schneider et al., 1969). Schneider et al. (1969) have shown that it is possible to approximate the entire spectrum with four appropriately selected distinct relaxation processes. Generally, mathematical analyses of the acoustic absorption spectrum for hemoglobin solutions have been undertaken with little attention to the actual mechanisms responsible for the absorption phenomenon.

More recently other globular proteins have been examined. Kessler (1968a) and Kessler and Dunn (1969) studied aqueous solutions of bovine serum albumin and attributed the ultrasonic absorption in the neutral pH region with solvent-solute interactions. Outside of the neutral pH range, the absorption behavior is correlated with conformation changes. Sadykhova and El'piner (1970) examined the acoustic absorption spectrum of a number of muscle and globular proteins over the limited frequency range 12 to 68 MHz near their isoelectric point. Generally in their study the absorption magnitudes of actin and actomyosin appeared much greater than those of myosin and albumin. However, their albumin spectrum did not compare

favorably with that of Kessler's (1968a). Wada et al. (1967) investigated the ultrsonic absorption of gelatin at 3 MHz as a function of pH. The peak in the absorption around pH 4 is interpreted as a result of a dissociation type reaction of the protein side chains. Also it has been reported that the absorption magnitude of gelatin solutions within the frequency range 0.7 to 10 MHz is approximately half that in hemoglobin and albumin solutions (Dunn et al., 1969). For all of these proteins, the ultrasonic absorption spectrum exhibited a distribution of relaxation times.

Two synthetic polyamino acids have been examined extensively under varying environmental conditions with respect to their ultrasonic absorption, viz., poly-L-glutamic acid (Burke et al., 1965; Schwarz, 1965; Wada et al., 1967) and poly-L-lysine (Parker et al., 1968). The primary mechanism proposed to explain the excess ultrasonic absorption in poly-L-glutamic acid solutions by Burke et al. (1965) is that of solvent-solute interaction whereas Schwarz (1965) attributes it to the helix coil transition. The examination by Wada et al. (1967) of poly-L-glutamic revealed that at 50 KHz, the absorption mechanism is that of helix coil transition while at 3 MHz the absorption is attributed to side chain dissociation. Parker et al. (1968) showed that the observed ultrasonic absorption behavior in aqueous poly-L-lysine solution can be attributed to the helix coil transition.

The carbohydrate, dextran, a linear $\alpha(1\text{-}6)$ anhydroglucose polysaccharide, assumes a random coil conformation in solution whereas most proteins exist as a compact, rigid molecule. The ultrasonic absorption spectrum of dextran, in the frequency range 3 to 69 MHz, can be represented by a distribution of relaxation times (Hawley et al., 1965; Hawley, 1966; Hawley and Dunn, 1970) while the absorption is considerably less than that exhibited by proteins.

This difference has been attributed to the proteins possessing a secondary and tertiary structure whereas dextran does not. In addition, the protein gelatin, which does not possess a tertiary structure, has a lesser absorption magnitude than those proteins with a tertiary structure. Thus Hawley et al. (1965) have suggested that the tertiary structure may be responsible for some of the excess ultrasonic absorption observed in protein solutions.

A biological polymer with a conformation quite different from that of the globular proteins and carbohydrates is deoxyribose nucleic acid, a rod-like molecule. Acoustic measurements were first reported by Litzler and Cerf (1963) in aqueous solutions of calf thymus DNA in which a maximum in the α/f^2 as a function of frequency curve resulted, indicating that a resonance type phenomenon occurred in native DNA. However, subsequent work (Lang and Cerf, 1969) has shown that this is not the case, and that the frequency free absorption decreases monotonically with increasing frequency within the range 3 to 58 MHz. Lang and Cerf (1969) also examined the dependence of the ultrasonic absorption on DNA solutions (molecular weight $4\text{-}7 \times 10^6$) as a function of alkaline pH within the range 6 to 12.5. A maximum was observed around pH 12 and attributed to alkaline denaturation of the DNA molecule. The mechanism responsible for the acoustic absorption within the neutral pH region has not been discussed.

The purpose of this investigation is to examine the ultrasonic spectrograms of aqueous solutions of biological macromolecules (hemoglobin, ovalbumin, serum albumin and deoxyribose nucleic acid) under varying environmental conditions, correlate these with known conformational changes of the biopolymer involved, and consider appropriate absorption mechanisms.

It is apparent from the above discussion that the mechanisms responsible for the ultrasonic absorption are unsettled. Generally three mechanisms have been suggested to explain the excess ultrasonic absorption in aqueous protein solutions, viz., proton transfer reaction, solvent-solute interaction and shear viscosity relaxation. A fourth, helix coil transition, has been suggested in reference with polypeptides. In globular proteins, the helical sections of the polypeptide chain are usually buried and thus not able to partake in interaction with the solvent. To this investigator's knowledge, no mechanisms have been proposed to explain the absorption behavior of native DNA solutions.

Chapter 2 presents the necessary acoustic theory in order to discuss a number of acoustic absorption mechanisms (which may be implicated in this work) in liquid media in general and in aqueous solutions in particular. Chapter 3 discusses the methods by which the acoustical data is obtained, which is then presented in chapter 4. The discussion of the results, along with proposed absorption mechanisms, is presented in chapter 5 and the last chapter summarizes the material of the thesis and includes a brief discussion of the "next steps" to be in elucidating the mechanisms of interaction of ultrasound and biological media.

CHAPTER 2 ACOUSTIC THEORY

In order for acoustic energy to propagate, the medium must possess both inertia and elasticity. The inertial force, which results by virtue of the molecules possessing a finite mass, functions to resist the system from being changed whereas the elasticity or restoring force acts to restore the system, once it is changed, to its initial state, and is a result of the interaction forces between molecules. Fluids, as well as solids, possess both inertial and elastic properties which are manifest in the thermodynamic quantities of density and compressibility, respectively. For the development of the equations describing sound propagation, three constitutive equations are required, viz., the continuity equation, the equation of motion and the equation of state (Markham et al., 1951). The first two are given by

$$\rho_o = (1 + \frac{\partial \xi}{\partial x})\rho \tag{2-1}$$

and

$$\frac{\partial p}{\partial x} = - \rho_o \frac{\partial^2 \xi}{\partial t^2} \tag{2-2}$$

where ρ and ρ_o are the disturbed and undisturbed densities, respectively, ξ is the particle displacement and p is the acoustic pressure. The equation of state of a fluid relates its thermodynamic state variables such as pressure-volume or stress-strain. When an acoustic disturbance perturbs the system, the process assumed is adiabatic since the entropy content remains relatively constant. The simplest equation of state is that of

$$p = Ks \tag{2-3}$$

which is the general first order form of the static stress-strain adiabatic process where K is the adiabatic bulk modulus. However, this relationship

must be modified if the absorption phenomenon is to be considered.

2.1 Classical Mechanisms of Absorption

Stokes (1845) modified (2-3) to contain the time rate of change of strain to include a resistive term, ζ, which represented a viscosity factor. As a result he derived the one dimensional lossy wave equation

$$\frac{\partial^2 \xi}{\partial t^2} = \frac{K}{\rho_o} \frac{\partial^2 \xi}{\partial x^2} + \frac{\zeta}{\rho_o} \frac{\partial^3 \xi}{\partial x^2 \partial t} . \tag{2-4}$$

If the solution to (2-4) is assumed to be of the form

$$\xi = \xi_o e^{j(\omega t - k^* x)} \tag{2-5}$$

where k^* $(=k-j\alpha)$ is the complex wave number, and k and α are the real wave number and absorption coefficient, respectively, then the solution to (2-4) is given by

$$\alpha = \left(\frac{\rho_o}{2K}\right)^{1/2} \omega \left\{ \frac{\sqrt{1 + \omega^2\tau^2} - 1}{1 + \omega^2\tau^2} \right\}^{1/2} \tag{2-6a}$$

$$c = \left(\frac{2K}{\rho_o}\right)^{1/2} \frac{1}{\omega\tau} \left\{ (1 + \omega^2\tau^2) \sqrt{1 + \omega^2\tau^2} - 1 \right\}^{1/2} \tag{2-6b}$$

where c is the phase velocity of the acoustic wave and τ, representing a relaxation time, is defined as ζ/K.

Stokes was cognizant of the fact that liquids possess both a shear, η_s, and a bulk (or volume), η_v, viscosity, but had no direct method for measuring the latter. Thus, even though the viscosity factor, ζ, represented both viscosities, Stokes assumed $\eta_v = 0$ which resulted in

$$\zeta = \frac{4}{3} \eta_s \tag{2-7}$$

yielding

$$\tau = \frac{4\eta_s}{3\rho_o c^2} . \tag{2-8}$$

Under the assumption that $\omega\tau << 1$, (2-6a) and (2-6b) become

$$\alpha_s = \frac{2\eta_s \omega^2}{3\rho_o c_o^3} \tag{2-9a}$$

and

$$c_o = \left(\frac{K}{\rho_o}\right)^{1/2} \tag{2-9b}$$

where the subscript s indicates the acoustic absorption coefficient due to shear viscosity.

A few years later, Kirchhoff (1868) considered heat conductivity, κ, as a mechanism of acoustic absorption in fluid media. Since the fluids under consideration in the present study are all aqueous, the effect due to thermal conductivity is negligible compared with that due to shear viscosity. Thus, the result of Kirchhoff is

$$\alpha_{hc} = \frac{\kappa(\gamma-1)\omega^2}{2\rho_o c_o^3 c_p} \tag{2-10}$$

where the subscript refers to the acoustic absorption coefficient due to heat conduction, and γ is the ratio of specific heats at constant pressure to constant volume (c_p/c_v).

The sum of the acoustic absorption coefficient terms of Stokes, (2-9a), and Kirchhoff, (2-10), is termed the classical value,

$$\alpha_{class} = \frac{\omega^2}{2\rho_o c_o^3}\left[\frac{4\eta_s}{3} + \frac{\kappa(\gamma-1)}{c_p}\right]. \qquad (2\text{-}11)$$

The classical absorption coefficient divided by the frequency squared is a constant for a given fluid at a stated temperature and pressure, viz.,

$$\frac{\alpha_{class}}{f^2} = \frac{2\pi^2}{\rho_o c_o^3}\left[\frac{4\eta_s}{3} + \frac{\kappa(\gamma-1)}{c_p}\right]. \qquad (2\text{-}12)$$

2.2 General Discussion of Relaxational Mechanisms of Absorption

Phenomenologically, when the density (or volume) and pressure are out of phase, sound absorption results. This occurs when the fluid, as a result of its possessing a finite viscosity, produces a frictional lag (Markham et al., 1951), such as Stokes (1845) developed. Lindsay (1948) described another cause in which the bulk modulus of the fluid changes as a result of the modulus possessing different rates. This latter cause is called a relaxation mechanism and will be discussed in considerable detail. Since the observed ultrasonic absorption coefficient in fluids is generally several times greater than that due to the classical mechanisms, it is usually attempted to explain this difference by suggesting that one or more relaxation processes are present. Generally three major relaxational effects can occur in aqueous solutions to explain the excess absorption above the classical losses which are always present. These three are classified as structural relaxation, thermal relaxation and chemical relaxation. Each of these will be considered in detail but first the general phenomenon of relaxation is treated.

Consider in a fluid medium that the individual molecules can exist in two or more equilibrium states of differing energy levels. The propagation

of an acoustic disturbance through this fluid will perturb the equilibrium states of these molecules, some extracting energy from the wave process while others release energy into the medium, depending upon whether their energy levels are increased or decreased by the disturbance. Consider, for example, a first order reaction, i.e., the molecules within the fluid reside in one of two equilibrium states, E_1, or E_2. In response to a disturbance, the rate constants, k_{12} and k_{21}, will determine the rate at which the population of molecules change states. This reaction can be pictured as

$$E_1 \underset{k_{21}}{\overset{k_{12}}{\rightleftharpoons}} E_2 \ . \tag{2-13}$$

Since an acoustic pressure wave consists of rarefied and compressional phases, let it be assumed that all of the molecules exist in energy state E_1 when subjected to static rarefication and in state E_2 when subjected to static compression. So, if the pressure of the fluid is increased instantaneously with all the molecules initially in E_1, and it is assumed that all the molecules change to E_2 exponentially, then the time for 63% of the molecules to change energy states is defined as the relaxation time τ and is related to the rate constants by

$$\tau = (k_{12} + k_{21})^{-1} \ . \tag{2-14}$$

It is seen in this example that even though the pressure changed instantaneously, the response lagged behind.

Now suppose, instead of the pressure changing as above, it varies harmonically with period T. At a very slow rate, the acoustic period will be much greater than τ ($T >> \tau$). In this case the energy population densities will follow the pressure changes with negligible time lag. In other words, the

pressure change and population density change are in phase, and T is large enough so that all of the molecules are able to change states. Now, as the acoustic frequency increases so that its period is within an octive or so of τ, the time necessary for the molecules to change their energy levels causes them to lag behind the pressure changes. Further increasing the frequency increases the lag, and also decreases the number of molecules which change energy levels. For the extreme case when $T << \tau$, none of the molecules have time to change their energy state which results in the process being relaxed out.

If the population density change results in a volume change, dV, then the work done on the system by the acoustic pressure wave, P, is given by

$$W = - \int P \, dV \, . \qquad (2\text{-}15)$$

As long as the changes in P and V are in phase (as for $T >> \tau$), no net work is done since the energy that is supplied from the acoustic wave to increase the molecules' energy states is returned, in phase, to the wave. Thermodynamically, this condition is termed a reversible process. At the other extreme ($T << \tau$) dV is virtually zero as only a small fraction of the population has time to change energy states. Therefore, since (2-15) represents an absorption of the acoustic wave when work is accomplished, virtually no absorption per acoustic period (or wavelength) occurs under the conditions $T >> \tau$ and $T << \tau$. When the above conditions are not valid, the volume change lags behind the pressure, and work is done on the system resulting in an absorption per wavelength, which is a maxima when $T = \tau$.

This first order reaction is an example of a single relaxation mechanism. The general expression representing the frequency-free absorption due to a single relaxation mechanism can be written as

$$\frac{\alpha}{f^2} = \frac{A}{1+\omega^2\tau^2} + B \quad . \qquad (2\text{-}16)$$

The term frequency-free is associated with the classical absorption mechanism, (2-12) where α/f^2 is independent of frequency. In (2-16) B includes the classical absorption mechanisms in addition to any relaxation process which possesses a characteristic frequency much greater than τ^{-1}. However, single relaxation mechanisms have not generally been known to occur in aqueous solutions of polymers and, thus, it has been necessary to describe the absorption spectra of these solutions by distributions of relaxation processes (see for example Dunn et al., 1969 or Philippoff, 1965).

2.2.1 Structural Relaxation

During the compressional phase of the propagated acoustic wave, the molecules within the fluid under investigation are brought closer together than they were under ambient conditions. In addition to being moved closer to one another, they are also rearranged, or repacked, into a closer packed lattice structure. This structural rearranging of the molecules requires redistribution of the molecules' mutual orientation with one another, i.e., changing their degree of association. Such configurational changes within the liquid are influenced by the molecule's shape and the forces of mutual attraction. These changes result from either the breaking of intermolecular bonds or the accumulation of sufficient kinetic energy to overcome the potential energy barrier which restrains such bonds from being broken. These structural rearrangements are attended by a volume change resulting from the pressure change which suggests that the liquid has a volume (or bulk) viscosity. Since these structural changes are a result of molecular energy level shifts, these being time dependent, a relaxation phenomenon results. Generally a structural relaxation mechanism is characterized by a distribution of

relaxation times (Litovitz and Davis, 1965).

Liquid water is an excellent example of a fluid whose excess ultrasonic absorption is a result of structural relaxation. Thermal relaxation (to be discussed next) is quite easily eliminated due to the anomalous property that the coefficient of thermal expansion at 4°C is zero (Fox and Rock, 1946). At this temperature, fluctuations of the temperature cannot occur as the pressure is varied, thus eliminating the perturbant force (the thermal wave) required for thermal relaxation. In addition, since liquid water is the solvent medium of biological macromolecules, it is appropriate to discuss its properties, first concentrating on its liquid structure itself and then commenting on the ultrasonic absorption and velocity properties of liquid water.

Any theory which attempts to explain the structure of liquid water must satisfactorily account for its anomalous properties such as unusually high heat capacity, high dielectric constant, negative thermal expansion from 0 to 4°C, decrease in compressibility from 0 to 46°C, initial decrease in the viscosity to the application of pressure between 0 and 30°C, etc. (Eisenberg and Kauzmann, 1969). These properties are attributed to the strong intermolecular interactions consisting mainly of hydrogen bonding between the water molecules (Kavanau, 1964). A significant feature of water molecules is their ability both to give and to receive hydrogen bonds. Also it is not necessary for these bonds to remain absolutely straight (Pople, 1951; Cannon, 1958).

Two classifications of water models exist, viz., continuum and mixed, depending upon whether the hydrogen-bonded networks are respectively continuous or discrete. Continuum models describe liquid water as a three-dimensional lattice of uninterrupted, tetrahedrally coordinated, hydrogen-bonded molecules. Lennard-Jones and Pople (1951) and Pople (1951) developed

a continuum model for which hydrogen bond stretching and bending deformations resulted in an increase in the number of nearest neighbors in the first two water shells surrounding a given water molecule. This occurs when ice melts, resulting in an increase in the flexibility of the hydrogen bonds, instead of breaking these bonds. Thus each water molecule participates in four hydrogen bonds (Barnes, 1929); two involving the hydrogen atoms of the molecule and two connecting the oxygen atom of the molecule to two neighboring hydrogen atoms. This model is in good agreement with the observed variation of the X-ray radial distribution function at different temperatures. However, the entropy for this model is not in accord with that calculated from thermodynamic data since little freedom of ratation is allowed in such a rigid model (Némethy and Scheraga, 1962a). Recent observations of vibrational spectroscopic data obtained from infrared (Falk and Ford, 1966; Schiffer and Hornig, 1968) and Raman Spectra (Wall and Hornig, 1965) measurements give strong support to the continuum model of liquid water. However, Walrafen (1969) does not agree with the results of Hornig and his coworkers since he has been able to show that the Raman Spectra shows evidence for a mixture model of water structure.

Mixture models describe liquid water as an equilibrium of discrete groupings in which each water molecule within these groups can vary its number of hydrogen bonds from none (monomer water) to all four (such as in ice or continuum models). Röntgen (1892) was the first to suggest that there are ice molecules in water, i.e., partial retention of the tetrahedrally directed hydrogen-bonding involved in the crystalline structure of ice.

The "vacant-lattice-point" model of Forslind (1952) is considered essentially a crystalline (tetrahedrally structured) system with spaces between the groups of molecules large enough to accommodate single, monomer, water molecules. As the temperature of the system is increased, localized

thermal amplitude peaks of sufficient strength disrupt the weakest bonds of the lattice structure causing water molecules to break off (producing a vacant lattice point) and pass into these cavities or interstitial voids. This interstitial model is able to account for the observed volume, viscosity and self-diffusion properties of water.

Frank and Wen (1957) and Frank (1958) have suggested that the formation of liquid water is a cooperative phenomena, i.e., many water molecules will come together in the form of a short-lived cluster and will similarly break apart as a whole. To illustrate: when two water molecules are connected by a hydrogen bond, one of the molecules develops a local positive charge whereas the other develops a local negative charge. These charges promote the formation of an additional hydrogen bond to a third water molecule, and so on. It has been suggested that the lifetime of these "flickering clusters" is 10^{-10} to 10^{-11} sec. based upon dielectric relaxation time (Collie et al., 1948) and bulk relaxation time (Hall, 1948) in water. The local energy fluctuations within the liquid water govern the formation and dissociation of these clusters. The only assumption regarding the formation of the clusters is that the largest possible number of hydrogen bonds be formed, without undue bond linearly deformation. This means that the clusters should be compact and contain as many four hydrogen-bonded water molecules as possible. These clusters are surrounded by, and in equilibrium with, monomeric unbounded water, this water lacking hydrogen bonds but being acted upon by strong dipole-dipole and London forces with neighboring molecules. The water molecules at the surface of the clusters participate in one, two or three hydrogen bonds.

Némethy and Scheraga (1962a), assuming the flickering cluster model of Frank and Wen, developed a partition function and were able to calculate thermodynamic parameters of this liquid water system as a function of

temperature. Their calculated cluster size ranged from 91 to 25 water molecules as the temperature varied from 0 to 70°C. To derive this partition function, each of the water molecules is assigned a particular energy, depending upon the number of hydrogen bonds it possesses. The ground energy state relates to the molecules within the interior of the cluster, the four hydrogen-bonded molecules. The energy levels increase as the number of hydrogen bonds decrease. Thus five energy levels are represented although the main structure of this model is represented by two species, the bulky (clusters) and dense (monomoer water) species. The energy required to break the hydrogen bond in liquid water is a matter of controversy with values ranging from 1.3 kcal/mole (Grjotheim and Krough-Moe, 1954) to 6.8 kcal/mole (Verwey, 1941). Némethy and Scheraga (1962a) performed their calculations using a value of 1.32 kcal/mole. The calculated values of the free energy, enthalpy and entropy are within 3% of the experimental data within the temperature range 0-70°C. However, the agreement is not as good for the heat capacity, as they pointed out.

Ultrasonic measurements have supported the mixture model for the structure of water (Hall, 1948; Smith and Lawson, 1954; Litovitz and Carneval, 1955; Litovitz and Davis, 1965). Hall (1948) developed a theory of the volume viscosity in liquid water in terms of a two energy state model to explain the excess ultrasonic absorption. The observed absorption must take into consideration the volume viscosity, η_v, (Litovitz and Davis, 1965)

$$\alpha_{OBS} = \frac{2\pi^2 f^2}{\rho_o c_o^3}\left[\eta_v + \frac{4}{3}\eta_s\right]. \qquad (2\text{-}17)$$

In water the observed ultrasonic absorption is approximately three times greater than the classical absorption due to shear viscosity only. Thus

it is concluded that the volume viscosity of water is roughly three times greater than the shear viscosity and Hall's theory attempts to explain this. Hall (1948) assumes that only the volume change between the two states is significant since Fox and Rock (1946) showed that the excess loss in water persists around 4°C where no rise in temperature can occur upon compression. The lower or ground energy state relates to the bulky species, i.e., that which occurs during the rarefied part of the wave, and the upper energy state refers to the dense species. Némethy and Scheraga (1962a) used the same convention where the unbounded (dense) water represent the highest energy state and the tetrahedrally bounded (bulky) water refers to the ground energy state. Hall's theory agrees with the excess ultrasonic absorption over the temperature range 0 to 80°C to within 10% or better.

Smith and Lawson (1954), investigating velocity of sound as a function of pressure and temperature, conclude that their measurements support Hall's model. Litovitz and Carnevale (1955), utilizing high pressure ultrasonic absorption and velocity measurements, conclude that Hall's two state theory is accurate only if the close packed (dense) configuration is assumed to be the ground energy state and bulky species in the upper energy state.

At the present time no single model explains all the known properties of liquid water (Narten and Levy, 1969) although several have, to a reasonable degree, explained a number of the measurable thermodynamic properties (Kavanau, 1964; Eisenberg and Kauzmann, 1969; von Hippel and Schleich, 1969). The Némethy and Scheraga (1962a, b, c) statistical-thermodynamic treatment of Frank and Wen (1957) and Frank's (1958) flickering-cluster model have received more widespread use since it has been developed more extensively, both quantitatively and qualitatively than any other model.

When biological macromolecules, such as hemoglobin, are in aqueous solution, a certain amount of the solvent will become an inherent part of the molecule since the polymer possesses ionic and polar groups which associate with water molecules. In addition, proteins contain a number of nonpolar side chains (hydrocarbon groups) such that within the vicinity of the macromolecule, some water structuring will occur, as described by the Frank and Evans (1945) "iceberg" mechanism. Due to entropy considerations of a nonpolar solute within an aqueous environment, these investigators suggested that the water molecules order (structure) themselves around the nonpolar molecule to form clusters, or "icebergs," interconnected by hydrogen bonds. Thus it is quite possible that the structure of liquid water increases in the neighborhood of the biological macromolecule. Any increase in water structuring such as this is termed the hydration layer and is not to be confused with the bound water.

Thus, when an acoustic wave is propagated through an aqueous solution of biological macromolecules, interaction between the perturbing wave and the hydration layer surrounding the solute molecule results. It is quite possible that the nature of this interaction is one of disrupting, or breaking, and making of these clusters. If this were the case, energy would be extracted from the acoustic wave when these clusters are formed, and returned to the wave, but not necessarily in phase, when dissolved. Returning the energy out of phase would then result in an absorption due to a structural relaxation process.

2.2.2 Thermal Relaxation

Ultrasonic absorption measurements indicate that for most liquids, a volume viscosity must be postulated, although several different mechanisms

can be responsible for the observed excess absorption, and hence the volume viscosity. Thermal relaxation requires that the propagation of a harmonically varying compressional wave results in a similar fluctuation in temperature, a consequence of the propagated acoustic wave being an adiabatic phenomenon. The temperature fluctuations are associated with the energy exchange processes between the external and the internal degrees of freedom of the constituent molecules (Lamb, 1965), wherein the latter is a function of the vibrational and rotational modes of the molecules. For example, in the non-associated (nonpolar) liquids, rotational isomeric and vibrational relaxation are the major causes of the volume viscosity, and hence the excess ultrasonic absorption. When it is necessary to distinguish between structural and thermal relaxation, generally the latter process is characterized by a single relaxation mechanism with negligible velocity dispersion through the relaxation region, whereas structural relaxation generally results in a distribution of relaxation times with measurable dispersion (Lamb, 1965). Since the ultrasonic absorption in associative-type liquids, such as water or alcohol solutions, is rarely characterized by a thermal relaxation mechanism, this process is thus expected to play little, if any, role in the solutions of this study.

2.2.3 Chemical Relaxation

Einstein, in 1920, was the first to discuss the possibility of a propagating acoustic wave perturbing a chemical reaction, though since then many other investigators have discussed this form of a relaxation process (see Herzfeld and Litovitz, 1959). Generally when an acoustic wave is propagated through a liquid media, the volume change which results is due to the perturbation of a chemical reaction from equilibrium by the pressure

disturbance. Of importance in ultrasonic measurements of aqueous solutions of globular proteins is the protolytic reactions which can generally be described by (Eigen and De Maeyer, 1963)

$$A + B \underset{k_{21}}{\overset{k_{12}}{\rightleftarrows}} C \tag{2-18}$$

where k_{12} and k_{21} are the forward and reverse rate constants, respectively. The complete rate equation for this reaction is given by

$$-\frac{dc_A}{dt} = -\frac{dc_B}{dt} = \frac{dc_C}{dt} = k_{12}c_A c_B - k_{21}c_c \tag{2-19}$$

where c_A, c_B and c_C are the instantaneous concentrations of the respective components. When the reaction is at equilibrium, that is, when the medium is not being perturbed by external forces, the time derivatives of (2-19) become zero, yielding the equilibrium constant, K, defined as

$$K = \frac{k_{12}}{k_{21}} = \frac{\bar{c}_C}{\bar{c}_A \bar{c}_B} \tag{2-20}$$

where the bar identifies equilibrium quantities. Assuming that the particle displacement gradient is infinitesimal, the perturbation from equilibrium of the protolytic reaction of (2-18) is small, which allows for linearization of the rate equation, yielding

$$\frac{dx_i}{dt} + \frac{1}{\tau} x_i = \frac{1}{\tau} \bar{x}_i \tag{2-21}$$

where

$$\begin{aligned} x_i &= c_i - c_i^o \\ \bar{x}_i &= \bar{c}_i - c_i^o \end{aligned} \tag{2-22a}$$

and

$$\bar{x}_i - x_i << c_i \tag{2-22b}$$

where x_i is the difference between the instantaneous concentration of species i (i = A, B or C) and some time-independent concentration reference, c_i^o, and the assumption in (2-22b) is a result of infinitesimal deviations from equilibrium. Substituting (2-22a) into the first order differential equation, (2-19), and applying the assumption, (2-22b), results in

$$\frac{dx_A}{dt} + \{k_{21}+k_{12}(\bar{c}_A+\bar{c}_B)\}x_A = \{k_{21}+k_{12}(\bar{c}_A+\bar{c}_B)\}\bar{x}_A \tag{2-23}$$

where the characteristic time, otherwise known as the chemical relaxation time, of this single step reaction is

$$\tau = \{k_{21}+k_{12}(\bar{c}_A+\bar{c}_B)\}^{-1}. \tag{2-24}$$

A single-step reaction, which is represented by a single relaxation time, is always inadequate for describing more complex reactions. Higher order reactions require a spectrum of relaxation times to describe their behavior, which modifies (2-21) to

$$\frac{dx_i}{dt} + \sum_k a_{ik}x_k = \sum_k a_{ik}\bar{x}_k \tag{2-25}$$

where a_{ik} is a function of the rate constants of the particular reaction, or series of reactions, and their corresponding equilibrium constants. It must be kept in mind that chemical relaxation processes are always represented by discrete, single relaxation times. However, it can occur that these relaxation times can be sufficiently close together that a

continuous relaxation spectrum appears to result, and the elucidation of each of the separate relaxation times is extremely difficult. From (2-23) it is obvious that the chemical relaxation time, and the ultrasonic absorption coefficient (as will be shown), is a function of the concentration of the reactants (Eigen and De Maeyer, 1963).

For a single relaxation process, the frequency free absorption is represented by (2-17), where τ, in this case, is the chemical relaxation time such as in (2-23). The absorption parameter of (2-17) represents the low frequency ($\omega\tau << 1$) absorption due to the perturbation of a chemical process and is given by (Applegate et al., 1968)

$$A = \frac{2\pi^2 \tau \rho_o c_o \Gamma}{RT} (\Delta u)^2 \qquad (2\text{-}26a)$$

where Δu, the change in internal energy is

$$\Delta u = \Delta v - \frac{\beta \bar{v}}{c_p} \Delta H \qquad (2\text{-}26b)$$

where Δv and ΔH are the standard volume and enthalpy changes, v is the volume per mole of the solution, β is the thermal expansion coefficient, c_p is the heat capacity at constant pressure, R is the gas constant and T is the absolute temperature. The parameters τ, ρ_o and c_o have been defined previously, and the parameter Γ is given by the equilibrium constant K, (2-19), and the reaction concentrations as

$$\Gamma = \frac{\bar{v} K c_t \bar{c}_B}{K c_t + (K \bar{c}_B + 1)^2} \qquad (2\text{-}27)$$

where

$$c_t = \bar{c}_A + \bar{c}_B \, . \qquad (2\text{-}27a)$$

Typically for aqueous solutions of electrolytes, the magnitude of Δv [see (2-26b)] is the order of 20-30 cc/mole whereas ΔH is less than 1 kcal/mole with $\beta\bar{v}\Delta H/c_p$ generally negligible (Eigen and De Maeyer, 1963; Applegate et al., 1968; Parker et al., 1968). Therefore, the A parameter of (2-26a) becomes

$$A = \frac{2\pi^2 \tau \rho_o c_o \Gamma (\Delta v)^2}{RT} \tag{2-28}$$

which means that for this type of solution, the pressure variations due to the acoustic wave perturb the chemical reaction from equilibrium. On the other hand, if a nonaqueous solution were under investigation, ΔH would be the order of 10 kcal/mole or more and $\beta\bar{v}/c_p > 1$ cc/kcal while $\Delta v < 1$ cc/mole, resulting in the internal energy being a function of only the enthalpy term (Eigen and De Maeyer, 1963). This would imply that for a nonaqueous solution, the thermal wave, which accompanies the pressure wave of the acoustic disturbance, is the primary perturbing agent of the chemical equilibrium.

One example which can occur in protein solutions is the single-step proton-transfer reaction, that is, when the acoustic wave perturbs the system, the proton is exchanged between water and the solute radical. For example, the reaction with a carboxyl group (Michels and Zana, 1969) is of the form

$$R\text{-}COO^- + H_3O^+ \rightleftarrows R\text{-}COOH + H_2O \tag{2-29}$$

where

$$K = \frac{[R\text{-}COOH + H_2O]}{[R\text{-}COO^-][H_3O^+]} \tag{2-30}$$

$$\frac{\Gamma}{\bar{v}} = \frac{Kc_t[H_3O^+]}{Kc_t + (K[H_3O^+] + 1)^2} \tag{2-31}$$

$$pH = -\log_{10}[H_3O^+] \tag{2-32}$$

$$c_t = [R\text{-}COO^-] + [R\text{-}COOH + H_2O]. \tag{2-33}$$

If the reaction with a primary amine group is considered

$$R\text{-}NH_3^+ + OH^- \rightleftarrows R\text{-}NH_2 + H_2O \tag{2-34}$$

$$\frac{\Gamma}{\bar{v}} = \frac{Kc_t[OH^-]}{Kc_t + (K[OH^-] + 1)^2} \tag{2-35}$$

$$pH = 14 + \log_{10}[OH^-] \tag{2-36}$$

$$c_t = [R\text{-}NH_3^+] + [R\text{-}NH_2 + H_2O]. \tag{2-37}$$

From (2-27), if $\Gamma/\bar{v}$ is plotted as a function of $pB(-\log_{10}\bar{c}_B)$, as is shown in Fig. 2-1, the resultant curve is bell-shaped with the maximum value occurring at

$$pB_{MAX} = -\frac{1}{2}[\log_{10}K + \log_{10}c_t]. \tag{2-38}$$

If the reactions in (2-29) and (2-34) represent, for example, the β-carboxyl of aspartic acid and the ε-amino of lysine, respectively, then for these free amino acids in aqueous solution, the $\Gamma/\bar{v}$ peak would occur close to pH 3.9 and pH 10.5, respectively, depending upon their concentration. If,

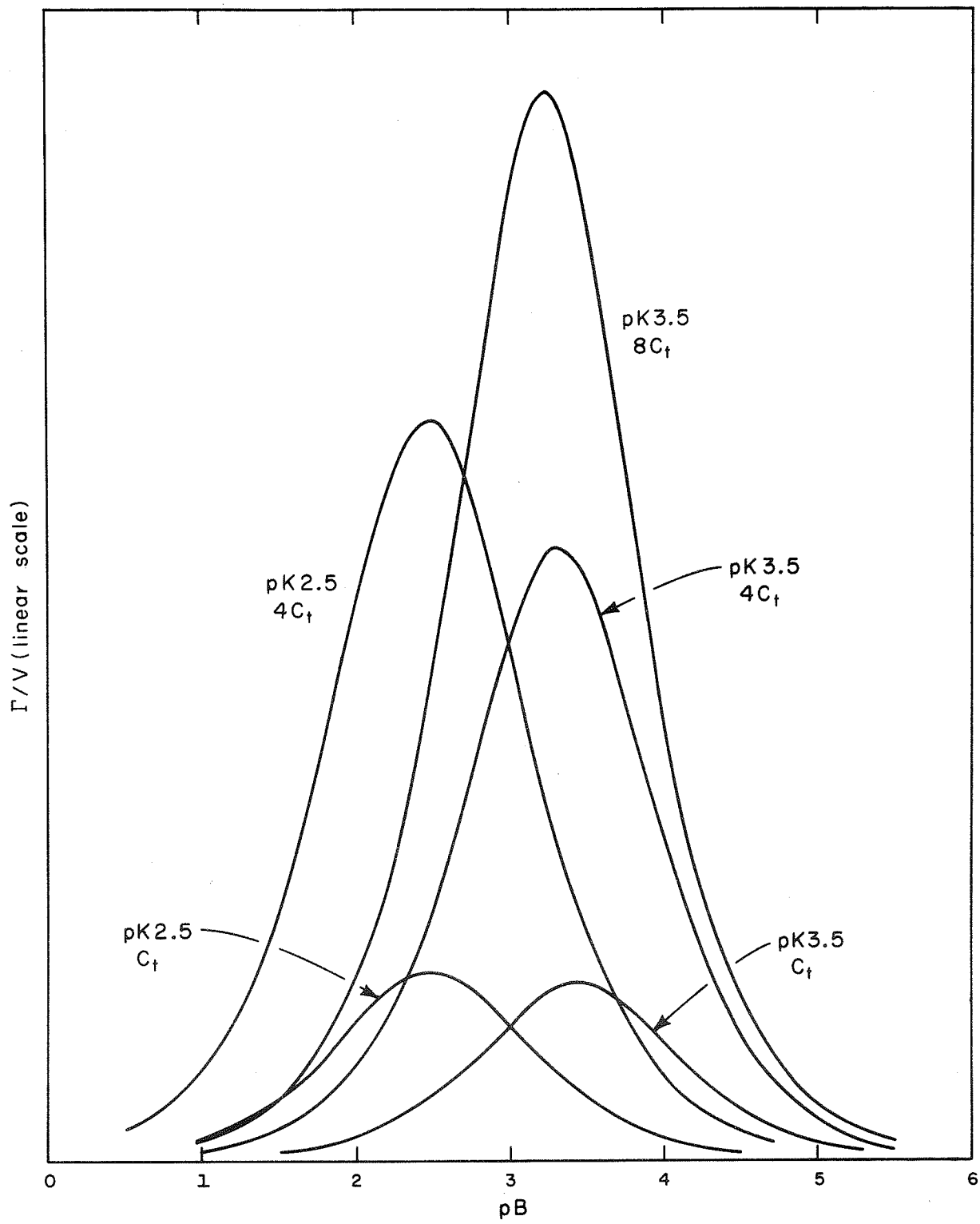

FIGURE 2-1

BEHAVIOR OF $\Gamma/\bar{v}$ PARAMETER AS A FUNCTION OF pB

on the other hand, these same amino acids were a protein side chain in aqueous solution, the pH at which the peak could occur would be within the approximate range, for aspartic acid, pH 3.0-4.7, and for lysine, pH 9.4-10.6 (Clark, 1964). Other examples are listed in Table 2-1.

Hussey (1970) studied the contribution of the proton transfer reaction of amino acid side chains of proteins and has proposed that this is the primary cause of the ultrasonic absorption in aqueous solutions of protein within the pH ranges 2-4 and 10-12. Outside of this pH range, $4<pH<10$, he concluded the ultrasonic absorption does not depend upon proton-transfer. Also, Zana and Lang (1970) disputed the conclusions of Kessler and Dunn (1969) regarding the ultrasonic absorption peaks around pH 3 in bovine serum albumin. Zana and Lang correlated the peaking to the protonation reaction involving protein side chains whereas Kessler and Dunn attributed it to the conformation change of the BSA molecule.

Table 2-1

Dissociation of Ionizable Groups of Proteins (Clark, 1964)

Group (Amino Acid)	pK Range (on a protein)
Carboxyl	
α - (All)	1.8-2.5
β - (Aspartic Acid)	3.0-4.7
γ - (Glutamic Acid)	
Amino	
α - (All)	7.9-10.0
ε - (Lysine)	9.4-10.6
Phenolic hydroxyl (Tyrosine)	9.8-10.4
Imidazolium (Histidine)	5.6-7.0
Guanidinium (Arginine)	11.6-12.6
Sulfhydryl (Cysteine)	9.4-10.8

2.3 Viscoelastic Relaxation--General Discussion

Liquids do not support static shear stresses as do solids. Substances are said to be elastic when they can remain in equilibrium under the presence of a shear stress. Liquids can, however, support dynamic shear stresses as a result of possessing finite viscosity. Thus a viscoelastic material is one which exhibits both an elasticity and a viscosity when it is mechanically stressed (Philippoff, 1965; Litovitz and Davis, 1965). For viscoelastic materials which have stress-strain properties that are time dependent, the Stokes equation of state is modified to include the stress time derivative, which yields a more general stress-strain acoustic equation of state for the compressional wave (Litovitz and Davis, 1965), viz.,

$$p + \tau_v \frac{\partial p}{\partial t} = K_o \left[s + \tau_p \frac{\partial s}{\partial t} \right] \tag{2-39}$$

where p and s represent the stress and strain of the disturbance, respectively. In this equation of state τ_v represents the time necessary for the pressure to change when the perturbing force is the volume change whereas τ_p represents the corresponding time except that the perturbing force is now the pressure change. These two relaxation times are related to one another by the ratio of the high frequency to low frequency compressional moduli, as

$$\tau_p = \frac{K_\infty}{K_o} \tau_v . \tag{2-40}$$

Applying a sinusoidal stress to the liquid, which is represented by the equation of state of (2-39), yields the complex compressional modulus, K^*, given by

$$K^* = K_o + \frac{K_r \omega^2 \tau_v^2}{1+\omega^2 \tau_v^2} + j\omega \frac{\tau_v K_r}{1+\omega^2 \tau_v^2} \tag{2-41}$$

where $K_r (= K_\infty - K_o)$ is the relaxational bulk modulus. The imaginary part of the modulus is proportional to the frequency dependent volume viscosity

$$\eta_v(\omega) = \frac{K_r \tau_v}{1+\omega^2 \tau_v^2} . \tag{2-42}$$

A similar equation of state relating the shear components of stress p' and strain s' can be written, viz.,

$$p' + \tau_s \frac{\partial p'}{\partial t} = G_\infty \tau_s \frac{\partial s'}{\partial t} \tag{2-43}$$

where τ_s is the shear relaxation time and G_∞ is the high frequency shear rigidity. There is no time independent strain term since a viscoelastic material cannot support a low frequency shear strain. Again, applying a sinusoidal stress to the material represented by this equation of state yields an expression for the complex modulus of shear, G^*, viz.,

$$G^* = \frac{G_\infty \omega^2 \tau_s^2}{1+\omega^2 \tau_s^2} + j\omega \frac{G_\infty \tau_s}{1+\omega^2 \tau_s^2} \tag{2-44}$$

where the frequency dependent shear viscosity is given by

$$\eta(\omega) = \frac{G_\infty \tau_s}{1+\omega^2 \tau_s^2} . \tag{2-45}$$

Since a viscoelastic medium possesses both compressional and shear complex moduli, the one-dimensional longitudinal acoustic wave equation for a harmonic disturbance is

$$\frac{\partial^2 \xi}{\partial t^2} = c^{*2} \frac{\partial^2 \xi}{\partial x^2} \tag{2-46}$$

where the complex velocity of propagation is

$$c^* = \left\{\frac{1}{\rho_o}\left(K^* + \frac{4}{3}G^*\right)\right\}^{1/2} . \tag{2-47}$$

Assuming the solution of (2-46) to be (2-5) yields

$$\alpha\lambda = \pi \left[\frac{\dfrac{K_r\omega\tau_v}{1+\omega^2\tau_v^2} + \dfrac{\frac{4}{3}G_\infty\omega\tau_s}{1+\omega^2\tau_s^2}}{K_o + \dfrac{K_r\omega^2\tau_v^2}{1+\omega^2\tau_v^2} + \dfrac{\frac{4}{3}G_\infty\omega^2\tau_s^2}{1+\omega^2\tau_s^2}} \right] \tag{2-48}$$

and

$$c = \left\{\frac{1}{\rho_o}\left(K_o + \frac{K_r\omega^2\tau_v^2}{1+\omega^2\tau_v^2} + \frac{\frac{4}{3}G_\infty\omega^2\tau_s^2}{1+\omega^2\tau_s^2}\right)\right\}^{1/2} . \tag{2-49}$$

For the frequency approximations, viz., $\omega\tau_v \ll 1$ and $\omega\tau_s \ll 1$, (2-48) and (2-49) reduce to

$$\frac{\alpha}{f^2} = \frac{2\pi^2}{K_o c_o}\left(K_r\tau_v + \frac{4}{3}G_\infty\tau_s\right) \tag{2-50}$$

and

$$c_o = \sqrt{K_o/\rho_o} . \tag{2-51}$$

Since the low frequency approximations to (2-42) and (2-45) are $K_r\tau_v$ and $G_\infty\tau_s$, respectively, substitution of these into (2-50) yields

$$\frac{\alpha}{f^2} = \frac{2\pi^3}{\rho_o c_o^3}\left(\eta_v + \frac{4}{3}\eta_s\right). \tag{2-52}$$

Assuming that the volume viscosity in (2-52) is zero yields the acoustic absorption coefficient of Stokes, (2-9a). Also the acoustic velocities of (2-51) and (2-9b) are identical.

2.3.1 Viscoelastic Relaxation of Rigid Ellipsoidal Particles

Globular proteins are polyampholytes, that is, polyelectrolytes which possess both positive and negative charges. When these proteins are in aqueous solution at or near their isoelectric point, the pH at which the net charge of the molecule is zero, they possess relatively compact (rigid) configurations, due to, among other things, the attractions between equally numbered and oppositely charged side chains. For this discussion, proteins in aqueous solutions are to be considered as rigid spherical or ellipsoidal particles.

When the rigid solute particles are much greater in size than the solvent molecules, the macroscopic viscosity increases due to the particle cutting across a large number of so called flow lines producing a distorted flow pattern (Tanford, 1961). The effect on this solution viscosity, η_{SOLN}, due to rigid spherical shaped molecules has been computed by Einstein (1906, 1911) to be

$$\eta_{SOLN} = \eta(1 + 2.5\phi) \tag{2-53}$$

where η is the shear viscosity of the pure solution and ϕ is the volume fraction of the particles in solution. Extending Einstein's computations to particles having the shape of ellipsoid of revolution causes the solution viscosity to be dependent on the particle orientation as well. Solutions of such molecules in linear solvents possess nonlinear stress-strain relationships and are termed non-Newtonian. In the following discussion it is to be assumed that the shear rate is low, thus minimizing the non-Newtonian effects.

The ellipsoidal particle orientation is modified by a shear effect of the molecules attempting to align themselves toward the direction of flow and rotational Brownian motion which tends to disorient the particle (Frisch

and Simha, 1956). This solution viscosity dependence on the velocity gradients of rigid ellipsoid of revolution particles has been treated by a number of workers (see refs. 2-7 in Scheraga (1955)). Of these, one (Scheraga, 1955) has computed theoretical values for intrinsic viscosity over a wide range of axial ratios and the parameter σ in terms of the viscosity factor ν, where

$$\eta_{SOLN} = \eta(1 + \nu\phi). \tag{2-54}$$

The σ parameter is given by G/θ where the numerator is the velocity gradient of the liquid and θ is the rotary diffusion constant, the latter also a function of volume and shape of the particle. Since σ is an important parameter in Scheraga's (1955) theory, it is necessary to investigate its relative magnitude for acoustically propagating waves through aqueous solutions of globular proteins. The expression for the amplitude velocity gradient is

$$G = \left|\frac{\partial^2 \xi}{\partial x \partial t}\right| = \frac{\omega^2 \xi_o}{c_o} \tag{2-55}$$

where ξ_o is the amplitude particle displacement. Relating (2-55) to the intensity

$$I = \frac{1}{2}\, \xi_o^2 \omega^2 \rho_o c_o \tag{2-56}$$

yields

$$G = \frac{\omega}{c_o}\sqrt{\frac{2I}{\rho_o c_o}}\,. \tag{2-57}$$

Assuming a maximum intensity of 100 mw/cm^2, a sound velocity of 0.15 cm/μs, a density of 1 gm/cm^3 and an upper frequency limit of 100 MHz yields a

velocity gradient of 15,300/sec. Tanford (1961, page 445) reports that for serum albumin, a compact molecule (p = 4.9, a = 84 Å), the rotatory diffusion constant is of the order 10^6/sec. (0.84×10^6 by flow birefringence and 1.39×10^6 by dielectric dispersion methods). Thus, the ratio of these two yields

$$\sigma = \frac{G}{\theta} = 0.015 \tag{2-58}$$

which is small enough, according to the Scheraga (1955) theory, to utilize the $\sigma = 0$ case.

The intrinsic viscosity is defined by

$$[\eta] = \lim_{c \to o} \frac{\eta_{SOLN} - \eta}{\eta c} \tag{2-59}$$

where c is the concentration in units of gm/cc. Assuming that the concentration dependence can be neglected for low concentrations and substituting into (2-59), (2-54), yields

$$[\eta] = \frac{\phi}{c} \nu = \frac{N_A \nu_h}{M} \nu \tag{2-60}$$

where N_A is Avogadro's number, M is the particle's molecular weight and ν_h is its hydrodynamic volume given by

$$\nu_h = \frac{M}{N_A} (\nu_2 + \delta_1 \nu_1) \tag{2-61}$$

where ν_2 is the average specific volume of the solute molecule, ν_1 is the average specific volume of the solvent molecule bound to the solute molecule and δ_1 is a parameter which relates the mass of bound solvent to mass of dry polymer (typically $\delta_1 \simeq 0.2$ for globular proteins). Finally, the intrinsic viscosity becomes

$$[\eta] = (\nu_2 + \delta_1\nu_1)\nu. \tag{2-62}$$

Equating (2-59) and (2-62), and assuming negligible concentration dependence, yields

$$\frac{\eta_{SOLN}-\eta}{\eta c} = (\nu_2 + \delta_1\nu_1)\nu. \tag{2-63}$$

Cerf (1952) determined that for $\sigma = 0$, the frequency dependence of the shape parameter ν is

$$\nu = \nu_A + \frac{\nu_B}{1+\omega^2\tau^2} \tag{2-64}$$

where $\tau = 1/6\theta$, θ being the rotatory diffusion constant, and ν_A and ν_B are parameters which Scheraga's (1955) theory yields.

Assuming that the excess ultrasonic absorption, $\Delta\alpha_s$, is due to the shear viscosity mechanism of rigid ellipsoidal particles, the ultrasonic excess absorption can be defined as

$$A = \frac{\Delta\alpha}{cf^2} \tag{2-65}$$

where

$$\Delta\alpha = \Delta\alpha_s = \alpha - \alpha_s \tag{2-65a}$$

α is the solution absorption, and α_s is the absorption due to the pure solvent. Applying the general form of (2-9a), (2-65) yields

$$A_s = \frac{\Delta\alpha_s}{cf^2} = \frac{8\pi^2}{3\rho_o c_o^3}\left[\frac{\eta_{SOLN}-\eta}{c}\right]. \tag{2-66}$$

Substituting (2-63) and (2-64) into (2-66) gives

$$A_s = \frac{8\pi^2\eta}{3\rho_o c_o^3}(\nu_2+\delta_1\nu_1)(\nu_A + \frac{\nu_B}{1+\omega^2\tau^2}) \qquad (2\text{-}67)$$

where the rotational relaxation, τ, is given by (Tanford, 1961, page 436)

$$\tau = \frac{8\pi^2\eta a^3}{9kT[2\ \ell n(2p)-1]} \, . \qquad (2\text{-}68)$$

2.3.2 Viscoelastic Relaxation of Electroviscous Particles

Bull (1940) has pointed out that for aqueous solutions of proteins, a minimum in the solution viscosity versus pH curve generally occurs at the isoelectric point. This indicates that the electrostatic charges which the proteins possess play an important role in the solution viscosity since the net charge of the molecule is zero at the isoelectric point. Consider a solution of macromolecular particles which can possess either a net positive or negative charge, the solvent being an aqueous electrolytic solution of known molar concentration. Since the total solution must be electrically neutral, the counterions of the electrolytic solution neutralize the charges on the surface layer of the macromolecule. The layer which contains the counterions is regarded as diffuse and its charge distribution is that calculated by the Debye-Hückel theory.

Einstein's equation, (2-53), which represents the macroscopic viscosity of a suspension or solution of spherical rigid particles, is inadequate for describing electrically charged particles. In 1916, von Smoluchowski first pointed out that if a charge is present on an impermeable spherical macromolecule of radius a in very dilute aqueous solution, then the viscosity will increase as a result of increasing electrostatic potential on the particle, and sixteen years later, Krasny-Ergen (1932) developed the

detailed derivation of the solution viscosity as a function of particle charge. Since then a number of modifications have been made on their theory, resulting in (Conway and Dobry-Duclaux, 1960)

$$\eta_{SOLN} = \eta(1 + 2.5\ \phi\nu') \tag{2-69}$$

where the electroviscous parameter ν' is

$$\nu' = 1 + \frac{77}{25}\frac{\varepsilon\ \bar{\rho}\ \zeta^2}{\pi(\kappa a)^2 kT\eta} \tag{2-70}$$

where ε is the dielectric constant of the solvent, $\bar{\rho}$ the average frictional coefficient of the ions, κ the Debye-Hückel reciprocal thickness and kT the thermal energy at the appropriate temperature. The parameter ζ, known as the zeta potential, is the electrokinetic potential at the surface of the hydrodynamic particle with respect to the electrolyte and is given by

$$\zeta = \frac{ze}{\varepsilon\kappa a^2} \tag{2-71}$$

where ze is the charge which is evenly distributed over the surface of the particle.

Since most proteins are ellipsoids of revolution rather than spheres, as Einstein's equation assumes, it is necessary to modify (2-69) to include both Scheraga's (1955) shape parameter, ν, and the electroviscous parameter, ν', to give

$$\eta_{SOLN} = \eta(1 + \phi\nu\nu') \tag{2-72}$$

and rearranging into the form of (2-63) results in

$$\frac{\eta_{SOLN} - \eta}{\eta c} = (\nu_2 + \delta_1\nu_1)\nu\nu'. \tag{2-73}$$

Tanford (1961) points out that although δ_1 in (2-73) does not represent exactly the same thing as that in (2-63), the differences are negligible, and should be treated identically.

Even though Bull (1940) realized the von Smoluchowski-Krasny-Ergen's electroviscous theory had considerable shortcomings with respect to their basic assumption that proteins could not fulfill, he still deemed it worthwhile to examine their equation against some experimental data, namely ovalbumin. Bull showed that the von Smoluchowski-Krasny-Ergen theory gave values as high as ninety times that observed.

More recently Booth (1950) derived an expression for the electroviscous parameter for solid, charged, non-conducting particles in an electrolyte, given by

$$\nu' = 1 + \frac{1}{\sigma\eta a^2}\left(\frac{\zeta\varepsilon}{2\pi}\right)^2 \pi b^2(1+b)^2 Z(b) \qquad (2\text{-}74)$$

where $b = \kappa a$, σ is the specific conductivity of the solution and $Z(b)$ is evaluated numerically in Booth's paper.

2.4 Relative Motion, Scattering Losses and Particulate Relaxation Mechanisms

When particles are suspended in a fluid, as can be assumed for globular proteins at their isoelectric point where electroviscous forces can be neglected, ultrasonic absorption mechanisms other than those discussed above, can occur, viz., (1) mode conversion, (2) scattering, (3) friction between particle and fluid and (4) their disparate thermal properties, each having their relative importance depending upon the magnitude of ka, where k is the acoustic wave number and a is the particle radius. The condition $ka \ll 1$ is assumed in this study as the protein radius is typically no greater than 50 Å, resulting in $ka \simeq 0.002$ for 100 MHz.

Epstein (1941) treated very generally the absorption mechanism of spherical particles suspended in a fluid under the conditions ka << 1 in which the propagated longitudinal acoustic wave, when incident upon the particles, results in reflected longitudinal and transverse waves, the latter due to boundary mode conversion. These highly damped shear waves are degraded into heat generally within distance of one wavelength from the particle. Thus, Epstein's absorption coefficient, due to mode conversion, to a first approximation is

$$2\alpha_{MC} = k\phi(\delta-1)\mathrm{Re}\left\{\frac{b + j(1-b^2/3)}{\delta-(2+\delta)b^2/9-j\delta b}\right\} \tag{2-75}$$

and

$$b^2 = j\,\frac{\omega\rho_o a^2}{\eta} \tag{2-76}$$

where δ is the ratios of particle, ρ_p, to fluid, ρ_o, density, respectively, and ϕ is the particle volume fraction given by $\phi = \frac{4}{3}\pi a^3 n$, n being the number of particles per cm^3. The method of Carstensen and Schwan (1959a) is utilized to evaluate the real part by employing the parameter

$$\gamma^2 = \frac{\rho_o a^2}{2\eta} \tag{2-77}$$

which, when substituted into (2-76), results in $b^2 = j2\gamma^2\omega$, and finally when combined with (2-75) yields

$$\alpha_{MC} = \frac{2}{9}\,\frac{\phi}{c_o}\,\left(\frac{\delta-1}{\delta}\right)^2 \frac{\gamma^2\omega^2[1 + \gamma\omega^{1/2}]}{[1+\gamma\omega^{1/2}]^2 + \gamma^2\omega[1+\frac{2}{9}(\frac{2}{\delta}+1)\gamma\omega^{1/2}]^{1/2}} \tag{2-78}$$

where c_o is the sound velocity of propagation. Rewriting (2-78) in the

usual form for a relaxation process and rearranging to yield the form of (2-65)

$$A_{MC} = \frac{\alpha_{MC}}{cf^2} = \frac{2\pi^2 N_A \nu}{Mc_o} \left(\frac{\delta-1}{\delta}\right)^2 \frac{m}{M_e} \frac{\tau_o}{1+\omega^2\tau_o^2} \tag{2-79}$$

where

$$\nu = \frac{4}{3}\pi a^3 \tag{2-79a}$$

$$m = \frac{4}{3}\pi a^2 \rho_o \tag{2-79b}$$

$$M = \frac{4}{3}\pi a^3 \rho_p \tag{2-79c}$$

$$\tau_o = M_e/R_e \tag{2-79d}$$

$$M_e = M + m\left[\frac{1}{2} + \frac{9}{4}\frac{1}{\gamma\omega^{1/2}}\right] \tag{2-79e}$$

$$R_e = 6\pi a\eta[1 + \gamma\omega^{1/2}] \tag{2-79f}$$

N_A is Avogadro's number and M is the particles' molecular weight. In (2-79) α_{MC} is the total ultrasonic absorption, to a first approximation, due to mode conversion. In Epstein's (1941) development, as the particle size increases (ka increases), a second order term to the above mode conversion expression is necessary. This term represents a correction of $\Delta\alpha_{MC}$ to (2-78), resulting in an increase absorption of

$$\Delta\alpha_{MC} = \phi k^3 a^2 \, \mathrm{Re}\left\{\frac{10}{9b} + j\,\frac{23}{4b^2}\right\}. \tag{2-80}$$

Extracting the real part by assuming the ratio of particle density to solvent density is about unity, yields in the form of (2-79)

$$\Delta A_{MC} = \frac{\Delta\alpha_{MC}}{cf^2} = \frac{4\pi^2 N_A \nu a^2}{M c_o^3 \gamma}\left[\frac{5}{9}\ \omega^{1/2} + \frac{23}{8\gamma}\right]. \qquad (2\text{-}81)$$

In addition to the second order mode conversion term, Epstein (1941) derived an expression due to the scattering of the acoustic energy. The scattering is a result only of redirecting the energy, not dissipating it into heat, but neverless, it does yield an apparent absorption given by

$$A_{SCAT} = \frac{\alpha_{SCAT}}{cf^2} = \frac{4\pi^2 N_A \nu \omega^2 a^3}{M c_o^4}\left[\left(\frac{\delta-1}{\delta+2}\right)^2 + \frac{1}{3}\left(1 - \frac{K_o'}{K_p'}\right)^2\right] \qquad (2\text{-}82)$$

where K_o' and K_p' are, respectively, the real parts of the bulk modulus of the fluid and particle.

Urick (1948) extended the theory of Lamb (1946), which led to an expression accounting for the ultrasonic absorption due to the viscous drag, or friction, between the so called stationary particle and the moving fluid, this phenomenon otherwise called relative motion. In addition, scattering of energy from the suspended particles was considered. Urick's expression for sound absorption and scattering by spherical particles of radius a is

$$\alpha_u = \frac{\phi}{2}\left\{\frac{1}{3}k^4 a^3 + \frac{k(\delta-1)^2 s}{s^2 + (\delta+\tau)^2}\right\} \qquad (2\text{-}83)$$

where

$$s = \frac{9}{4\beta a}\left[1 + \frac{1}{\beta a}\right] \qquad (2\text{-}83a)$$

$$\tau = \frac{1}{2} + \frac{9}{4}\frac{1}{\beta a} \qquad (2\text{-}83b)$$

$$\beta = \sqrt{\frac{\omega\rho_o}{\eta}}\ . \qquad (2\text{-}83c)$$

Rearranging yields

$$A_u = \frac{\alpha_u}{cf^2} = \frac{2\pi^2 N_A \nu}{M}\left\{\frac{k^2 a^3}{3} + \frac{(\delta-1)^2 s}{k(s^2+(\delta+\tau)^2)}\right\} . \qquad (2\text{-}84)$$

Carstensen and Schwan (1959a) pointed out that the expressions for sound absorption derived by Epstein, (2-79), and Urick, (2-84), are completely equivalent. In concluding this, they indicated, as Urick (1948) also did, that the mechanism of mode conversion is describing quantitatively the effect of shearing which is occurring between the fixed particle relative to the moving fluid.

Hawley (1966) was unable to explain the excess ultrasonic absorption behavior in aqueous suspensions of polydisperse polystyrene lattices simply on the basis of the Lamb-Urick-Epstein theory (Lamb, 1946; Urick, 1948; Epstein, 1941). However, more recently Hawley and his colleagues (Allegra, 1970; Allegra et al., 1970a; Allegra et al., 1970b) have been able to account for this behavior by considering a thermal dissipation mechanism (Epstein and Carhart, 1953). When an adiabatic acoustic wave propagates through a solution or suspension of particles, a temperature effect will result at the fluid-particle discontinuity if their specific heats are different. Epstein and Carhart (1953) extended the model of Epstein (1941) to include the dissipation of energy due to irreversible heat transfer by assuming both media to be heat conductive. Chow (1964) improved upon the Epstein-Carhart (1953) theory by including the effect due to surface tension between particle and fluid, this resulting in an increased ultrasonic absorption coefficient due primarily to increased thermal dissipation. However, the surface tension effect is considered negligible in aqueous solutions of proteins. Epstein

(1941), Epstein and Carhart (1953) and Chow's (1964) theories were all derived utilizing similar analysis methods. Temkin and Dobbins (1966) approached the problem from a different point of view, namely, by assuming the fluid-rigid particle interaction is a combination of the two relaxation processes of viscous drag and heat conduction. In doing so, their theory agreed well with experimental data of Zink and Delsasso (1958). Morfey (1968) greatly extended the Temkin-Dobbins' (1966) theory by using their approach while including a third relaxational process resulting from the particle being compressible. Morfey's theory of sound attenuation by small particles in a fluid is now explained in some detail as it appears to be the most general particulate relaxation process developed to date that can have any applicability to aqueous solutions of globular proteins at their isoelectric point.

Assuming the acoustical wave is propagated in a very dilute solution of small ($ka << 1$) particles, the complex wave number is given by (Morfey, 1968)

$$k^* = \frac{\omega}{c_o} + \frac{\omega\phi}{2c_o}[E + \beta^2 B - h(1-\varepsilon)D] \qquad (2\text{-}85)$$

where the absorption coefficient is the imaginary part of k^*. In evaluating (2-85), the following definitions are necessary, noting the subscripts (0) and (1) refer to the fluid and particle, respectively:

a	particle radius
c	sound velocity
c_p	specific heat--constant pressure
k	thermal conductivity
m_o	mass of individual particle
m_1	mass of fluid displaced by particle

M molecular weight

N_A Avogadro's number

T absolute temperature

α absorption coefficient

γ ratio of specific heats

δ ratio of densities (ρ_1/ρ_o)

η coefficient of shear viscosity

ρ density

σ surface tension (assumed = 0)

ϕ volume fraction

ω radian frequency

τ_b bulk relaxation term

τ_c heat-conduction relaxation time

τ_d dynamic relaxation time

where

$$\beta = \rho_o c_o / \rho_1 c_1 \tag{2-85a}$$

$$h = \left[\frac{(\gamma_o - 1)T}{c_{p_o}} \right]^{1/2} \rho_o c_o \tag{2-85b}$$

$$\varepsilon = \frac{\rho_o c_o}{\rho_1 c_1} \sqrt{\frac{\gamma_1 - 1}{\gamma_o - 1}} \tag{2-85c}$$

$$y_o = \sqrt{\frac{\omega a^2 \rho_o}{2\eta_o}} = \sqrt{\frac{9}{4} \frac{\omega \tau_d}{\delta}} \tag{2-85d}$$

$$\tau_b = \frac{4}{3} \frac{\eta_o}{\rho_1 c_1^2} \tag{2-85e}$$

$$\tau_c = \frac{m_1 c_{p_1}}{4\pi k_o a} \tag{2-85f}$$

$$g' = \frac{2}{3}\frac{\sigma}{\rho_1 c_1^2 a} + \frac{1}{3\delta}\left(\frac{\omega a}{c_1}\right)^2 \tag{2-85g}$$

$$J = (1-j\omega\tau_c) - (\gamma_1 - j\omega\tau_c)(g'+j\omega\tau_b) \tag{2-85h}$$

and the complex parameters E, B and D are given by

$$E = \frac{\frac{3}{2}y_o^2 + \frac{9}{4}y_o + j\frac{9}{4}(1+y_o)}{(\delta+1/2)y_o^2 + \frac{9}{4}y_o + j\frac{9}{4}(1+y_o)} \tag{2-85i}$$

$$B = \frac{[\varepsilon(1+j\omega\tau_c) - (\gamma_1-1)(g'+j\omega\tau_b)]}{J\beta}\sqrt{\frac{\gamma_o-1}{\gamma_1-1}\cdot\frac{c_{p_1}}{c_{p_o}}} \tag{2-85j}$$

$$D = \frac{1-g'-\varepsilon-j\omega\tau_b}{J}\cdot\frac{c_{p_1}}{\rho_o c_o}\cdot\sqrt{\frac{\gamma_o-1}{Tc_{p_o}}} \tag{2-85k}$$

Substituting (2-85a) - (2-85h) into (2-85i, j, k) and then into (2-85) yields in the form of (2-65) the ultrasonic absorption parameter A_M, after Morfey (1968)

$$A_M = \frac{\alpha_M}{cf^2} = \frac{8\pi^3 a^3 N_A}{c_o\omega}\left[\mathrm{Im}(E) + \beta^2\,\mathrm{Im}(b) - h(1-\varepsilon)\,\mathrm{Im}(D)\right] . \tag{2-86}$$

The theories representing ultrasonic absorption mechanisms presented in this chapter will be evaluated and compared to the experimental data in the following chapters.

CHAPTER 3 MEASURING TECHNIQUE

Pellam and Galt (1946) and Pinkerton (1947, 1949a, 1949b) were among the first to apply electronic pulse-circuit techniques, which were developed as a result of World War II radar technology, to ultrasonic measurements of absorption and velocity in fluid media. Before this time, continuous wave techniques were used exclusively. The pulse method is presently the most widely used technique for making such measurements in both liquids and solids.

Pellam and Galt's (1946) system consisted of a single piezoelectric transducer plus an acoustic reflector, with the distance between the two variable. The two surfaces were aligned such as to be coaxially parallel. Ultrasonic absorption measurements were performed by recording the attenuation change in the electronic circuity necessary to compensate for the increase or decrease in the received acoustic signal as a function of the path length over which the acoustic pulse traversed. Sound velocity was measured by recording the time necessary for the pulse to traverse a known distance.

Two principle advantages of this pulse technique for ultrasonic measurements over continuous wave method are the elimination of standing waves and the minimization of localized heating effects (Herzfeld and Litovitz, 1959). To utilize the pulse technique, a sinusoidal signal of the desired frequency, and modulated by a square wave to yield an rf pulse, is impressed across a piezoelectric transducer (an X-cut quartz plate or cast piezoelectric ceramic material such as barium titinate). The carrier frequency is selected to be the fundamental or an odd multiple harmonic of the fundamental thickness mode of vibration of the piezoelectric element. For a piezoelectric thickness mode transducer, the amplitude of the applied

sinusoidal voltage is directly proportional to the acoustic pressure amplitude at the surface of the transducer as long as infinitisimal wave approximations are applied. After the pulse of acoustic energy is received by a second transducer, whose resonant frequency is matched to the transmitting transducer, or reflected back to the transmitting transducer, the signal is then processed electronically in such a way as to yield the desired information.

The received signal is amplified and detected yielding the envelope of the pulse (video signal), the peak of which is directly proportional to the received acoustic pressure amplitude. Assuming that the absorption behavior of the fluid is exponential in nature, the relationship between the acoustic pressure amplitude and the attenuation coefficient is

$$p = p_o e^{-\alpha x} \tag{3-1}$$

where p_o is the pressure amplitude at $x = 0$, and x is the acoustic path length over which the pulse travels. By detecting the peak amplitude of the video signal, taking the logarithm of this dc signal and recording it as a function of acoustic path length, x, yields a straight line whose slope is proportional to the attenuation coefficient. After all the transients have decayed from this pulse, the process is repeated, which typically allows for a repetition rate of about 200 pps.

3.1 High Frequency System

Two basic systems are utilized in this work (Hawley, 1966; Kessler, 1968a; Kessler et al., 1970). The high frequency system, shown in Fig. 3-1, is an automated version of that of Pellam and Galt (1946), which utilizes both a transmitting and a receiving transducer. The lower frequency limit

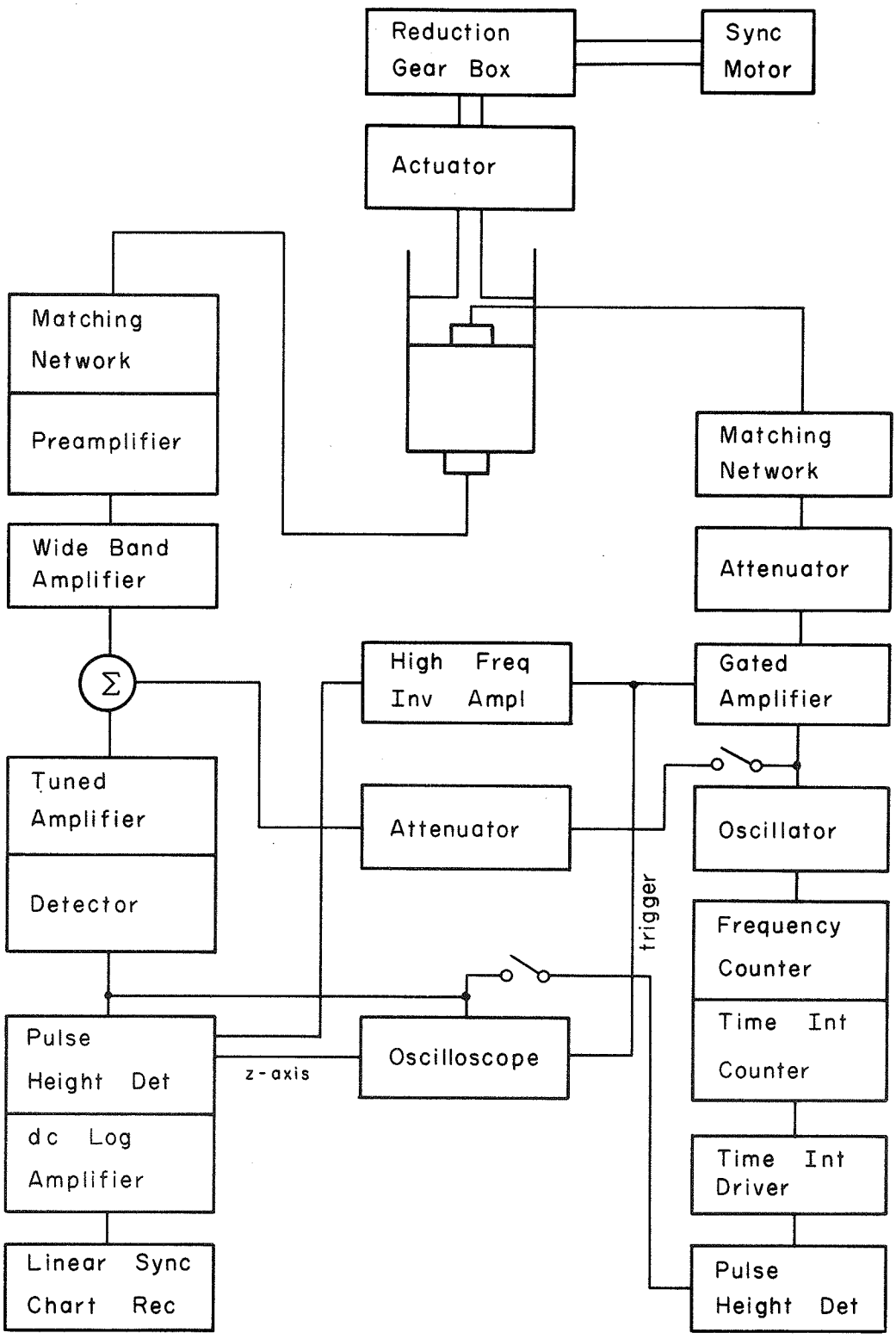

FIGURE 3-1

BLOCK DIAGRAM OF HIGH FREQUENCY ELECTRONIC SYSTEM
(SWITCHES OPEN FOR ABSORPTION AND CLOSED FOR VELOCITY)

of this system is approximately 5 MHz since the apparent attenuation due to diffraction effects, to be discussed later, become appreciable below this point. The upper frequency limit, around 200 MHz, depends upon the parallelism requirement between the two coaxially aligned transducers (Hawley, 1966), although the upper frequency limit in this study is around 50 MHz.

3.1.1 High Frequency Mechanical

This system consists of two matched sets of air-backed, 1 in. diameter, X-cut quartz piezoelectric transducers with fundamental thickness modes of vibration of 1 and 3 MHz. The lower receiving crystal is fixed to the bottom of a cylinder while the transmitting transducer is assembled onto the lower portion of a movable piston arrangement which traverses vertically within the cylinder (dimensions 3.5 in. diameter and 9 in. long) and thus varies the transducer separation distance. The two transducers are coaxial and parallel, the latter requirement being the primary high frequency limiting factor. The piston is connected to a 0.5 in. diameter rod, with the coaxial cable (RG62/U) inside, which supplies the electrical rf signal to the transmitting transducer. The piston employs Teflon O-rings which function as a bearing surface, allowing the two crystal surfaces to remain parallel during transducer displacement. All surfaces of the cylinder-piston arrangement which make contact with the liquid under investigation are stainless steel 316, save for the transducer surfaces which are gold plated.

The stainless steel rod is driven by a linear actuator unit (Duff-Norton Ball Screw Jactuator) via a one inch diameter threaded (4/inch) drill rod. The actuator transforms rotatory motion into linear displacement, viz., every 96 turns of the input shaft translates the piston one inch. The input

shaft is driven by a Bodine 1/25 horsepower, synchronous, reversible motor through an Apcor multiratio speed reducer allowing reduction ratios from 1:1 to 200:1 in 10 increments. The internal gearing of the 1800 rpm motor results in an output of 180 rpm into the reducing gear box, yielding, through proper reduction ratios, a linear velocity of the piston from 0.0793750 cm/sec to 0.000396875 cm/sec.

3.1.2 High Frequency Thermal

The cylinder is surrounded by an annular space which allows for circulation of an appropriate temperature controlling fluid, viz., water. See Fig. 3-2. This fluid is pumped (Jabsco self-priming pump, 1/8 horsepower motor) from a 15 liter, temperature controlled reservoir, through the chamber jacket and returned. The thermal regulation of the reservoir is maintained at the desired temperature by the balancing between a cooler and a heater. The former is cold fluid from a Tesumsah model F34-2JG refrigeration unit which is being circulated through 0.5 in. copper tubing which is coiled inside the perimeter of the reservoir and functions as a heat exchanger. The temperature of the fluid from the refrigeration unit is adjustable but usually remains fixed during constant temperature experimentation. The heater, a 1000 watt immersible heater controlled by a Yellow Spring Model 72 Proportional Temperature Controller, accomplishes the fine adjustment of the temperature. This controller senses the reservoir temperature by way of an immersed thermistor.

To achieve temperatures of the fluid under investigation below room temperature, say 10°C, the cold fluid being circulated through the heat exchanger is set at approximately 7°C. The proportional controller then functions as the only control of the reservoir temperature by regulating

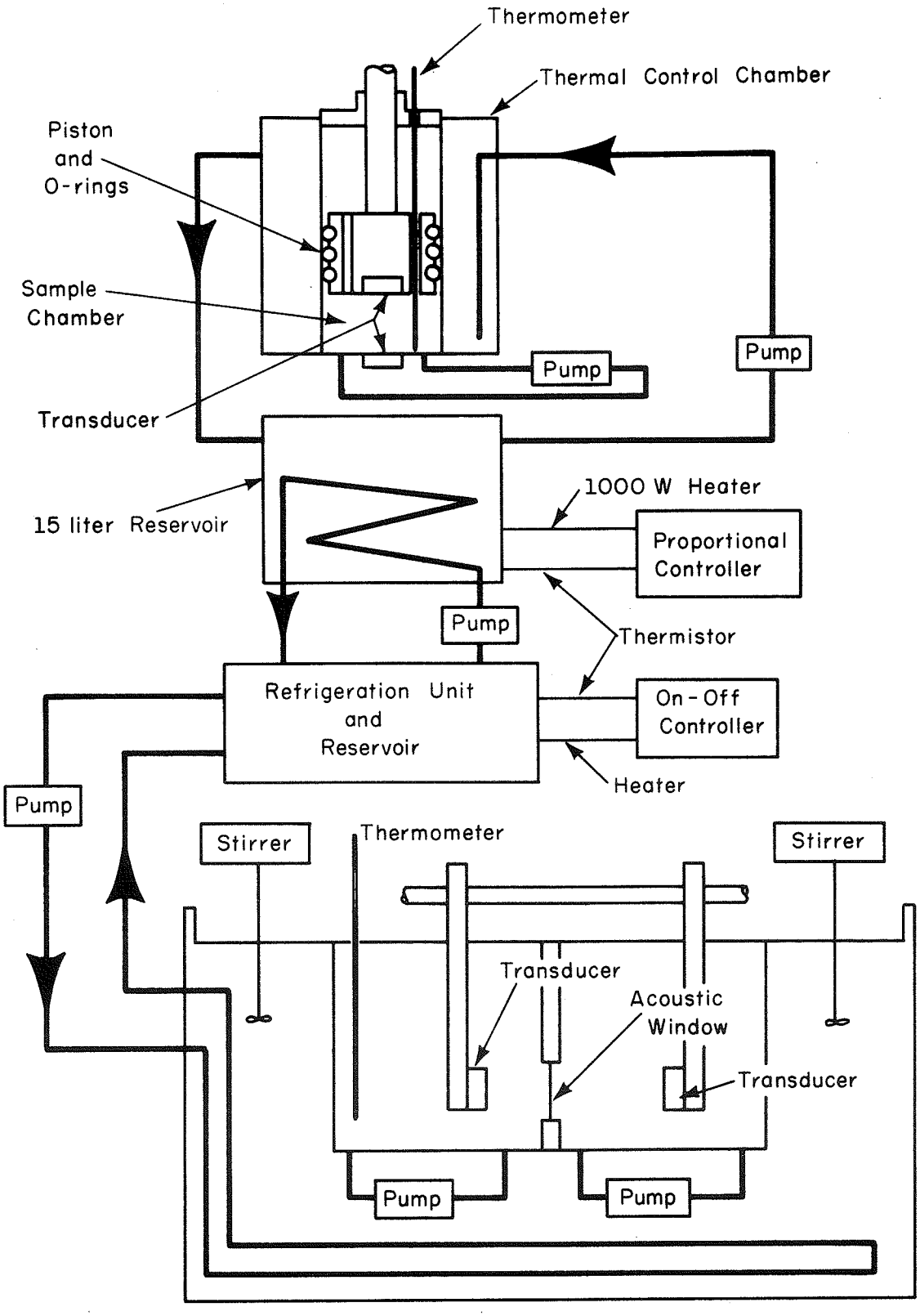

FIGURE 3-2

BLOCK DIAGRAM OF THERMAL CONTROL SYSTEM
FOR BOTH HIGH AND LOW FREQUENCY SYSTEM

the voltage being applied to the heater. The final temperature measurement of the unknown fluid is obtained from a thermometer immersed, through a hole in the cover plate of the cylinder, directly into the measuring chamber, which is done immediately prior to the ultrasonic measurement. When measurements are to be performed above room temperature, the cooling unit is disconnected and the ambient environment then provides the cooling balance. The system is capable of maintaining the temperature of the liquid under investigation to within $\pm$ 0.01°C. The temperature accuracy, as checked against a National Bureau of Standards calibrated thermometer, is within $\pm$ 0.05°C.

Finally, in order to avoid any thermal (and also concentration) gradients which might develop within the sample chamber, the liquid is continuously pumped through a total submersion, nylon head, variable speed, centrifugal type pump connected to a Variac, which allows a variable flow rate. Since the pump is external to the measuring cylinder, heating effects of the liquid result when the temperature of operation is much below room temperature. This problem is avoided by immersing the pump in water which is maintained at approximately the same temperature as that of the reservoir.

3.1.3 High Frequency Technique

The minimum volume of fluid needed for investigation is typically 650 ml, although the chamber will accommodate up to one liter. At the lowest operating frequency (5 MHz), the piston separation is the greatest, extending from about 2 cm to 7 cm, this still being well within the Fresnel zone of the acoustic wave ($a^2/\lambda = 54$ cm, c = 1500 m/s). The acoustic field is assumed to be of the free-field form, that is, radiation of the acoustic energy into a semi-infinite, half space, so that corrections for the apparent attenuation due to free-field diffraction can be made (Del Grosso, 1964).

The diffraction correction is discussed in more detail below. The effects due to guided mode (dispersion) effects can be ignored since the cylinder bore-to-transducer diameter ratio is greater than two (Del Grosso, 1965).

The transmitted pulse is formed by applying the continuous wave output of the Measurements Corporation Model 80-R Standard Signal Generator, which has a frequency range from 5 to 475 MHz, to the Arenberg PG650C pulsed oscillator operating in the gated amplifier mode, which gates the input signal to the desired duration and repetition rate, as is shown in Fig. 3-1. The frequency of the signal generator is continuously monitored by the Systron Donner Frequency Counter, model 1037, capable of direct frequency measurements up to 50 MHz and period measurements with a resolution of 0.1μ seconds. The plug-in model 1291, a heterodyne converter, extends the frequency range to 500 MHz. The output of the gated amplifier is fed through a 93 Ω attenuator (Arenberg Ultrasonic Laboratory) and impedance matched to the quartz crystal by an L-type network (Everitt and Anner, 1956).

The low level received signal is preamplified by the Arulab Preamplifier model PA-620-L and further amplified by the Hewlett Packard model 460A variable gain (0-20 dB) wide band amplifier, and finally amplified by the Matec tuned amplifier and detector model PR201, which contains a variable gain tuned amplifier from 8 to 380 MHz and a broad banded external receiver from 1-10 MHz. The video output is fed into the Matec Pulse Amplitude Monitor model 1235A which temporally selects a single pulse within an echo train and peak detects it. The dc voltage which results from the detection process is compared differentially to an internal reference voltage, resulting in a linear decibel output signal. The detected pulse is observed on the Tektronix type 453, dc to 50 MHz oscilloscope by intensity modulating it through the Z-axis. The oscilloscope will accept the negative triggering

pulse from the pulsed oscillator. However, a high frequency inverting amplifier (Nexus Operational Amplifier FSL-6) is necessary to supply the desired positive trigger to the Pulse Amplitude Monitor. The monitor's output dc signal is fed into the Sergent Recorder model SRL whose full scale deflection is set, by a range plug-in, to 10 mv. Thus the full scale chart recorder displacement is 1, 2, 5, 10, or 20 dB, which is determined from the Pulse Amplitude Monitor's range switch. As the transducer separation increases (or decreases) at a constant velocity, the processed dc signal which is applied to the chart recorder decreases (or increases) in amplitude as a function of time (10 inches per minute), yielding a straight line, the slope being proportional to the measured ultrasonic absorption of the liquid under investigation. Line voltage and/or frequency fluctuations are unimportant in absorption measurements as both the motor which drives the piston and the one which controls the chart recorder speed are synchronous.

The algebraic addition of a continuous wave reference signal, from the signal generator, at the input of the Matec tuned amplifier will produce a null (or peak) when both signals, of equal amplitude, are out of (or in) phase. However, when both signals are not of the same amplitude (in this case the reference signal is of lesser amplitude), the resultant video output will vary in amplitude as the two signals change their phase orientation. Thus, as the transducers move at a constant velocity, the peak amplitude of the video signal behaves as a full wave rectified sinusoidal, the period of the wave representing one acoustic wavelength, λ, in the liquid under investigation. If the rate at which the piston is moving is given by r_p, the acoustic period is then $T = \lambda/r_p$. By recording this time, the velocity of sound, c, within the unknown liquid is given by

$$c = T f r_p \qquad (3\text{-}2)$$

In practice T is averaged over 100 periods by feeding the video pulse into a pulse height detector and its output being processed by the time interval driver. The full wave rectified waveform from the pulse height detector is differentiated, zero detected resulting in a square wave of period T and finally passing through a pulse chaper yielding a pulse every time the pulse height detected signal passes through a minimum, which is every λ/r_p sec. These pulses are then fed into the Systron Donnor Time Interval Counter plug-in model 1926A which records the time it takes for the piston to travel 100 acoustic wavelengths by opening and closing the gate at the first and hundred and first pulse, respectively. By averaging in this way, short range variations in the piston velocity and stray noise effects are minimized (Kessler, 1968a; Kessler et al., 1970). A separate frequency counter is essential if fluctuations of the line frequency are known to occur so that the proper piston speed compensation is achieved.

3.2 Low Frequency System

Measurements at frequencies below 5 MHz in the modified Pellam and Galt (1946) system are impractical for the liquids under investigation in this study since the apparent attenuation due to diffraction becomes appreciable. Therefore a comparison technique, initially described by Schwan and Carstensen (1952), and later discussed in the use of absorption (Carstensen et al., 1953) and velocity (Carstensen, 1954) measurements, is used which minimizes the difficulties due to diffraction effects. It will be seen in the section on diffraction that if the velocities of the two media being compared are the same, the apparent attenuation due to diffraction

could be eliminated since the acoustic path length remains constant. This low frequency system is capable of measuring ultrasonic absorption and velocity over the frequency range 0.30-20 MHz.

3.2.1 Low Frequency Mechanical

In this system, the experimental vessel, fabricated from type 304 stainless steel, is divided into two chambers, separated by an acoustic window (stretched 0.003 in. polyethylene). See Fig. 3-3. One chamber contains a dispersionless reference liquid, viz., singly deionized and distilled water, for which its ultrasonic properties have been adequately characterized (Pinkerton, 1949a; Greenspan and Tschiegg, 1959) so that comparisons can be made with the liquid under investigation in the other chamber. Two different size experimental vessels were utilized. The chambers of the large vessel are each 7 in. long, 6 in. wide and has a volume of 4 liters. Its acoustic window is 5 in. in diameter. The smaller vessel's chambers contain one-fourth the volume, 1 liter, with dimensions 7 in. long and 3 in. wide with a 2.5 in. acoustic window diameter. Generally the smaller vessel was used in this study to minimize the volume needed to investigate the biopolymer aqueous solution. However, the larger vessel was used when less expensive, bulk materials were investigated. One difficulty which arises from the smaller vessel is that the so called chamber-to-transducer diameter ratio becomes less than 2 and guided mode effects (Del Grosso, 1965) are possible. However, comparisons between the identical solution in both tanks have indicated no differences in the ultrasonic absorption coefficient. In addition, diffraction effects increase with the smaller vessel, as compared to the larger one, simply because the transducer radius is smaller and this limits the lowest frequency that can be investigated.

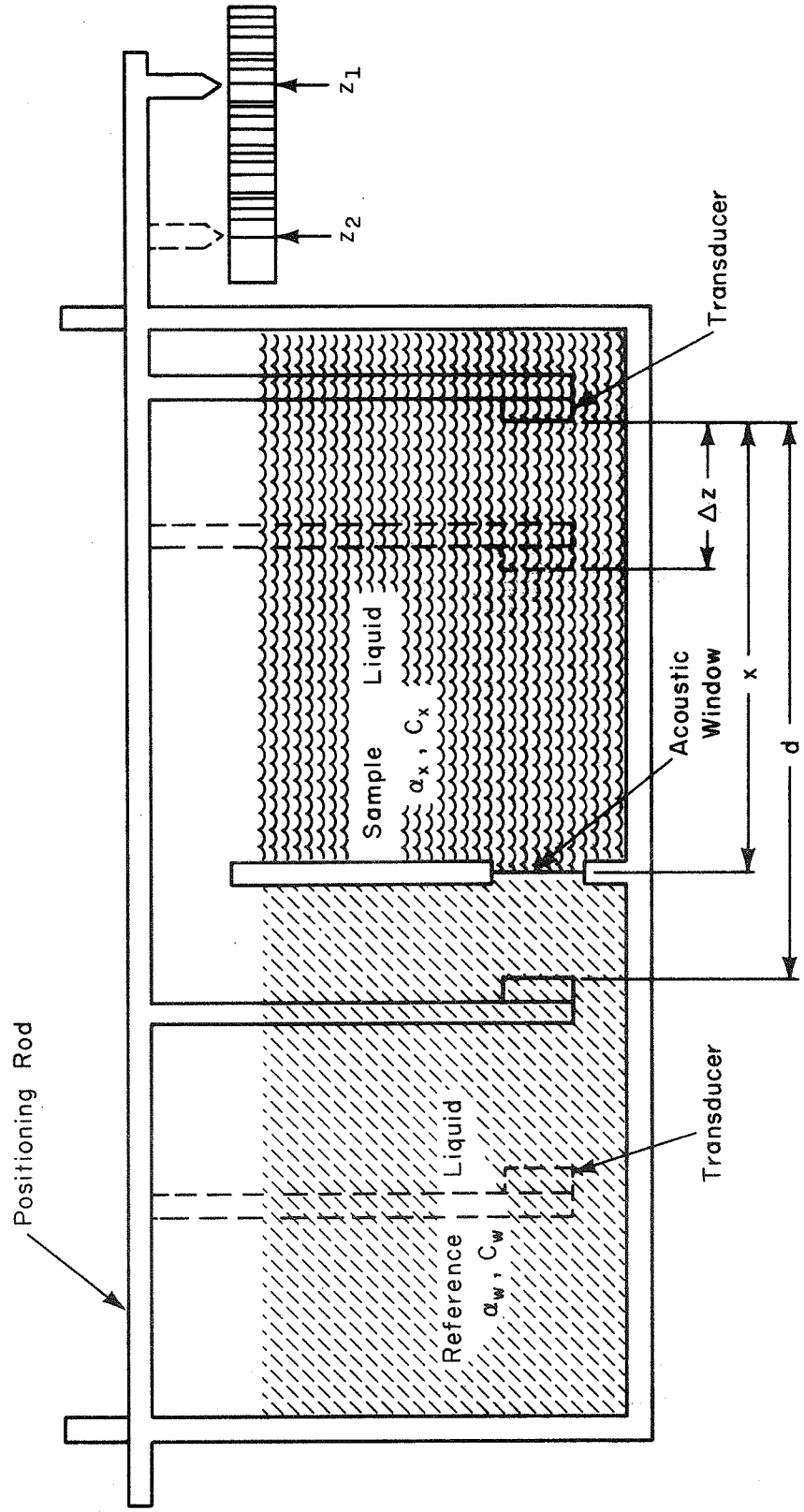

FIGURE 3-3

SCHEMATIC DIAGRAM OF LOW FREQUENCY MEASURING VESSEL

For example, with a transducer separation around 12 cm, at 1 MHz (c = 1500 m/s in both chambers), a^2/λ = 27 cm for the smaller chamber transducers while a^2/λ = 96 cm with the larger set up.

Two matched sets of air-backed, piezoelectric transducers (lead zirconate-lead titinate ceramic discs) are employed with the low frequency system. In conjunction with the larger vessel, 3 in. diameter transducers with a fundamental frequency thickness mode of 0.35 MHz are used, whereas 1 5/8 in. diameter, 0.56 MHz fundamental frequency transducers are employed with the smaller vessel. The transducers are mounted on a movable assembly by way of adjustment mechanisms, which are used to align the transducers coaxially parallel. The transducers are mounted on the horizontally traversing assembly in such a way that each is in one of the chambers, and the mechanical distance between the transducer surfaces always remaining fixed. The movable assembly is mounted on two precision tracking rods by precision fitted linear motion ball bushings. The lateral displacement is provided by a positioning rod, which is connected to the half inch diameter threaded (4/inch) drill rod of a linear actuator unit (Duff-Norton Ball Screw Miniature Jactuator) which translates rotatory (20 revolutions) into linear (one inch) motion. The input to this actuator is identical with that of the high frequency mechanical system. Thus, the speed at which the movable carriage translates is adjustable from 0.3810 cm/sec to 0.001905 cm/sec in 10 increments.

The acoustic window is three thousandths inch polyethylene sheet stretched to half thickness. Sealing of the 0.0015 in. acoustic window between the two chambers, which disassemble, is accomplished with neoprene gaskets. Major considerations of the type of material used for the acoustic window are: (1) it must be chemically inert to the fluids placed within the test chambers and (2) it must form a stiff planar membrane separating

the two liquids so that it does not function as an acoustic lens.

3.2.2 Low Frequency Thermal

The double chambered measuring vessel is supported by two brass bars in such a way as to be almost entirely submersed in a temperature regulated, circulating water bath. The regulation of this bath results from thermally controlled liquid being passed through 0.5 in. copper tubing, which completely lines two opposite sides of the bath and functions as a heat exchanger. The water within the bath is circulated through the heat exchanger and around the vessel by two three-bladed paddles connected to constant speed (1550 RPM) stirrer motors. The fluid which flows through the copper tubing originates in a 15 liter reservoir, the fluid being a solution of propylene glycol and water. The thermal control of this fluid originates at the Yellow Spring Thermistemp Temperature Controller model 71 (on-off type) which alternately turns on either the refrigeration unit to cool the 15 liter reservoir or the 450 watt knife-blade heater, depending upon whether the thermistor probe senses the reservoir fluid to be too warm or too cool, respectively. The thermal regulation of the liquids in each of the measuring chambers is equivalent to that for the high frequency system, viz., $\pm$ 0.01°C. The thermometer is placed within each of the chambers at the time the ultrasonic measurements are performed to measure the actual temperature of the fluid. The fluid within the chambers is circulated so as to eliminate concentration and thermal gradients.

3.2.3 Low Frequency Technique

Consider the transducer carriage of the low frequency comparison system in such a position so that the minority of the acoustic path traverses through

the reference liquid with an absorption coefficient α_w, this position denoted as 1. In this position, the distance, in the sample liquid, from the transducer surface to the acoustic window, assumed to be lossless, is X, and the remainder of the distance to the other transducer, located in the reference liquid, is d-Z. See Fig. 3-3. With the transmitting transducer immersed in the reference liquid, the second transducer receives a signal with the carriage in position 1 given by

$$p_1 = P_o e^{-\alpha_w (d-x)} e^{-\alpha_x X} \tag{3-3}$$

where P_o and p_1 are the acoustic pressure amplitudes at the surfaces of the transmitting and receiving transducers, respectively, and α_x is the ultrasonic absorption coefficient of the liquid under investigation. If the transducer carriage traverses a distance ΔZ, in the direction of the reference liquid, to position 2, the received acoustic pressure amplitude is then

$$p_2 = P_o e^{-\alpha_w (d-x+\Delta Z)} e^{-\alpha_x (X-\Delta Z)} . \tag{3-4}$$

As a result of the two liquids possessing unlike acoustic impedances (product of the liquid density times the sound speed), the acoustic energy which is incident normally onto the window will be partially reflected. However, since the reflection factor for the impedance discontinuity is a constant, besides being relatively small, the reflected energy will not affect the measurement. Taking the ratio of (3-4) to (3-3) yields

$$p_2 = p_1 e^{(\alpha_x - \alpha_w)\Delta Z} . \tag{3-5}$$

Thus, as the transducer carriage moves horizontally, the received ultrasonic pressure amplitude varies as a function of the difference in the ultrasonic absorption coefficients between the two liquids. To measure this difference (see Fig. 3-4) the electronic setup used is similar to that of the high frequency measuring system for frequencies greater than 5 MHz. For lesser frequencies, the Hewlett-Packard Test Oscillator model 650A (10 Hz to 10 MHz) is used to produce the carrier frequency of the transmitting pulse. Due to the low-frequency limitations of the amplifying equipment of the high frequency setup below 5 MHz, the signal received by the transducer is L-matched to the Arenberg Wideband Amplifier and Video Detector model WA-600-D. The video signal output from the Arenberg is then processed as described previously.

Figure 3-4a shows a modified electronic setup for the processing of the received acoustic signal, described in more detail by Christman (1970). This arrangement was utilized in the latter phases of the experimental work with the low frequency system, although it could also be applied to the high frequency system. Essentially, the Hewlett Packard Spectrum Analyzer 8553L/8552A functions as both tuned amplifier and detector, the output being taken from the Analyzer's vertical output. This 0-100 MHz Spectrum Analyzer is operated in the fixed frequency, linear mode with a 300 KHz bandwidth. In order to apply the proper signal to the pulse amplitude monitor, the Spectrum Analyzer's output is fed through a unity gain operational amplifier. The remainder of the system is the same as in Fig. 3-4.

Carstensen (1954) originally developed this system as an accurate method for direct measurement of the absolute sound velocity difference between two liquids, as a function of frequency. The reference liquid for

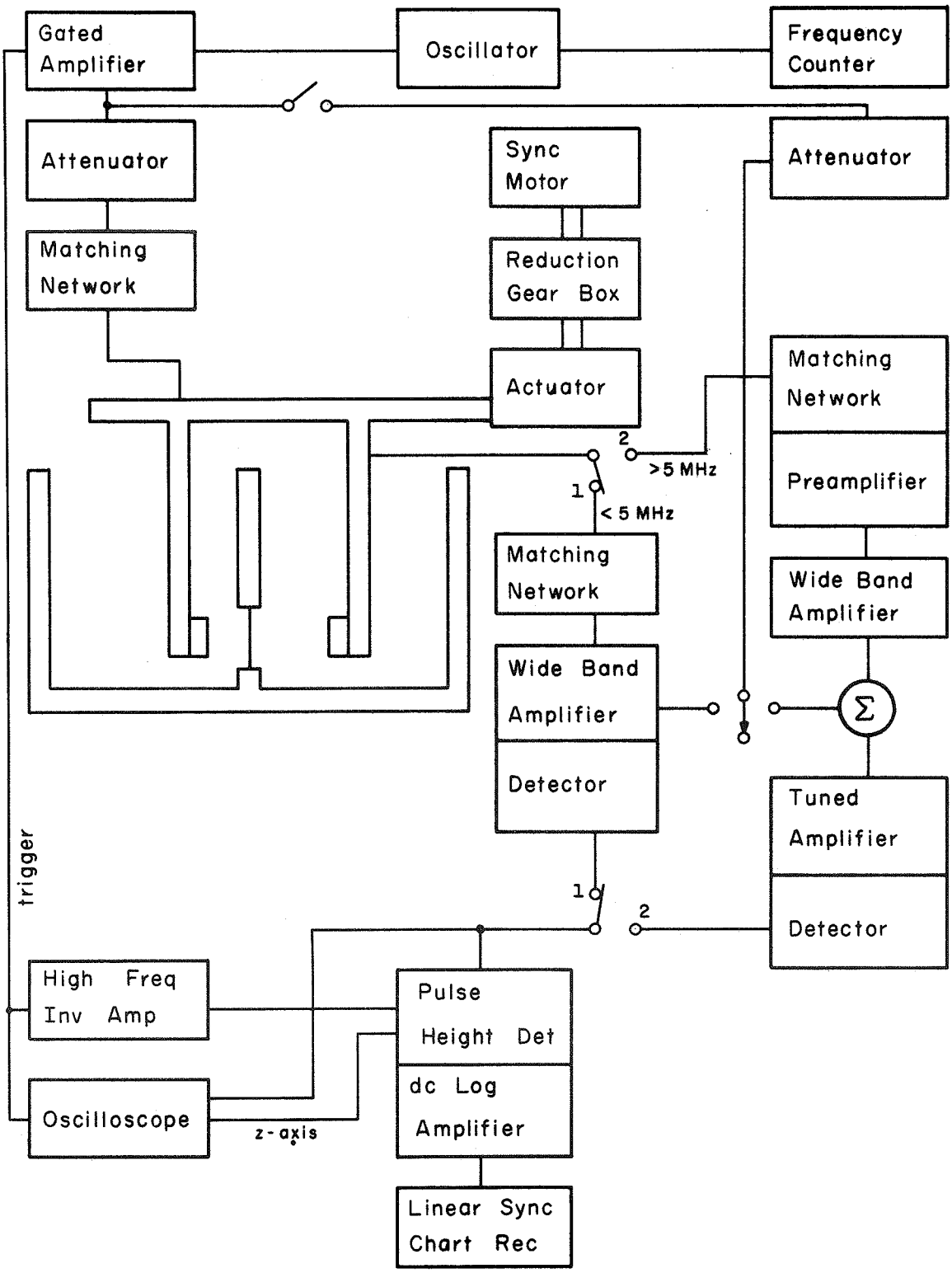

FIGURE 3-4

BLOCK DIAGRAM OF LOW FREQUENCY ELECTRONIC SYSTEM

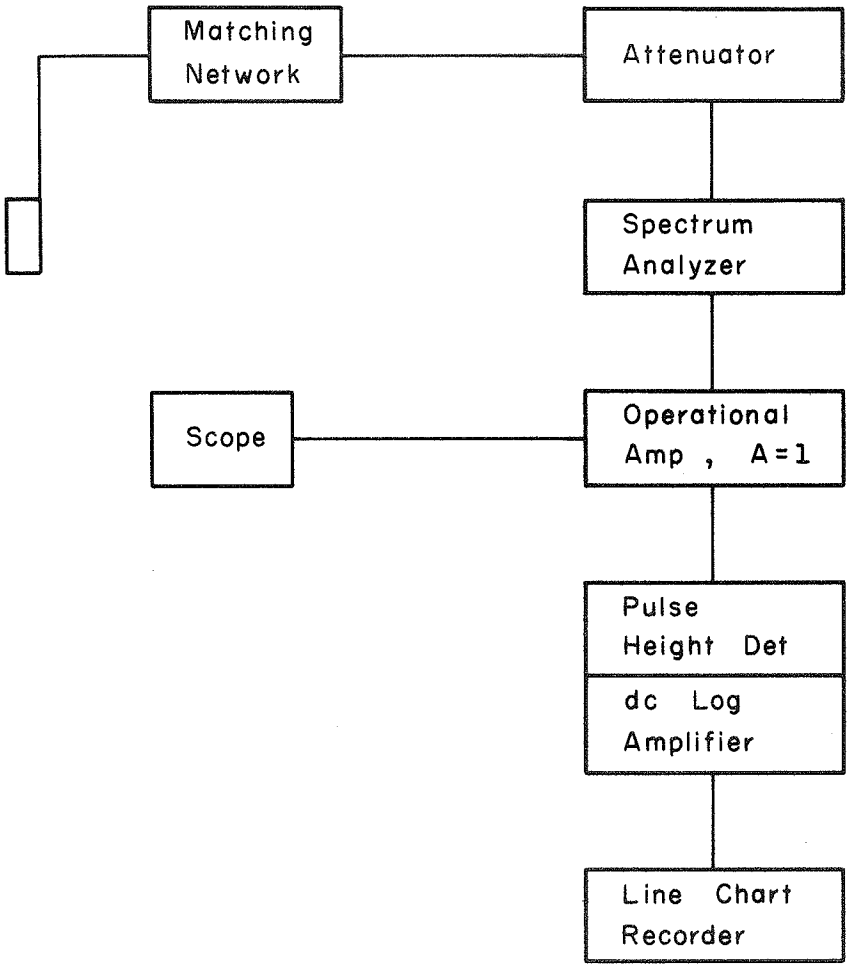

FIGURE 3-4a

BLOCK DIAGRAM OF MODIFIED RECEIVER SECTION
FOR LOW FREQUENCY ELECTRONIC SYSTEM

velocity measurements is also water, as in the absorption measurements, since it is dispersionless with its values of sound velocity known with considerable accuracy (Greenspan and Tschiegg, 1959). Depending upon the frequency of operation (i.e., greater than or less than 5 MHz), the continuous wave reference signal is added at the input to the Matec tuned amplifier or into a stage of the distributed amplfier of the Arenberg wideband amplifier. See Fig. 3-4. When the received and reference signals are of the same amplitude and out of phase at the adder junction, a null is observed on the oscilloscope. As the transducer assembly is moved along the axis of the measuring vessel, the acoustic path length will vary, provided the velocity of the liquid under investigation is different (usually greater) from that of the reference liquid. The phase of the received signal is dependent upon n, the number of acoustic wavelengths separating the two transducers. By changing the acoustic pathlength an integral number, m, of wavelengths, the absolute velocity difference can be determined. Using the notation of Fig. 3-3,

$$n = \frac{d-x}{\lambda_w} + \frac{x}{\lambda_x} \quad \text{(Position 1)} \tag{3-6}$$

where λ_w and λ_x are, respectively, the sound wavelengths in the reference (water) and the unknown liquid. Translating the carriage m number of 360° phase shifts, which results in a mechanical displacement of ΔZ, the acoustic pathlength is altered to

$$n \pm m = \frac{d-x+\Delta Z}{\lambda_w} + \frac{x-\Delta Z}{\lambda_x}. \quad \text{(Position 2)} \tag{3-7}$$

Eliminating n between (3-6) and (3-7), and rearranging the terms, yields

$$c_x = \frac{c_w}{1 \mp \frac{c_w M}{f\Delta Z}} \quad (3\text{-}8)$$

The number of 360° phase shifts is determined by observing the null pattern on the oscilloscope, and ΔZ is obtained with a Gaertner model M303 micrometer slide with a traveling microscope, which is mounted in such a way as to measure the carraige displacement directly to 10 microns. A separate procedure, however, must sometimes be performed if the sound velocity of liquid under examination is not known to be greater or less than that of the reference liquid as this technique yields only the absolute sound velocity difference.

3.3 Diffraction

Carstensen and his colleagues (1952, 1953, 1954) developed and described the comparison technique for obtaining ultrasonic absorption and dispersion measurements so as to minimize, or avoid completely, the irregular behavior of the acoustic near field. This effect, diffraction is defined as any change of rectilinear wave paths which cannot be explained by reflection or refraction (Goodman, 1968). Diffraction effects occur whenever waves are disrupted by an opaque object.

Free-field diffraction effects, which are considered in this study, result in an apparent attenuation with ultrasonic absorption measurements (Pinkerton, 1949b; Seki *et al.*, 1956) and an apparent increase in velocity (McSkimin, 1960). Figure 3-5 shows the decibel loss of acoustic energy and the phase advance due solely to diffraction as a function of normalized distance from the circular transducer of radius a, expressed in units of a^2/λ, λ being the acoustic wavelength (Papadakis, 1966). The distance

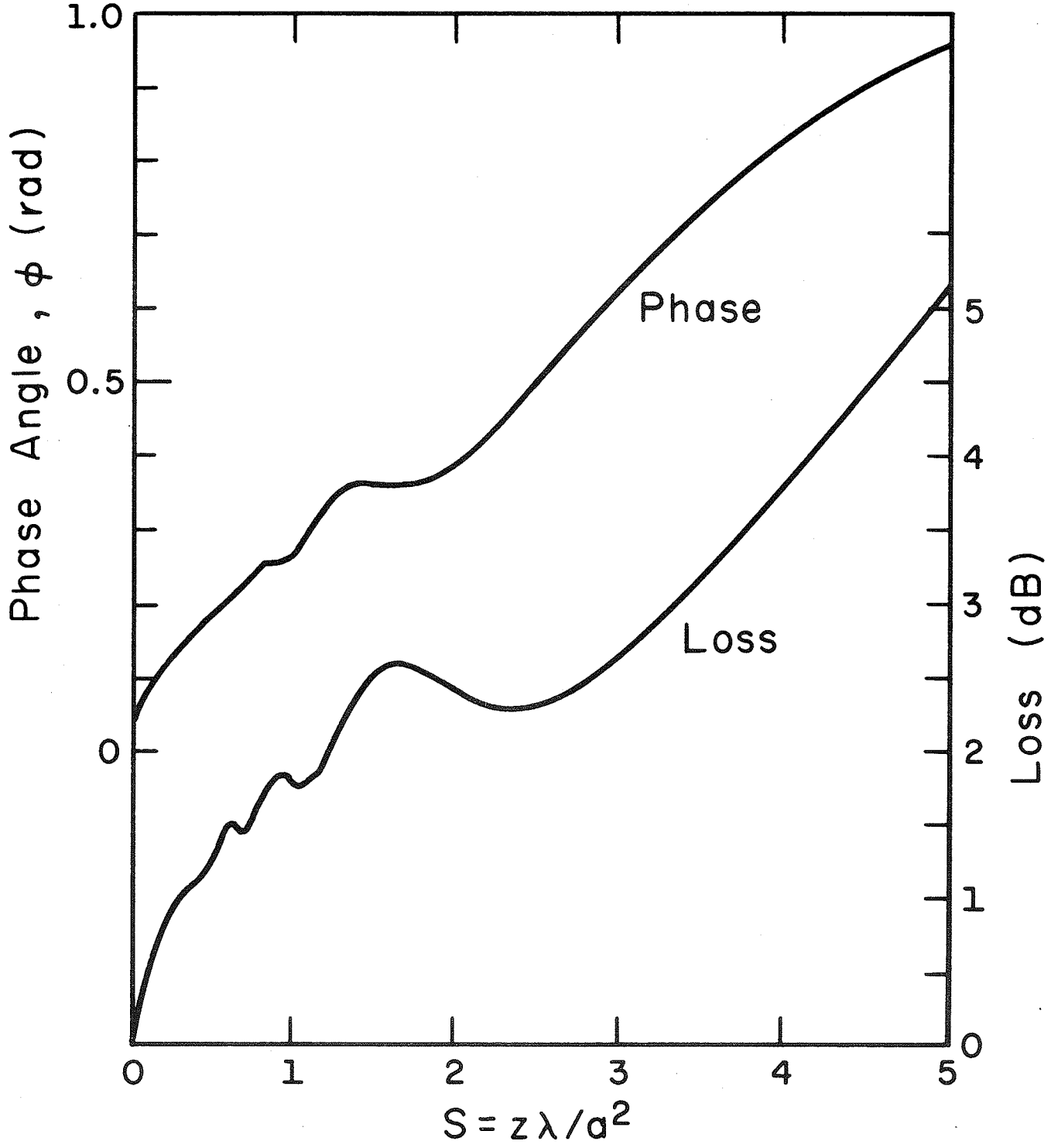

FIGURE 3-5

RELATIONSHIP BETWEEN THE PHASE ADVANCE AND THE LOSS IN THE FIELD OF A CIRCULAR PISTON SOURCE (Papadakis, 1966)

a^2/λ from the circular transducer is the point at which the last maximum occurs in the axial intensity plot. For distances greater than a^2/λ, the sound field is, to a reasonable approximation, spherically divergent, this region being known as the far or Fraunhoffer region whereas, for lesser distances from the source, the near or Fresnel region, the sound field is considered to be confined to the geometry of a cylinder of radius a (Kinsler and Frey, 1962). Seki et al. (1956) have also shown a similar plot, with the second dip at 1.05 a^2/λ and the third at 2.40 a^2/λ. Beyond the third dip the apparent loss due to diffraction increases monotonically. However, the area of concern in this study is for $a^2/\lambda < 1$, that is, the Fresnel type of diffraction, since all of the ultrasonic measurements are made within the Fresnel region. Within this region, the loss due to diffraction behaves in an irregular manner, thus resulting in an apparent loss or gain in the ultrasonic absorption measurement, depending upon a number of factors to be discussed. See Fig. 3-6.

With the imposition of boundary conditions to the Helmholtz equation for a circular piston source radiating into a semiinfinite half space, King (1934) derived an expression for the velocity potential in cylindrical coordinates at some point (r, Z) within the acoustic field,

$$\psi = aU_o e^{j\omega t} \int_o^\infty e^{-\mu z} J_o(\lambda r) J_1(\lambda a) \frac{d\lambda}{\mu} \tag{3-9}$$

$$\mu = \sqrt{\lambda^2 - k^2} \tag{3-9a}$$

where a is the piston source radius, J_o and J_1 are Bessel functions of the first kind of orders zero and one, respectively, with the indicated argument, $U_o e^{j\omega t}$ is the harmonically varying velocity amplitude at the

piston surface and μ is a parameter which can be complex (Del Grosso, 1964; Seki et al., 1956). By considering k, the acoustic wave number, to be real in this analysis, the sole losses are those associated with diffraction effects. On the other hand, if k were assumed to be complex, then the intrinsic ultrasonic absorption coefficient of the medium under investigation could be considered. However, it is assumed that the losses due to intrinsic absorption and diffraction effects are additive so that the simpler analysis, i.e., k real, can result (Bass, 1958).

A simplification results only when the relationship between the acoustic pressure at two points within the field is desired (relative pressure) rather than absolute pressure. Therefore, by evaluating for the real and imaginary parts of the velocity potential integral, and dividing them by similar quantities but for the plane wave, relative real and imaginary velocity potentials result. Thus the average RMS acoustic pressure relative to a plane wave is given by (Del Grosso, 1964)

$$\langle p \rangle_{rel} = \sqrt{(\text{Re } \langle \psi \rangle_{rel})^2 + (\text{Im } \langle \psi \rangle_{rel})^2} \quad . \tag{3-10}$$

Del Grosso's method for correction of diffraction effects is applied to the data of this study. He obtained the second order approximation to the work of Bass (1958) for the real and imaginary parts of the relative velocity potential integral given by

$$\text{Re } \langle \psi \rangle_{rel} = 1 - \left[J_o \cos x + J_1 \sin x \right] \left[1 - \frac{y^2}{2} - \frac{y^4}{8} \right]$$

$$- J_1 \frac{\sin x}{x} \left[y^2 + \frac{y^4}{4} \right] \tag{3-11}$$

$$\text{Im } \langle\psi\rangle_{rel} = \left[J_o \sin x - J_1 \cos x\right]\left[1 - \frac{y^2}{2} - \frac{y^4}{8}\right]$$

$$- J_1 \frac{\cos x}{x}\left[y^2 + \frac{y^4}{4}\right] \qquad (3\text{-}12)$$

where

$$y = x/ka \ . \qquad (3\text{-}13)$$

The argument M of J_o and J_1 is given by

$$M = \frac{ka^2}{Z} - \frac{ka^4}{Z} \qquad (3\text{-}14)$$

and

$$x = \frac{k}{2}\left[\sqrt{Z^2 + 4a^2} - Z\right] . \qquad (3\text{-}15)$$

The values of relative pressure $\langle p\rangle_{rel}$ are tabulated (Del Grosso, 1964) for eleven values of ka from 4π to 100π as a function of normalized distance from the source, the distance a^2/λ into the acoustic field along the Z-axis being the unity value. Figure 3-6 shows plots of the average RMS pressure relative to a plane wave $\langle p\rangle_{rel}$ as a function of normalized distance $Z\lambda/a^2$ for the given ka values. Note that if the transducer separation traverses a relatively large normalized distance, the irregularities in the curves of Fig. 3-6 do not have to be considered, whereas, over short distances, the diffraction effects could appear as a gain, as opposed to a loss, in acoustic energy. As Pinkerton (1949b) observed, to minimize the contribution of diffraction effects to the observed ultrasonic absorption, (1) the transducers should be as large as possible (large ka) and (2) the intrinsic absorption coefficient per unit length should be large.

Tables 3-1 and 3-2 demonstrate the mechanics of calculating the

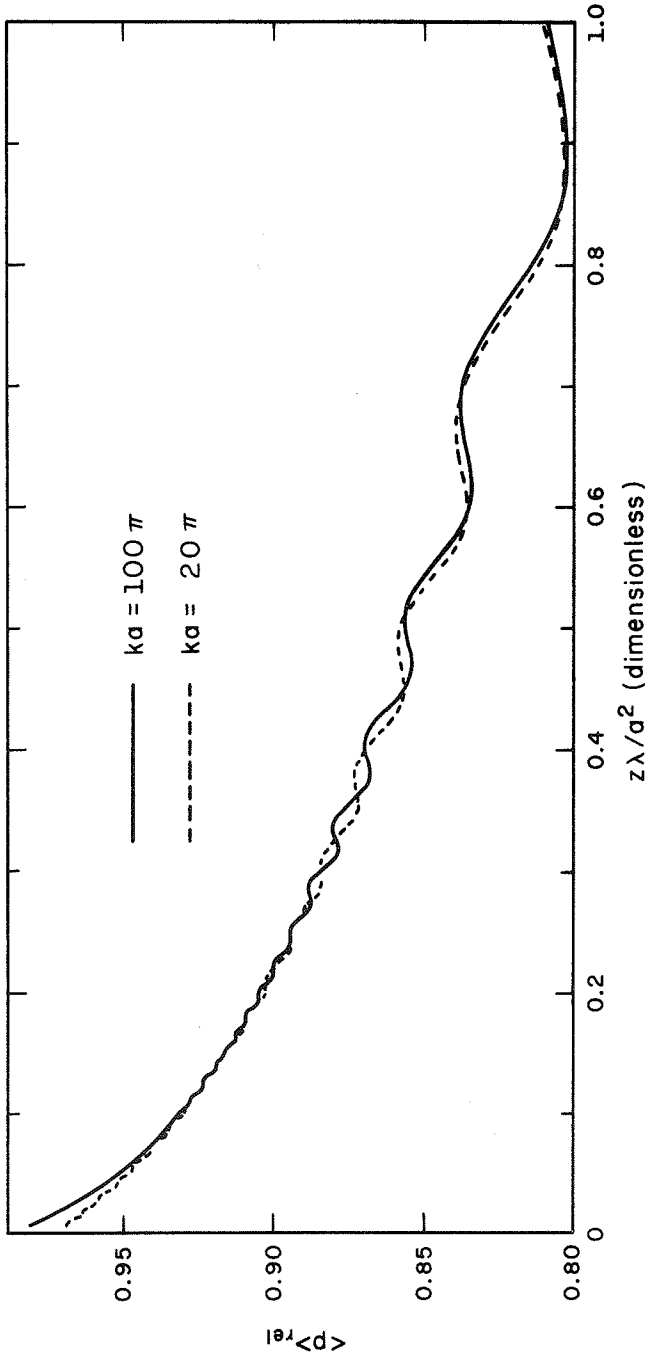

FIGURE 3-6

AVERAGE RELATIVE PRESSURE FROM A CIRCULAR PISTON SOURCE OF RADIUS a
(Del Grosso, 1964)

Table 3-1

Diffraction Correction-High Frequency System

Frequency of absorption measurement	f	10.22 MHz
Sound velocity in water at 25°C	c	0.15 cm/μsec
Wavelength	$\lambda = c/f$	0.01468 cm
Radius of transducer	a	1.27 cm
Normalized transducer radius	ka	173π
Near field length	a^2/λ	109.9 cm
Minimum transducer separation	Z_1	2.14 cm
Normalized separation	$Z_1\lambda/a^2$	0.01947
Relative acoustic pressure at Z_1 (*)	$\langle p \rangle_1$	970596
Maximum transducer separation	Z_2	6.90 cm
Normalized separation	$Z_2\lambda/a^2$	0.06278
Relative acoustic pressure at Z_2 (*)	$\langle p \rangle_2$	946628
Ratio of relative pressures	$\beta = \langle p \rangle_1/\langle p \rangle_2$	1.0253
Relative attenuation due to diffraction effect (**)	$A_D = \ell n(\beta)$	0.02497 nep
Absorption diffraction correction	$\alpha_D = A_D/Z_2-Z_1$	0.00525 nep/cm
Intrinsic absorption of water at 25°C (***)	α	0.02287 nep/cm
Percent difference due to diffraction	$\frac{\alpha_D}{\alpha}(100)$	23.2%

(*) Del Grosso (1964), Use $ka = 100\pi$

(**) Zucker (1964)

(***) Pinkerton (1949a)

Table 3-2

Diffraction Correction-Low Frequency System

Frequency of absorption measurement	f	1.691 MHz
Radius of transducer	a	2 cm
Sound velocity at 10°C		
Water (Ref.)	c_w	0.1450 cm/μsec
2% Protein solution (Unk.)	c_x	0.1470 cm/μsec
Wavelength		
Ref:	$\lambda_w = c_w/f$	0.0857 cm
Unk:	$\lambda_x = c_x/f$	0.0869 cm
Average normalized transducer radius		
$ka = \frac{4a}{\lambda_x + \lambda_x}$		46.3π
Mechanical transducer separation	d_o	12 cm
Near field length Ref:	a^2/λ_w	46.67 cm
Unk:	a^2/λ_x	46.03 cm
Normalized separation		
Ref:	$d_o\lambda_w/a^2$	0.2751
Unk:	$d_o\lambda_x/a^2$	0.2607
Relative acoustic pressure(*) Ref:	$\langle p\rangle_w$	891404
Unk:	$\langle p\rangle_x$	890109
Ratio of relative pressures	$\beta = \langle p\rangle_w/\langle p\rangle_x$	1.001454
Relative attenuation due to diffraction effects(**)	$A_D = \ln(\beta)$	0.0013 nep
Absorption diffraction correction	$\alpha_D = A_D/d_o$	0.00011 nep/cm
Difference in absorption between ref. and unk.	$\Delta\alpha = \lvert\alpha_w - \alpha_x\rvert$	0.0050 nep/cm
Percent difference due to diffraction	$\frac{\alpha_D}{\Delta\alpha}(100)$	2.2%

(*) Del Grosso (1964). Use $ka = 40\pi$

(**) Zucker (1964)

contribution to the apparent attenuation due to diffraction effects after Del Grosso (1964). For the high frequency system corrections, note that if distilled water at 25°C were being measured at 10.22 MHz, the observed absorption would be 23.2% higher due to diffraction effects. At higher frequencies, these effects decrease since the ultrasonic absorption of the media increases while the diffraction correction factor decreases.

The inherent advantage in the low frequency comparison technique has been mentioned previously, but is now demonstrated in Table 3-2 as the relatively small effect of diffraction. Ideally, if zero acoustic velocity differences between the two liquids were to exist, no diffraction effects would be present as the acoustic pathlength would remain constant. For the example given for approximately a 2% aqueous protein solution at 10°C, the velocity difference (estimated high to demonstrate the point) is 20 m/s, yielding an absorption correction due to diffraction of only 2.2% of the total observed difference in absorption.

The diffraction effects on the velocity of propagation, again using Del Grosso's (1964) method, is shown (O'Brien, 1968), at a frequency of 8.8 MHz and speed of sound of 1600 m/s, to be in error less than 0.0027% (or 0.04 m/s) which is insignificant compared to the accuracy of the experimental arrangement and will not be considered further.

3.4 Solution Preparation and Methods

The aqueous solutions of the biological chemicals which have been investigated in this study are all listed in Table 3-3 along with their control or lot number(s) and their source. The water used in all the experimentation is singly deionized and distilled and tests to, at most, 0.15 parts per million (Illinois State Water Survey).

Table 3-3

Biological Polymers Examined

MATERIAL	VENDOR
Uncrystallized Bovine Hemoglobin (Control #3099)	Nutritional Biochemicals Corporation Cleveland, Ohio
Hemoglobin Bovine 2X Crystalline (Control #1480, 8647, 8985)	Nutritional Biochemicals Corporation Cleveland, Ohio
Albumin Egg (Control #9133)	Nutritional Biochemicals Corporation Cleveland, Ohio
Albumin Egg 2X Crystalline (Control #9343)	Nutritional Biochemicals Corporation Cleveland, Ohio
Ovalbumin Crystalline 3X Salt Free (Control #9326)	Nutritional Biochemicals Corporation Cleveland, Ohio
Albumin, Bovine Fraction V (Lot #1058-1520)	Sigma Chemical Company St. Louis, Missouri
Deoxyribonucleic Acid Sodium Salt (Calf Thymus) (Lot #V1506)	Mann Research Laboratories, Inc. New York, New York
Deoxyribose Nucleic Acid Sodium Salt (Salmon Sperm) Highly polymerized, A grade (Lot #50075, 50209)	Calbiochem Los Angeles, California

All of the protein solutions were prepared by placing the proper amount of power or crystal on top of a measured volume of water and placed in the refrigerator until mixing was complete, usually 2-5 hours. The uncrystallized hemoglobin solution, which contained some red blood cell walls, was centrifuged at 20,000 g's for 2 hours to remove the heavier particles. This hemoglobin solution supernate, in addition to the other protein solutions were filtered twice through type A glass fiber filters (Gellman Inst. Co., Ann Arbor, Michigan) which removed particles larger than 0.3 μ in diameter and stored in the refrigerator at 7°C until use, usually not more than a couple of hours. The weight concentration of the acoustically measured solutions were determined, at room temperature, by evaporating over air 15 ml in a tared beaker until dry and placing in a vacuum desiccator for 24 hours before

measuring on an Ainsworth Type 10 Analytical Balance (Wm. Ainsworth and Sons, Inc., Denver, Colorado) which has a precision of $\pm$ 0.1 mg. The protein concentration accuracy is determined to better than $\pm$ 0.3%.

The Calf Thymus DNA solution, which required 3-4 hours to go into solution, was prepared in the same manner as the protein solutions. Also, its concentration was determined by evaporation.

The highly polymerized Salmon Sperm DNA required considerably more time to go into solution, of the order of 2 weeks. Its solvent was SSC, that is, a 0.15 M NaCl (Mallinckrodt Analytical Reagent) plus 0.015 M $Na_3C_6H_5O_7$ (Baker Analyzed) aqueous solution. Bacterial growth was inhibited in both types of DNA solutions during mixing and storage by the addition to the solution of chloroform (Allied Chemical Reagent Grade). As the maximum Salmon Sperm concentration was approximately 0.004 gm/cc, its concentration had to be determined spectrophotometrically with a Beckman Model DU Spectrophotometer using the extinction coefficient $E\Big|^{1\%}_{260}$ = 224 at pH at 12.

The pH of the Hb, Ov and DNA was changed, to obtain the ultrasonic absorption and velocity titration curves, by the addition of either 1.0 N HCl or KOH prepared from standard volumetric solutions (Acculute-Anachemia Chemicals Ltd.). The pH measurements were obtained with a Beckman 76006 Century SS pH Meter using a Beckman pH Combination Electrode (#39013) which fitted directly into the acoustic chamber. The pH Meter was standardized at pH 4.01, 7.00, 7.41, 9.18 and 12.45 with Beckman buffers (3005, 3007, 3008, 3009 and 3010, respectively) and at pH 2.01 with Coleman buffer tablets (Lot #68). The pH readings were obtained to a relative accuracy $\pm$ 0.01 pH unit.

The guanidine hydrochloride solutions were prepared by mixing a known

amount of GuHCl (Eastman Organic Chemicals, Rochester, New York, Lot #882K) into a measured volume of water to obtain a concentration of 8 Molar. The solution was filtered once through type A grass fiber to remove any particle greater than 0.3 μ. Its concentration was determined by evaporating, over air, to almost dryness, as it is highly hydroscopic, and dried in a vacuum desiccator over indicating anhydrous $CaSO_4$ (Hammond Drierite Company, Xenia, Ohio) for one week.

The concentration determinations of the acoustic titrations were calculated from the volume of KOH or HCl added to a known volume of solution within the measuring chamber. The acid or base was introduced via a hypodermic syringe and needle in very small amounts while monitoring the pH meter. The concentration determination of the GuHCl-Hb solutions were obtained by, first accurately determining the Hb solution concentration before GuHCl was added, and then while adding the GuHCl, measuring both the change in volume due to GuHCl and its dry weight. The concentration accuracies of this experiment are estimated to be from $\pm$ 0.3 to $\pm$ 3%, the accuracy decreasing as the GuHCl concentration increased.

CHAPTER 4 RESULTS

Ultrasonic absorption and velocity measurements were accomplished in aqueous solutions of four biological polymers, viz., hemoglobin (Hb), ovalbumin (OV), bovine serum albumin (BSA) and deoxyribose nucleic acid (DNA). The majority of the data were taken at 10.0°C over the frequency range 1.6-50 MHz. In order to correlate the acoustic data with absorption mechanisms, the following parameters were varied: biopolymer concentration to assure that infinite dilution assumptions were valid, ultrasonic frequency to determine the relaxation spectra, molecular purity to investigate whether or not the method of extraction affects the acoustically varied parameters, aqueous environment of the biopolymer by the addition of hydrochloric acid (HCl), potassium hydroxide (KOH) and guanidine hydrochloride (GuHCl) to examine the effect of conformal change and exposed side chains, temperature to obtain the energy of activation and salt concentration, or absence of by dialysis, to determine the effect of minute salt concentration.

In this report the absorption data is presented in terms of the frequency-free excess absorption obtained by subtracting from the observed absorption that due to the solvent, which in most cases will be distilled water, and to divide this difference by the square of the frequency at which the measurement is obtained, viz.,

$$\frac{\Delta\alpha}{f^2} = \frac{\alpha_{OBS} - \alpha_{SOLVENT}}{f^2} \,. \qquad (4\text{-}1)$$

In (4-1) α_{OBS} has been corrected for diffraction effects, when necessary. Pinkerton's (1949a) values of the frequency-free absorption coefficient for water as a function of concentration are listed in Table 4-1 and

Table 4-1

Ultrasonic Absorption in Water
(Pinkerton, 1949a)

T(°C)	$\alpha_{H_2O}/f^2 \times 10^{+17}$ (sec^2/cm)
0	56.9
5	44.1
10	35.8
15	29.8
20	25.3
30	19.1
40	14.61
50	11.99
60	10.15

plotted in Fig. 4-1. These values are termed frequency-free since they are independent of frequency at all ultrasonic frequencies thus far treated. In order to demonstrate whether or not the ultrasonic absorption is a linear function of solute concentration within the range the data were obtained, the parameter of (4-1) is plotted as a function of concentration. With linear dependence, the frequency-free absorption parameter is then divided by solute concentration in order to correct for differences in concentration when the ultrasonic absorption is compared at various frequencies, pH, etc., viz.,

$$A = \frac{\Delta\alpha}{cf^2} . \qquad (4\text{-}2)$$

This method of presenting the ultrasonic absorption data facilitates the examination of that portion of the data due to the solute. In the high frequency system, the solvent must be subtracted off to yield the excess absorption whereas in the low frequency system the excess absorption is obtained directly provided the solvent is used as its reference liquid.

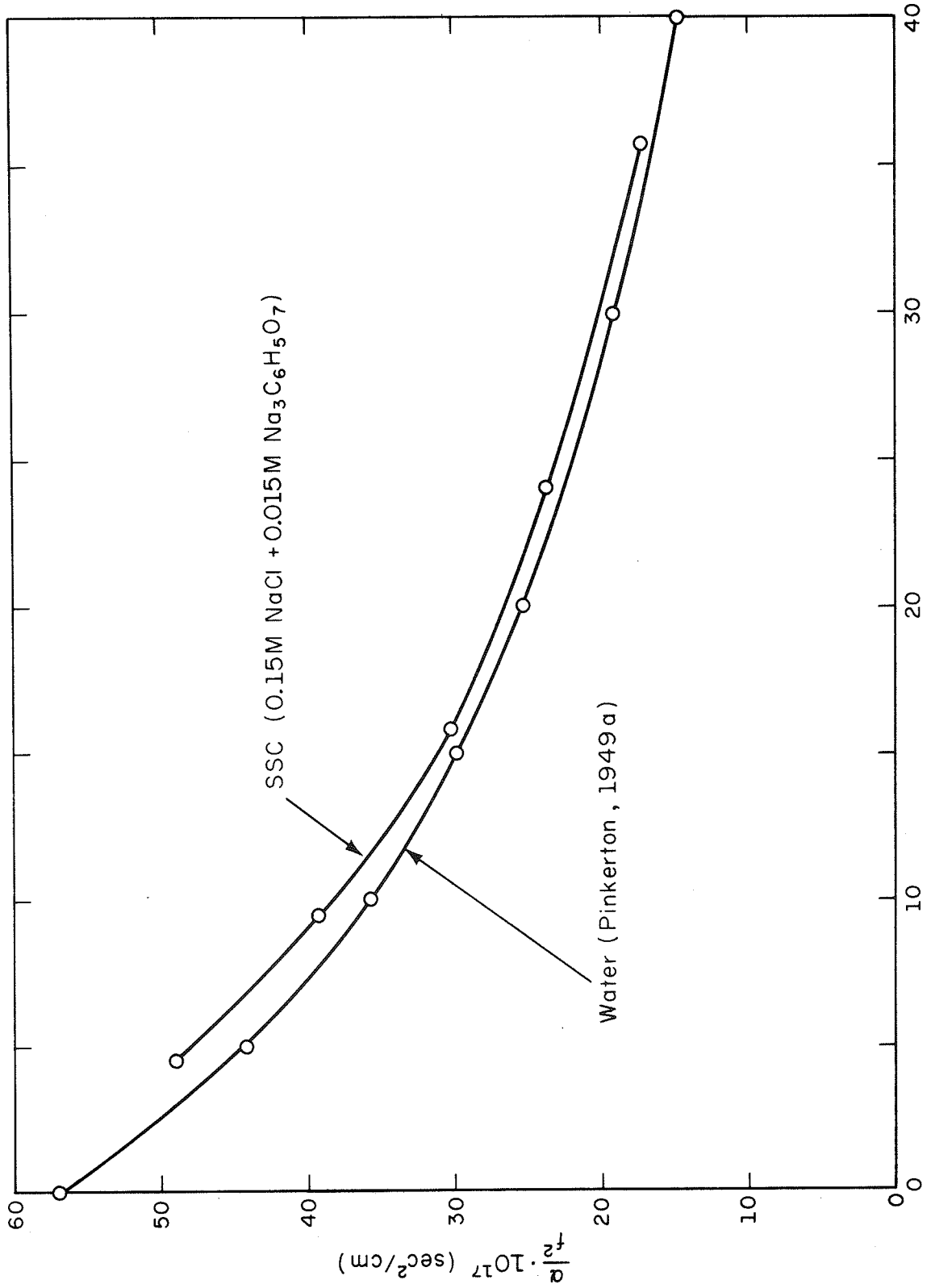

FIGURE 4-1

FREQUENCY FREE ABSORPTION AS A FUNCTION OF TEMPERATURE FOR DISTILLED WATER AND STANDARD SALINE CITRATE (SSC)

In order to assure that interaction between biopolymers (finite concentration effects) is not resulting in their aqueous solution when the acoustic wave is propagated, the excess ultrasonic absorption and velocity are examined as a function of solute concentration. Two grades of bovine hemoglobin are examined, one uncrystallized (0X) and the other twice crystallized (2X). The excess frequency-free absorption of aqueous solutions of both Hb-0X and Hb-2X are plotted, respectively, in Figs. 4-2 and 4-3 at 10.0°C for the frequencies indicated. It is apparent that for Hb-0X, deviation from linearity occurs around 0.10 gm/cc whereas that for the purer Hb occurs beyond 0.16 gm/cc. Carstensen and Schwan (1959b) reported that aqueous solutions of hemoglobin were linearly dependent upon concentration to at least 0.15 gm/cc. Comparing the ultrasonic velocity measurements as a function of concentration in Figs. 4-4 and 4-5 indicate deviation from linearity at lesser concentrations, viz., around 0.09 gm/cc for Hb-0X and 0.13 gm/cc for Hb-2X.

Figure 4-6 shows the excess absorption of aqueous solutions of uncrystallized ovalbumin (Ov-0X) to be linearly dependent on concentration to at least 0.15 gm/cc. The ultrasonic velocity of Ov-0X is also linearly dependent upon concentration to the same concentration, as is seen in Fig. 4-7, which also shows a different linear dependence for Ov-2X and Ov-3X up to 0.046 gm/cc.

Comparison of the concentration dependence of velocity for Hb and Ov shows, in Table 4-2, the slopes of both grades of Hb to be the same whereas markedly different slopes between Ov-0X and Ov-2X, 3X.

Since deviation from linearity of excess frequency-free absorption is usually attributed to interaction among the solute molecules, it would

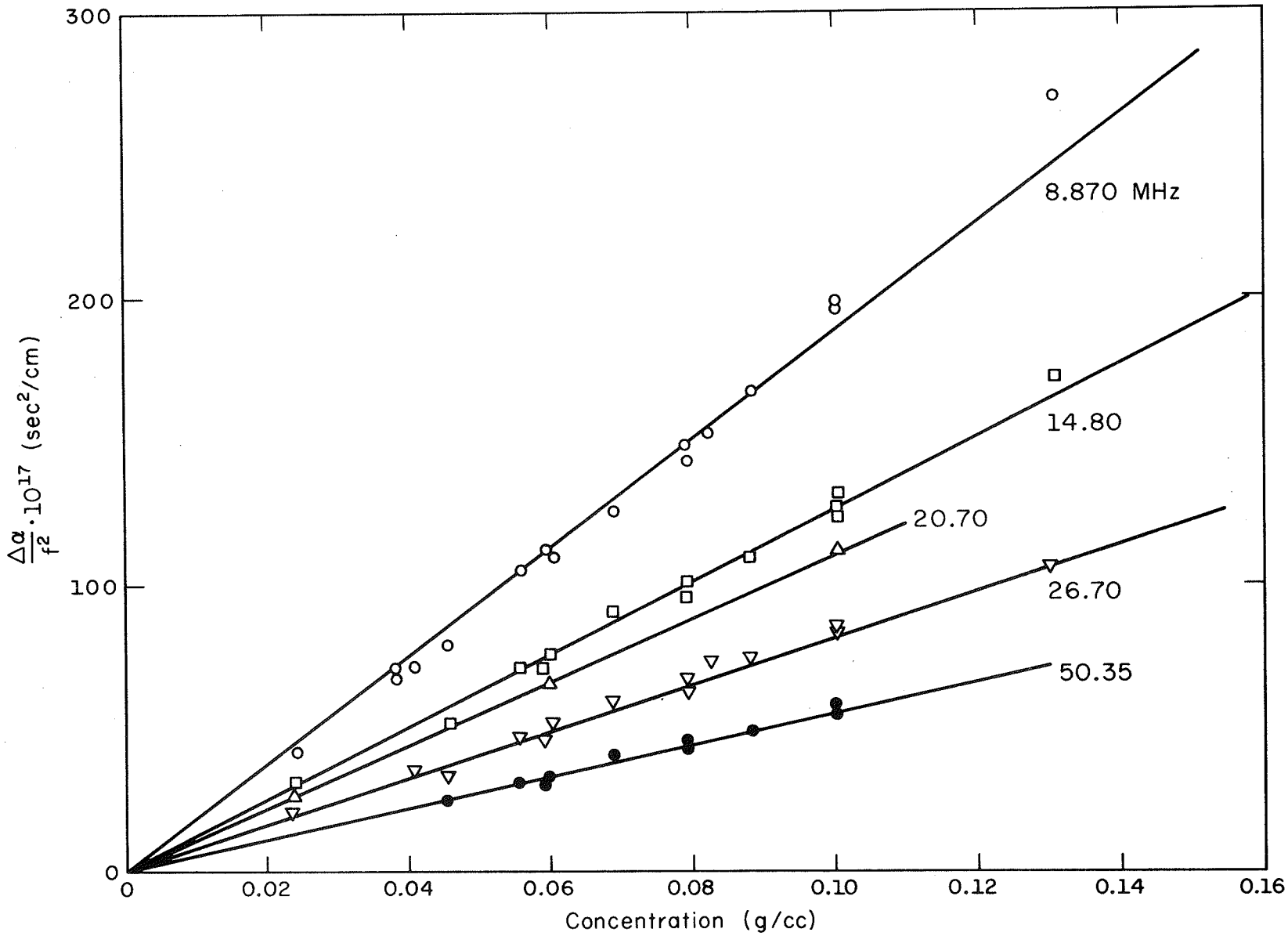

FIGURE 4-2

CONCENTRATION DEPENDENCE OF ABSORPTION
BOVINE HEMOGLOBIN-OX (T = 10.0°C)

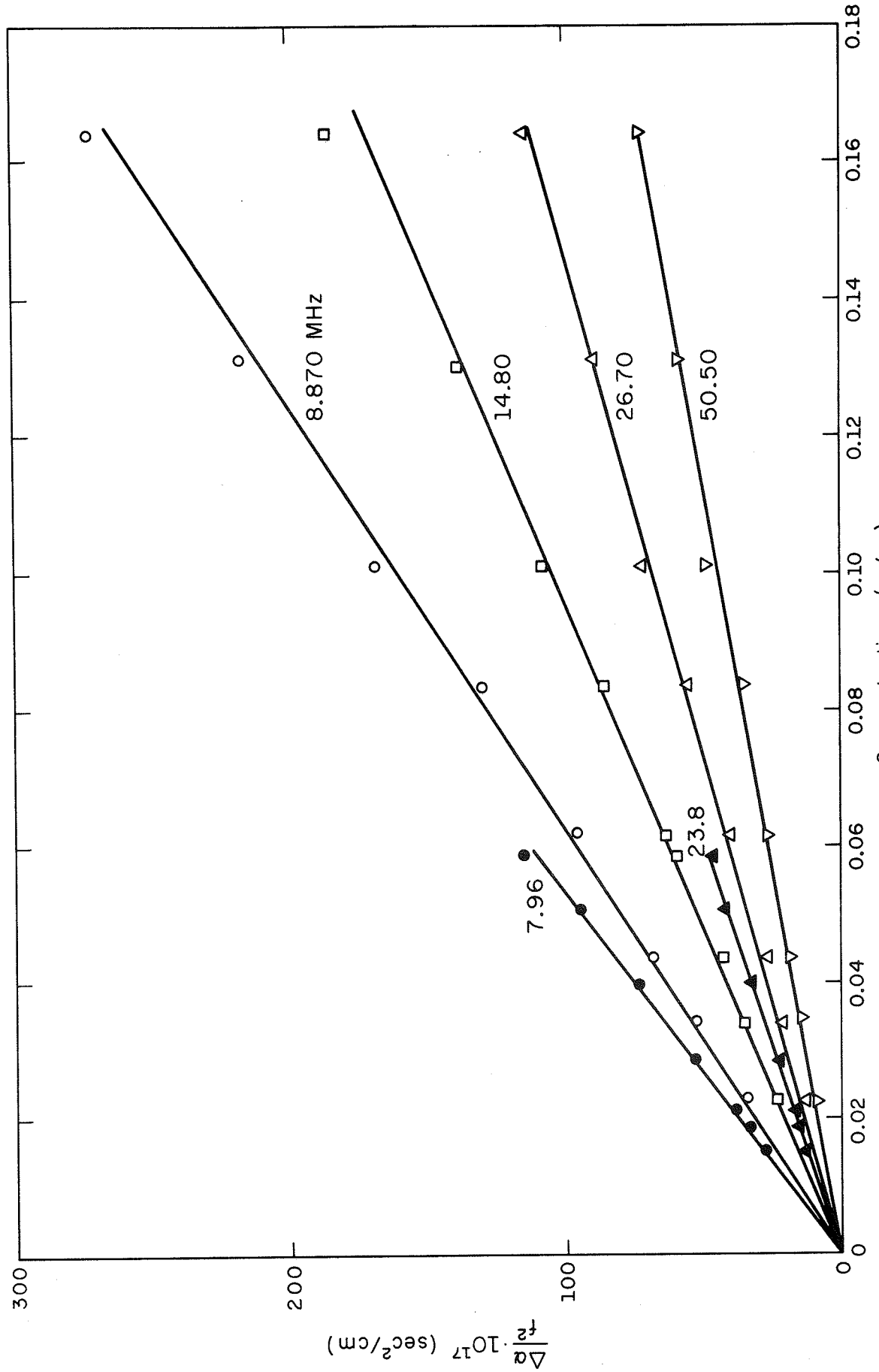

FIGURE 4-3

CONCENTRATION DEPENDENCE OF ABSORPTION
BOVINE HEMOGLOBIN-2X (T = 10.0°C)

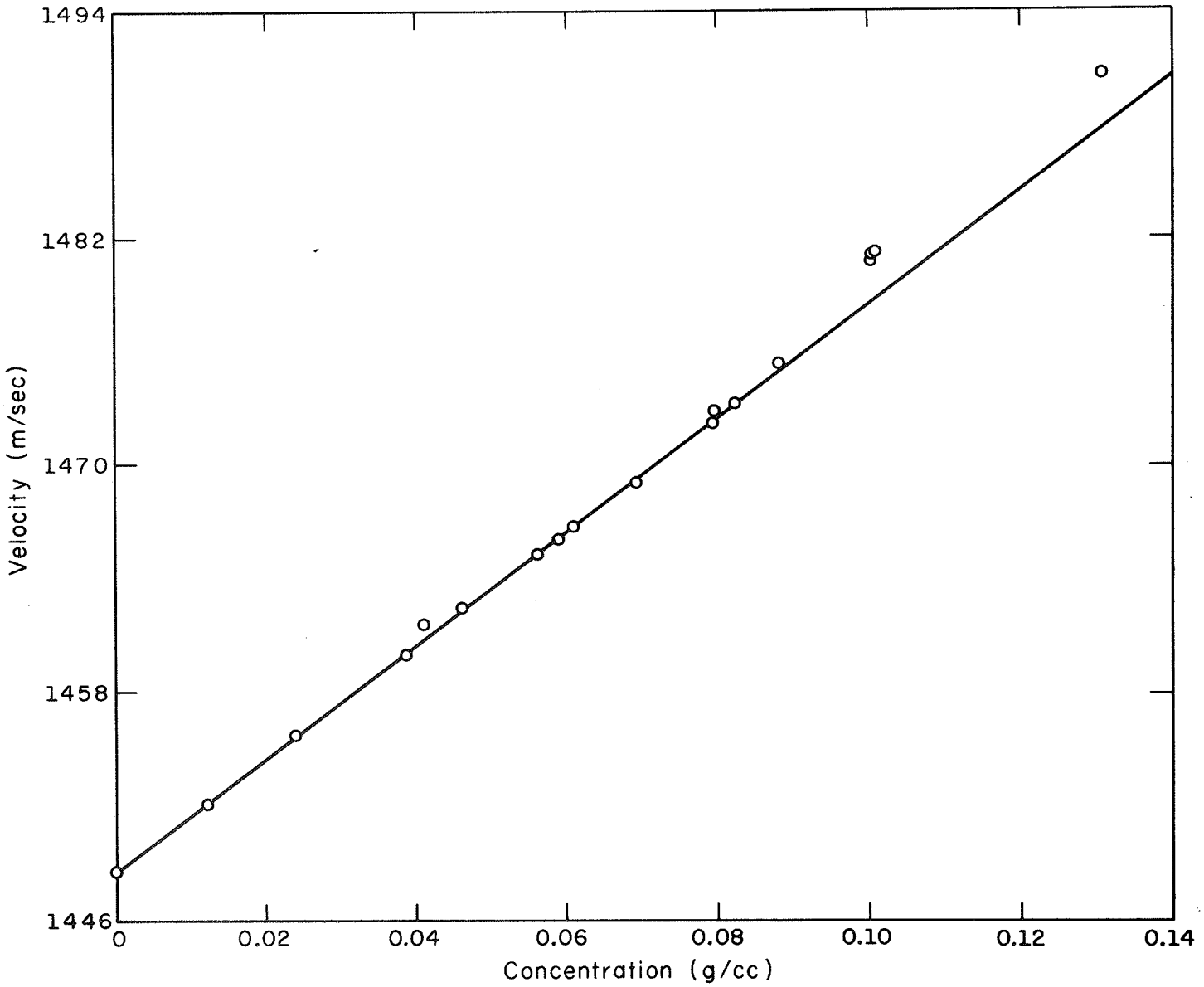

FIGURE 4-4

CONCENTRATION DEPENDENCE OF VELOCITY
BOVINE HEMOGLOBIN-OX (T = 10.0°C; f = 8.870 MHz)

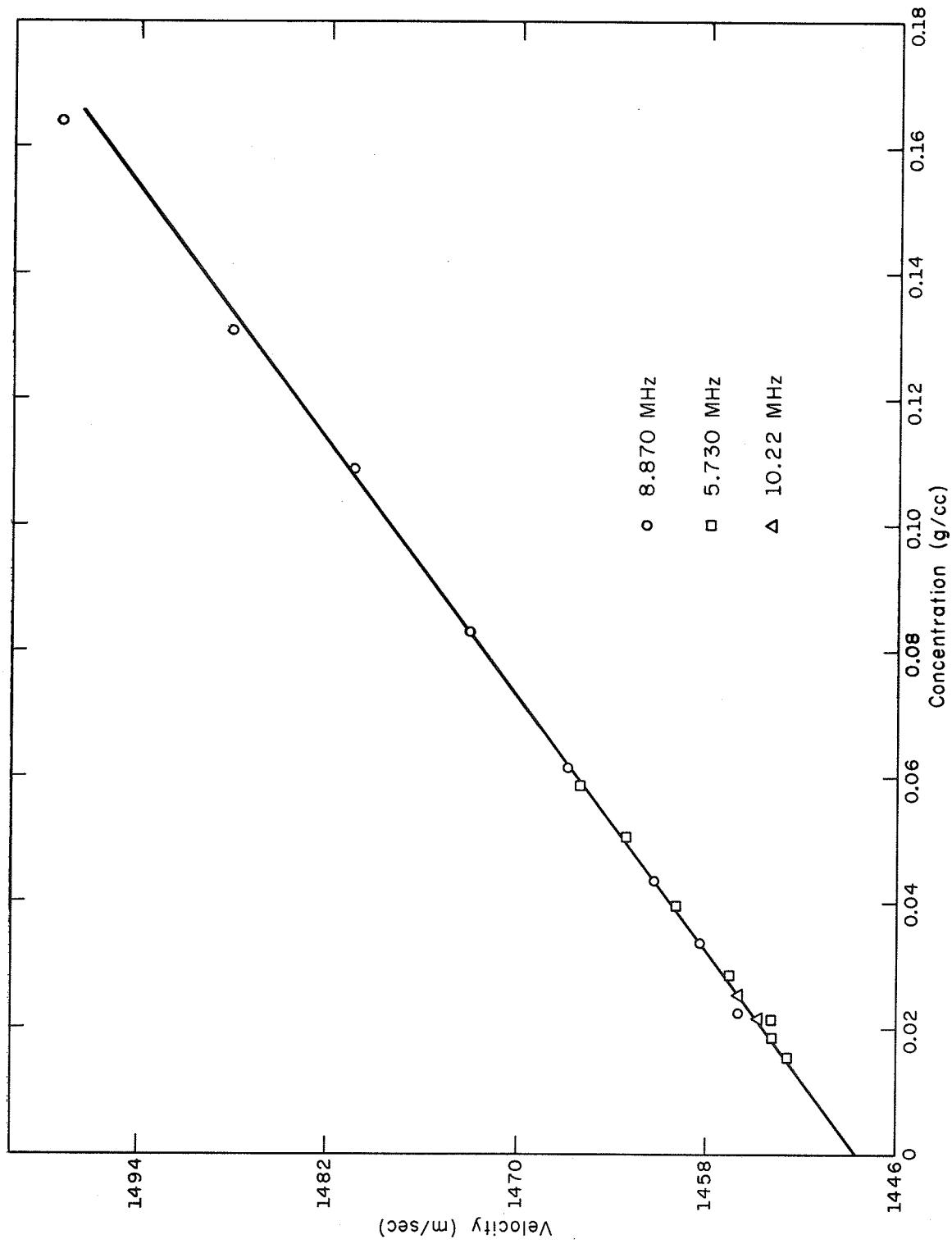

FIGURE 4-5

CONCENTRATION DEPENDENCE OF VELOCITY
BOVINE HEMOGLOBIN-2X (T = 10.0°C)

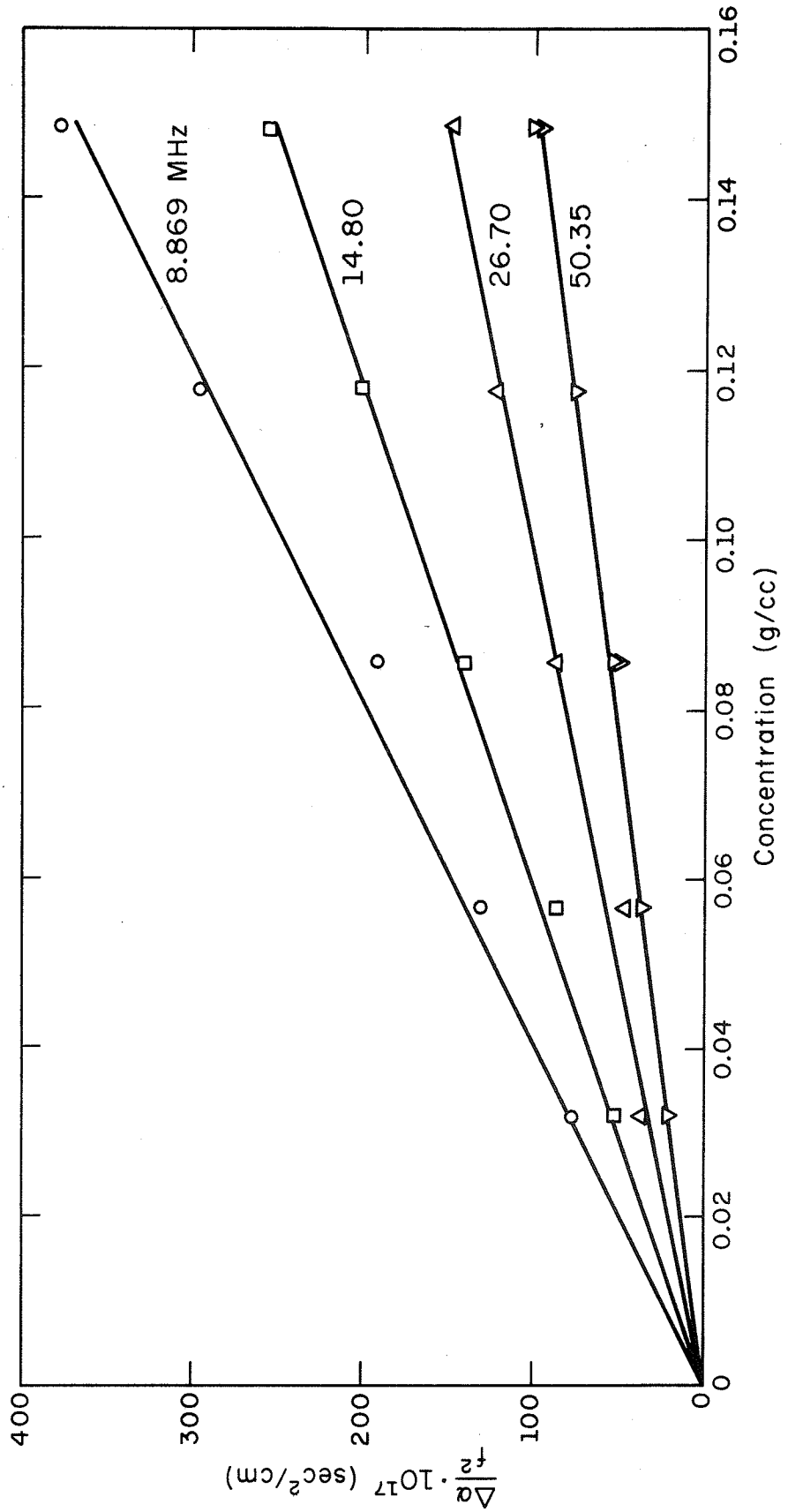

FIGURE 4-6
CONCENTRATION DEPENDENCE OF ABSORPTION
OVALBUMIN-OX (T = 10.0°C)

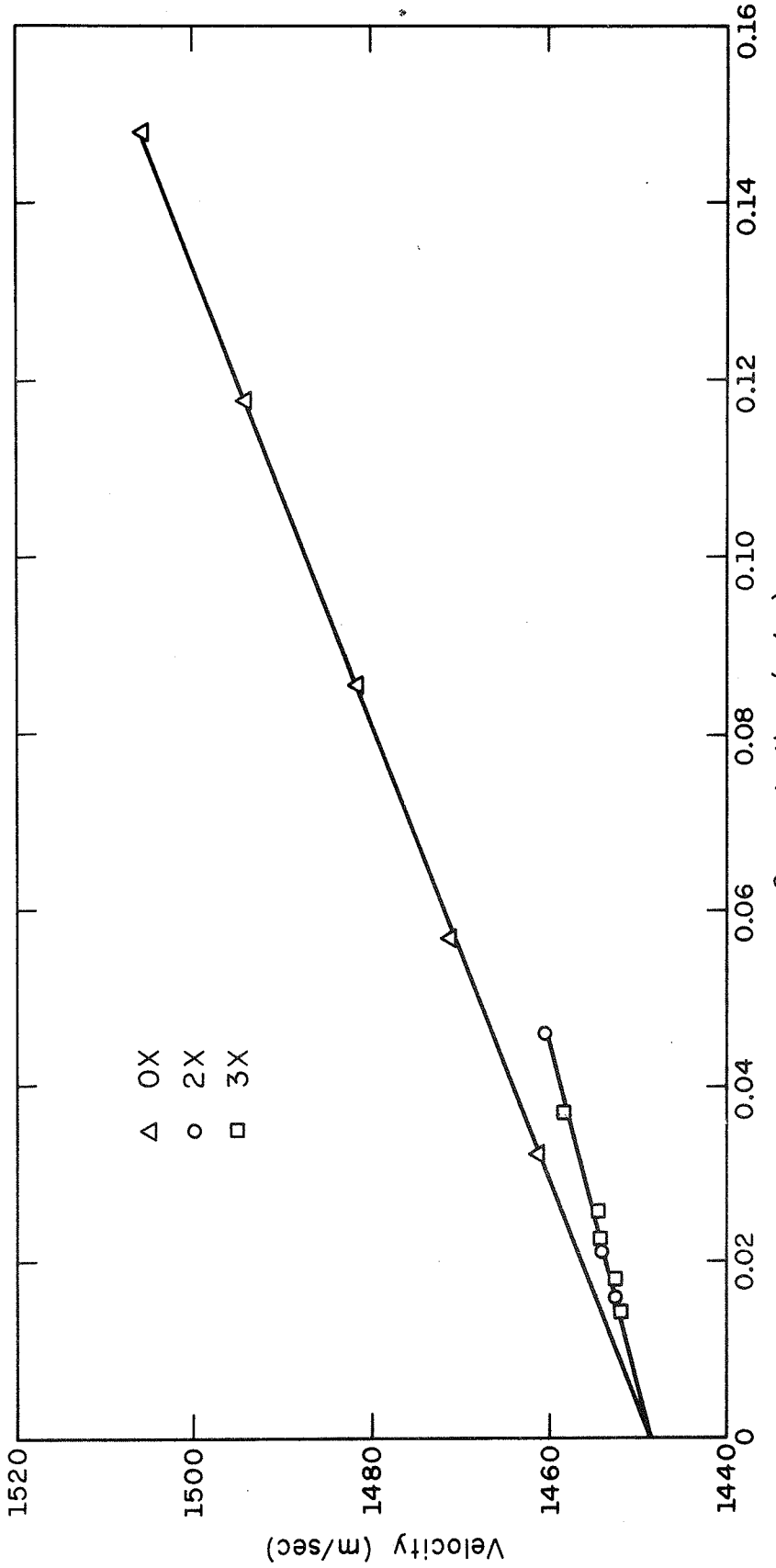

FIGURE 4-7

CONCENTRATION DEPENDENCE OF VELOCITY
OVALBUMIN-2X AND 3X (T = 10.0°C)
(2X-f = 8.870 MHz; 3X-f = 14.80 MHz)

Table 4-2

Comparison of Velocity Dependence upon Concentration

Material	Slope (m/s · cc/gm)
Hb-0X	300
Hb-2X	300
Ov-0X	390
Ov-2X, 3X	260

appear of interest to calculate the distance between these molecules where the excess absorption becomes nonlinear. To calculate the weight concentration at which these globular proteins contact one another, set the volume of an assumed spherical particle, $\frac{4}{3}\pi R^3$, equal to the volume per molecule, i.e.,

$$\frac{4}{3}\pi R^3 = \frac{cN_A}{M} \qquad (4\text{-}3)$$

where c is the solute weight concentration in gm/cc, M is the molecular weight of the biopolymer and N_A is Avogadro's number. Plotting R, the radius of the biopolymer, as a function of concentration at constant molecular weight, yields Fig. 4-8, where the two molecular weights 68,000 and 46,000 represent those of hemoglobin and ovalbumin, respectively. To a first approximation, using X-ray crystallographic techniques, Perutz et al., (1960) found the hemoglobin molecule to be roughly spherical with overall dimensions 64 Å by 55 Å by 50 Å. From Fig. 4-8, at the concentration 0.16 gm/cc, where the ultrasonic absorption begins to deviate from linearity, for Hb-2X, the radius is 54.4 Å, which is within the range where the individual molecules can, and most likely do, contact one another. In the following chapter, approximate calculations show the dimensions of the ovalbumin molecule to be 43 Å by 43 Å by 129 Å.

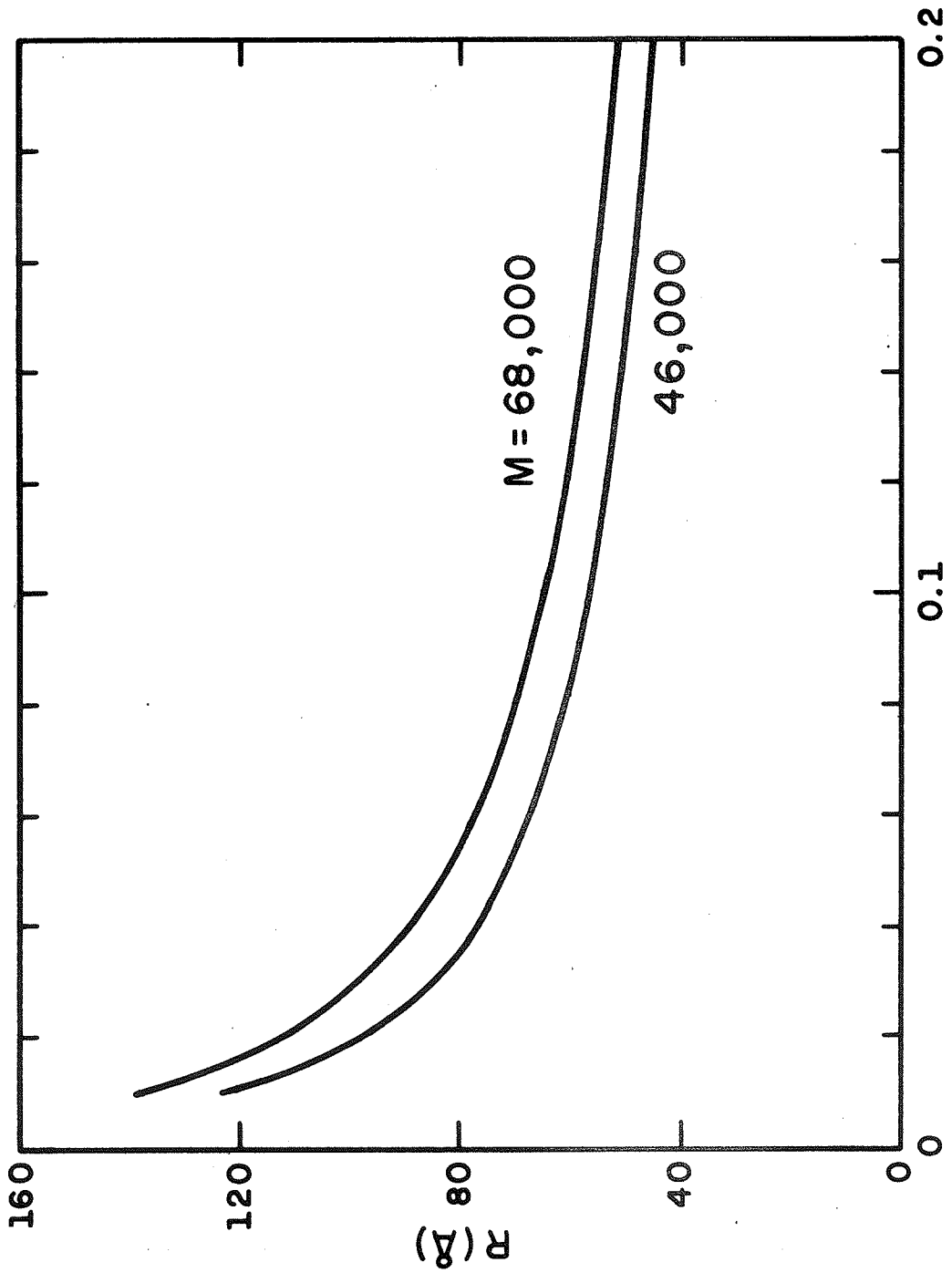

FIGURE 4-8

PARTICLE RADIUS VS CONCENTRATION
(See Text for Explanation)

Thus, if the ovalbumin absorption were to deviate from linearity at 0.16 gm/cc, the approximate molecular radius would be 48.5 Å which also is within contact distance.

To examine further this idea that when the solute molecules are within touching distance of one another, the absorption deviates from linearity, the excess frequency-free absorption of an aqueous solution of a random coil molecule, polyethylene glycol (PEG), molecular weight 4500, is plotted in Fig. 4-9 up to 0.41 gm/cc in concentration. Deviation from linearity occurs betwen 0.30 and 0.35 gm/cc. Being a random coil molecule, the statistical quantity average radius of gyration is used to determine the distance bwtween molecules in an aqueous solution. Assuming all mass elements of the macromolecule have the same mass, the average radius of gyration is defined by (Tanford, 1961)

$$R_G = \beta \sqrt{\frac{M}{6M_o}} \tag{4-4}$$

where β is the effective length of the monomer unit of molecular weight M_o, M being the polymer molecular weight. The effective segment length of the PEG molecule is calculated from (Kessler, 1968a; Kessler *et al.*, 1970)

$$\left[\frac{\beta}{\beta_o}\right]^3 = \frac{[\eta]_{o\ \text{OBSERVED}}}{[\eta]_{o\ \text{THEORETICAL}}} \tag{4-5}$$

where β_o is the theoretical segment length which, for PEG, equals 4.4 Å, $[\eta]_{o\ \text{THEORETICAL}}$ is the intrinsic viscosity at $\omega = 0$ calculated from the Zimm (1956) theory and $[\eta]_{o\ \text{OBSERVED}}$ is the intrinsic viscosity of aqueous solution of PEG, given by Sadron and Rempp (1958) to be

$$[\eta]_{o\ \text{OBSERVED}} = 2.0 + 0.033\ M^{0.72}. \tag{4-6}$$

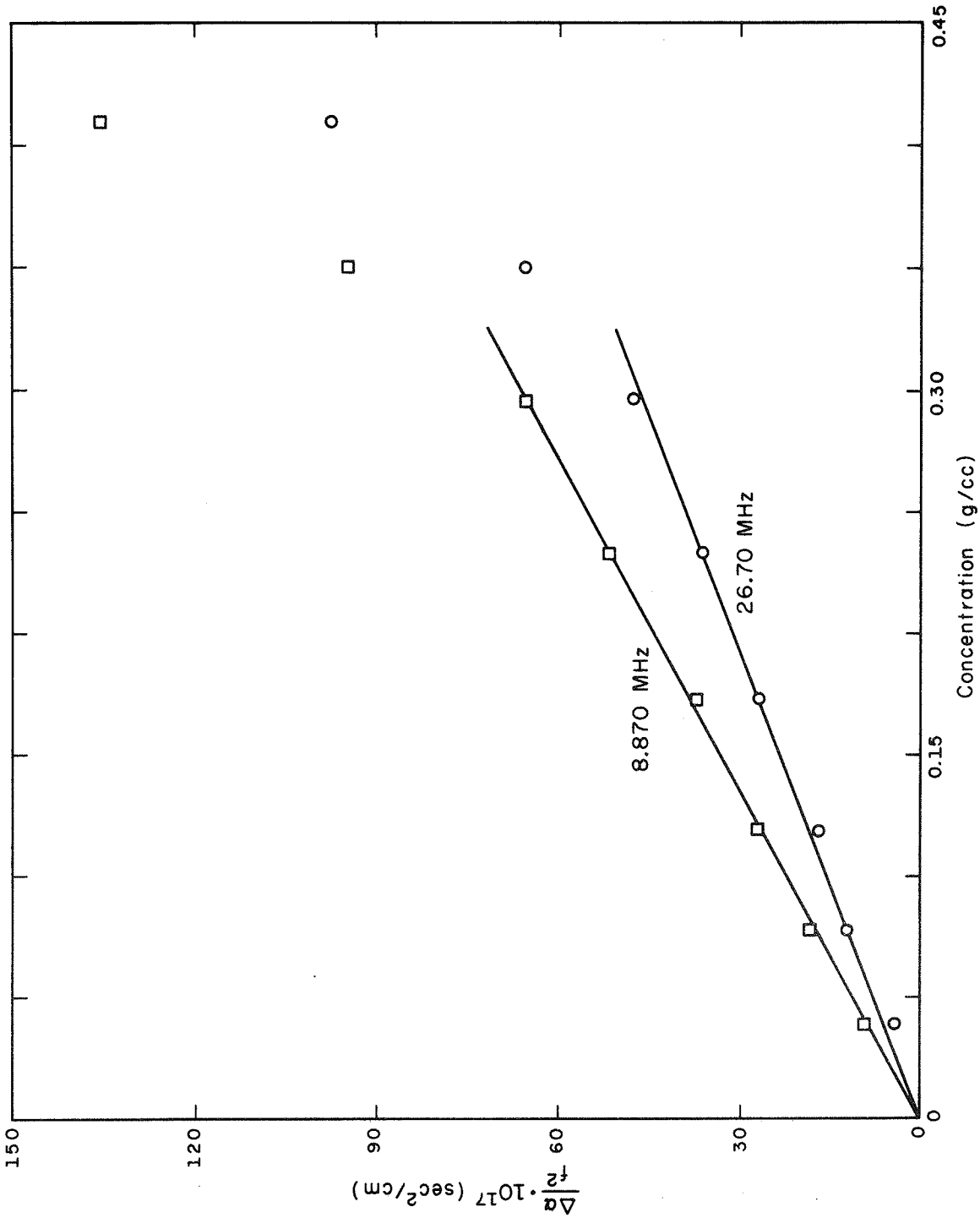

FIGURE 4-9

CONCENTRATION DEPENDENCE OF ABSORPTION
POLYETHYLENE GLYCOL-4500 (T = 20.7°C)

Substituting the PEG molecular weight into (4-3) and assuming R is approximately R_G, which is the extreme case for R_G, yields Fig. 4-10 for PEG of molecular weights 4500 and 20,000. According to Fig. 4-10, the average radius of gyration at 0.30 gm/cc is approximately half that calculated from (4-4) as tabulated in Tables 4-3 and 4-4. Thus it must be concluded that, for PEG at least, the polymer molecules interact with each other at lesser concentrations than those at which deviation from linearity is observed. Thus it is most likely that the effect resulting in the deviation from linearity in aqueous PEG solutions is completely different from that of the protein solutions. As for the two globular proteins investigated as a function of concentration, only hemoglobin, for certain, can be correlated with the solute-solute interaction causing the deviation from linearity.

The excess frequency-free absorption per unit concentration is plotted as a function of frequency for aqueous solutions of Hb-0X, 2X in Fig. 4-11, 0v-0X in Fig. 4-12, 0v-2X in Fig. 4-13, 0v-3X in Fig. 4-14, BSA in Fig. 4-15 and DNA in Fig. 4-16, all at their isoelectric point at 10.0°C and largely over the frequency range 1.6-50 MHz. The ultrasonic spectrograms of Figs. 4-11 through 4-16 are summarized in the composite ultrasonic spectrogram of Fig. 4-17 which indicates that the above aqueous solutions are characterized by a distribution of relaxation processes. Similar conclusions were reached for polyethylene glycol (O'Brien, 1968; Kessler, 1968a; Kessler *et al.*, 1970), dextran (Hawley *et al.*, 1965; Hawley, 1966), poly-L-glutamic acid (Lewis, 1965) and for other macromolecules.

The spectrogram, Fig. 4-11, for Hb-0X and 2X at neutral pH, indicates a slight decrease in the magnitude of the excess absorption of the purer

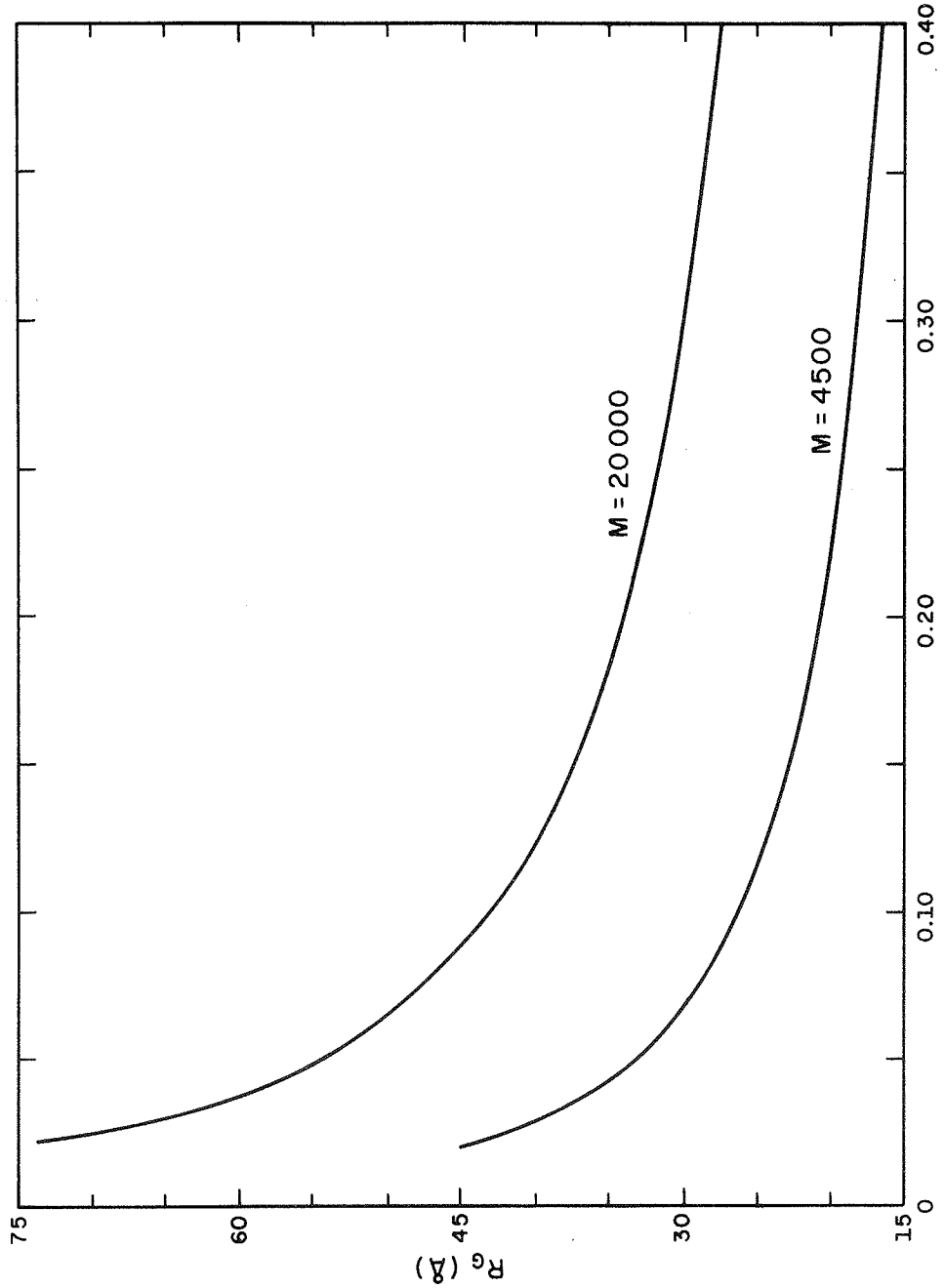

FIGURE 4-10
RADIUS OF GYRATION VS CONCENTRATION
(See Text for Explanation)

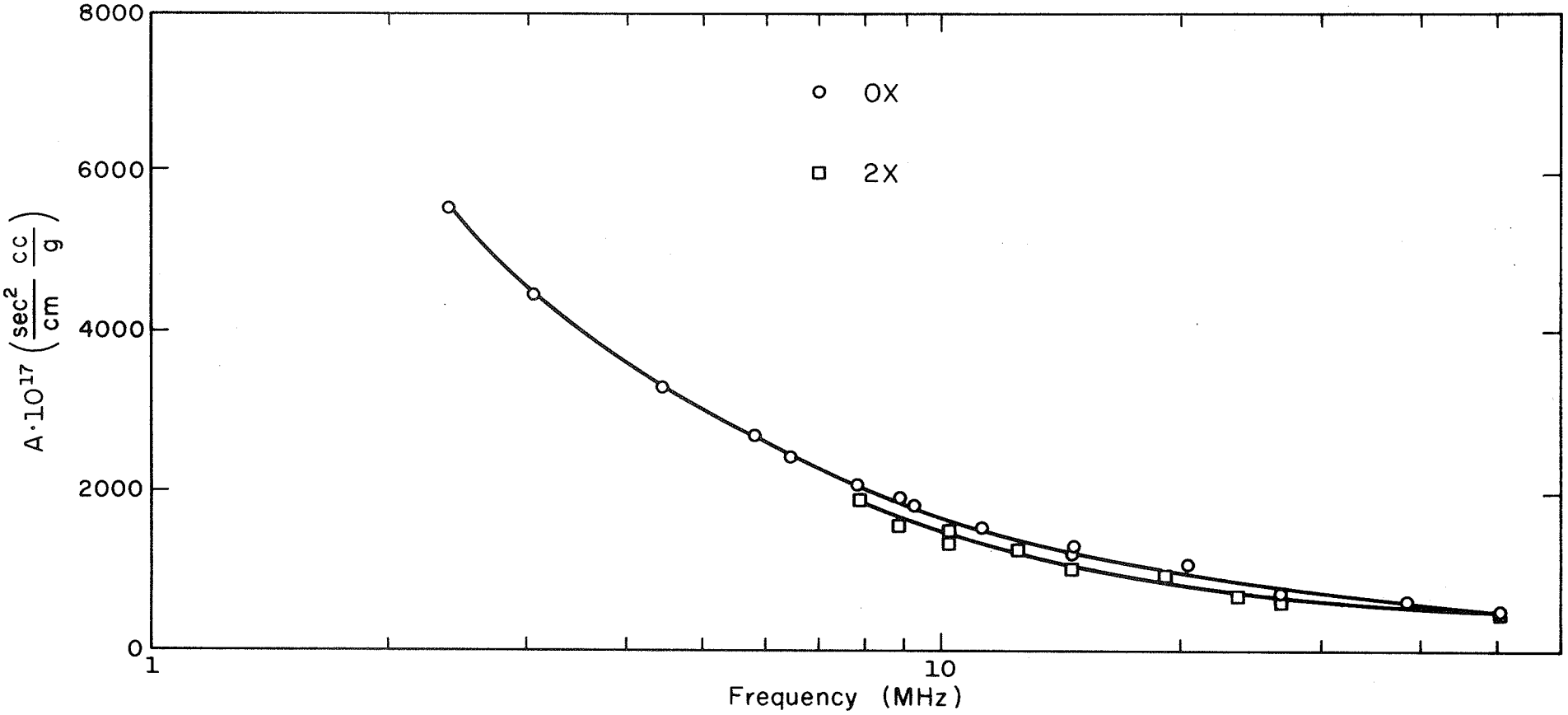

FIGURE 4-11

ULTRASONIC SPECTROGRAM
BOVINE HEMOGLOBIN-OX AND 2X (T = 10.0°C)

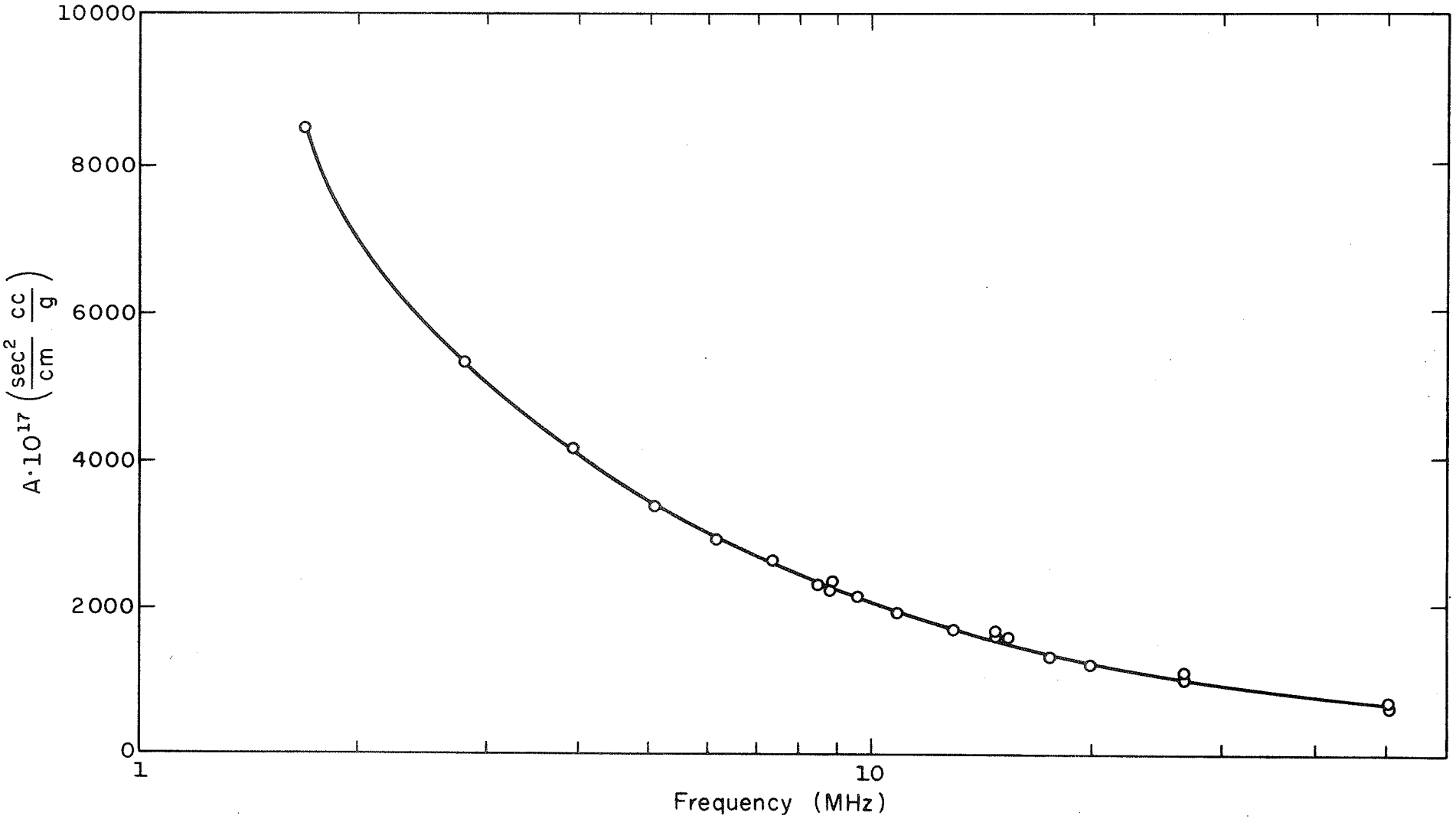

FIGURE 4-12

ULTRASONIC SPECTROGRAM
OVALBUMIN-OX (T = 10.0°C)

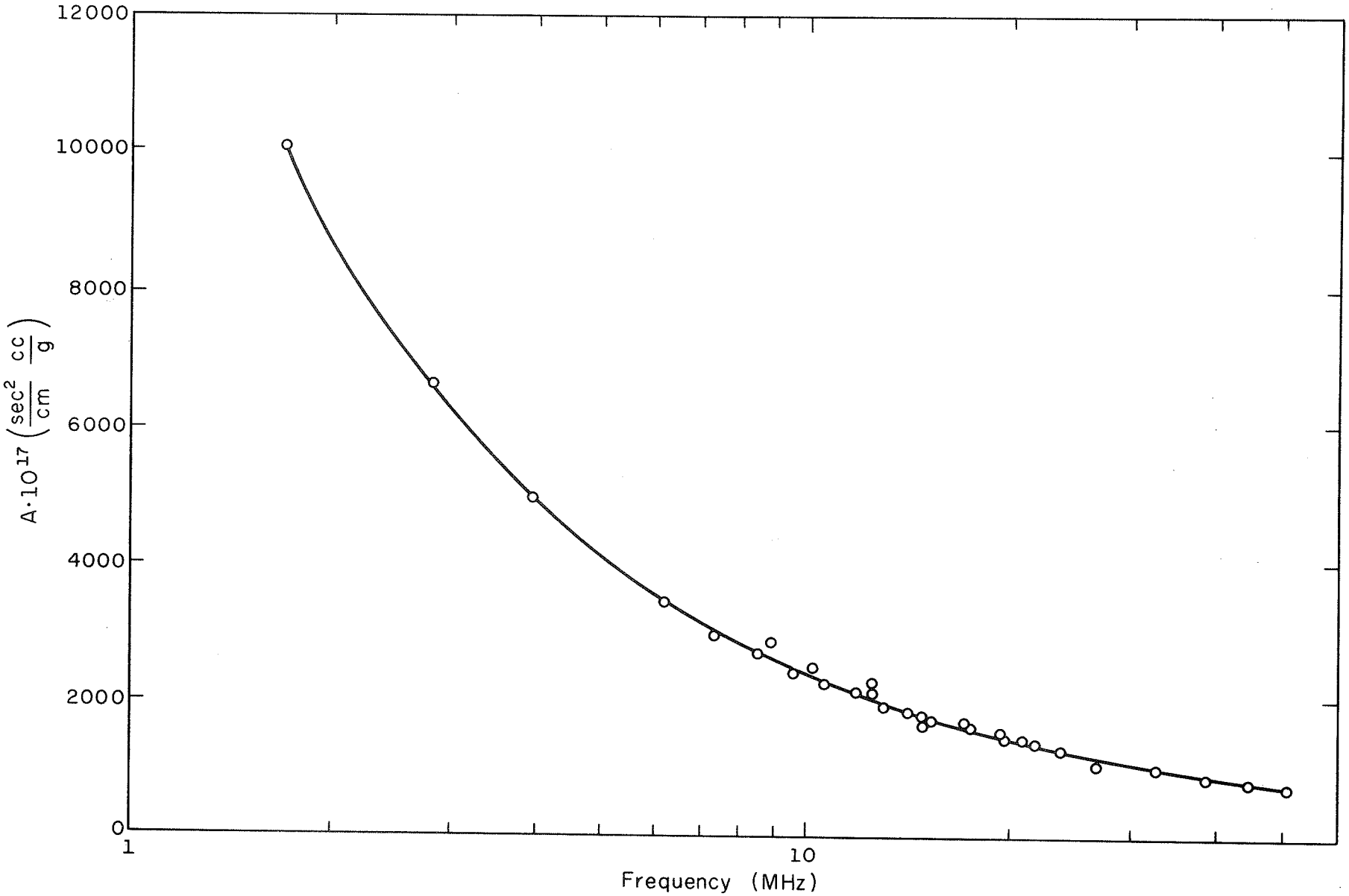

FIGURE 4-13

ULTRASONIC SPECTROGRAM
OVALBUMIN-2X (T = 10.0°C)

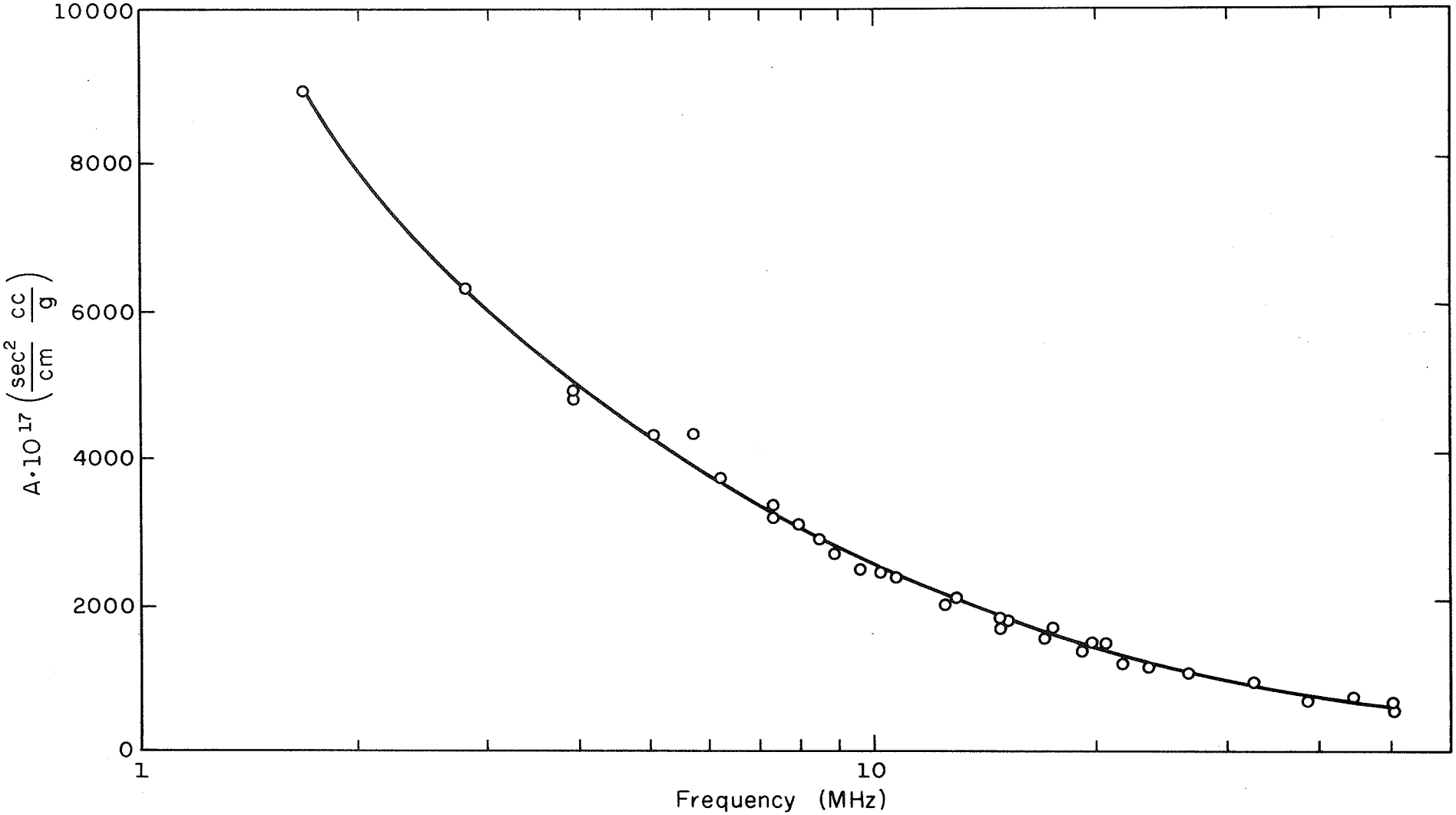

FIGURE 4-14

ULTRASONIC SPECTROGRAM
OVALBUMIN-3X SALT FREE (T = 10.0°C)

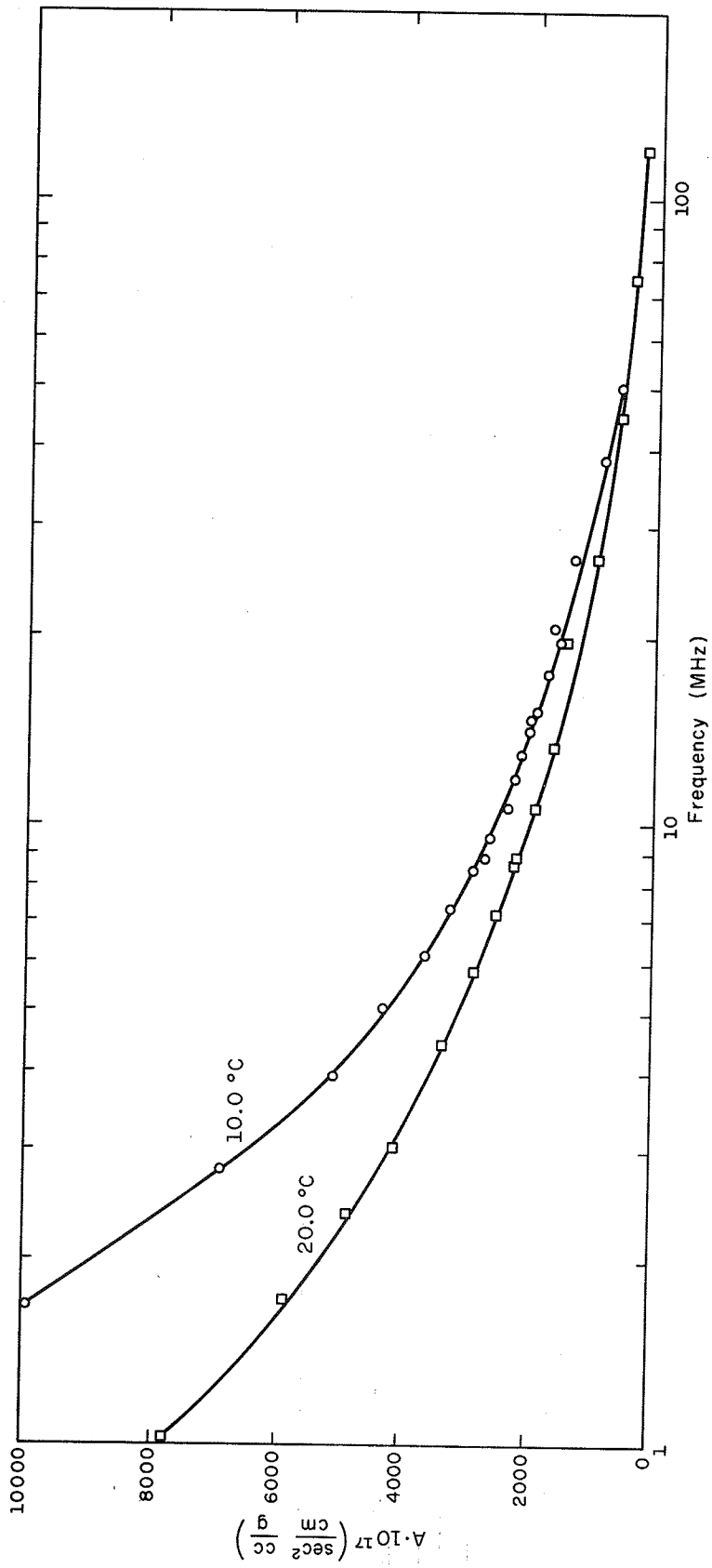

FIGURE 4-15
ULTRASONIC SPECTROGRAM
BOVINE SERUM ALBUMIN (T = 10.0°C AND 20.0°C)
(T = 20.0°C, Kessler, 1968a)

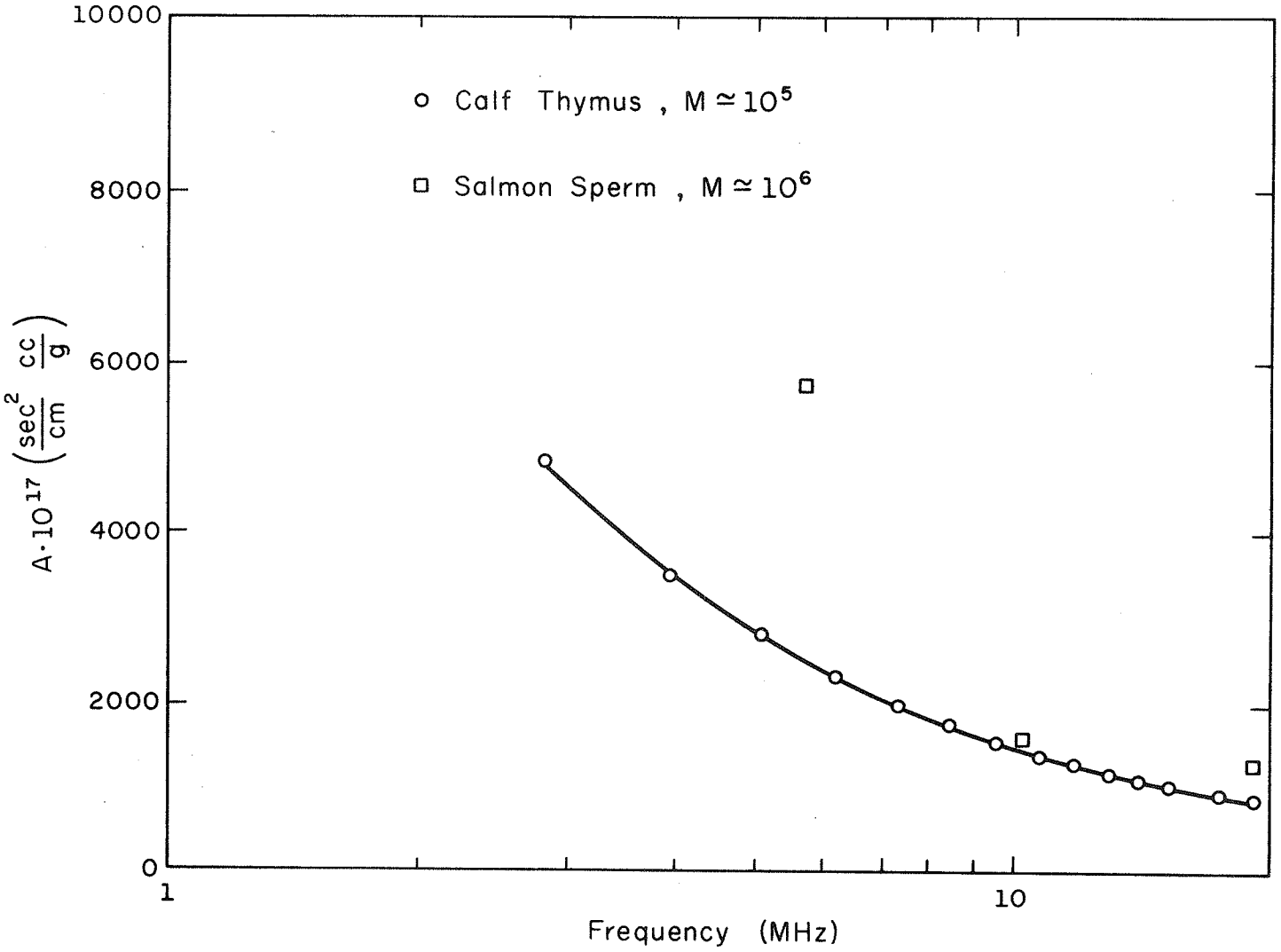

FIGURE 4-16

ULTRASONIC SPECTROGRAM
DEOXYRIBOSE NUCLEIC ACID (T = 10.0°C)

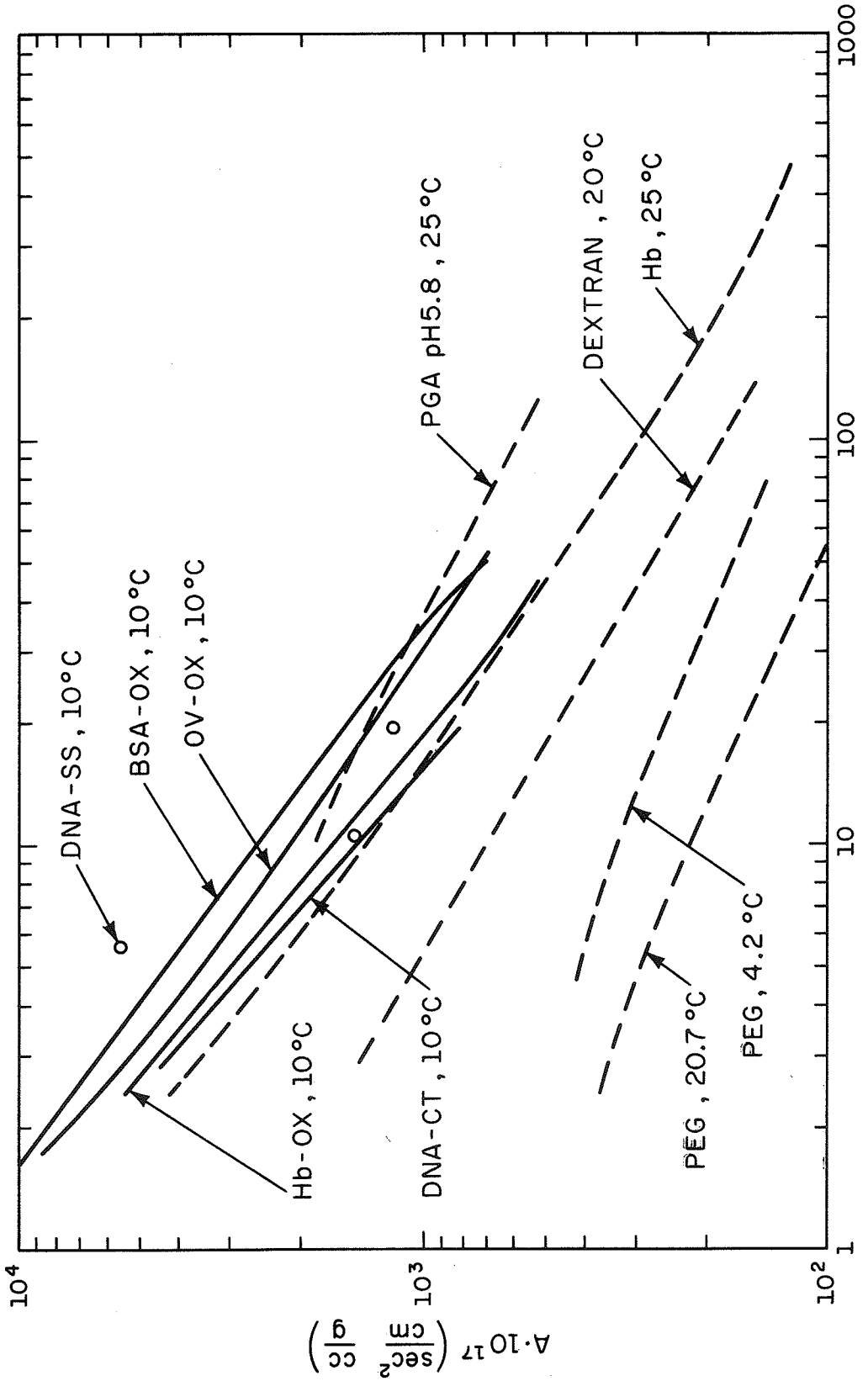

FIGURE 4-17

COMPOSITE ULTRASONIC SPECTROGRAM

PEG (Kessler, 1968a; O'Brien, 1968; Kessler et al., 1970),
PGA (Burke et al., 1965; Lewis, 1965),
DEXTRAN (Hawley et al., 1965; Hawley, 1966),
Hb, 25°C (Edmonds et al., 1970; Dunn et al., 1969)

Table 4-3

Properties of PEG Polymer Chains

(Kessler, 1968a; Kessler et al., 1970)

M	$[\eta]_o$ OBSERVED (cc/gm)	$[\eta]_o$ THEORETICAL (cc/gm)	β(Å)
4500	15.1	5.48	6.29
20,000	43.2	11.73	6.78

Table 4-4

Radius of Gyration for PEG from Indicated Source

M	R_G(Å) (Eqn. 4-4)	R_G(Å) (Fig. 4-10 - 0.30 gm/cc)
4500	26	16
20,000	59	30

Hb grade of about 10% at the lower frequencies, this difference disappearing at the higher frequencies. This possibly indicates the hemoglobin of lesser purity introduced some contaminant into the solvent which also possesses a relaxation behavior. This speculation is admittedly weak as the magnitude difference is small.

Figures 4-2, 4-13 and 4-14 are the ultrasonic spectrogram for aqueous solutions of the egg protein, ovalbumin, under varying degrees of purification, i.e., uncrystallized, twice crystallized and three times crystallized-salt free (dialyzed) all at 10.0°C over the frequency range 1.680-50.50 MHz. All three spectrograms are results of the molecule having zero net charge, that is, at the isoelectric point. Comparison of the absorption magnitudes of these three spectrograms is facilitated by the composite diagram of Fig. 4-18. The uncrystallized preparation shows a 10-20% lesser absorption than the Ov-2X with both indicating a similar frequency dependence. The

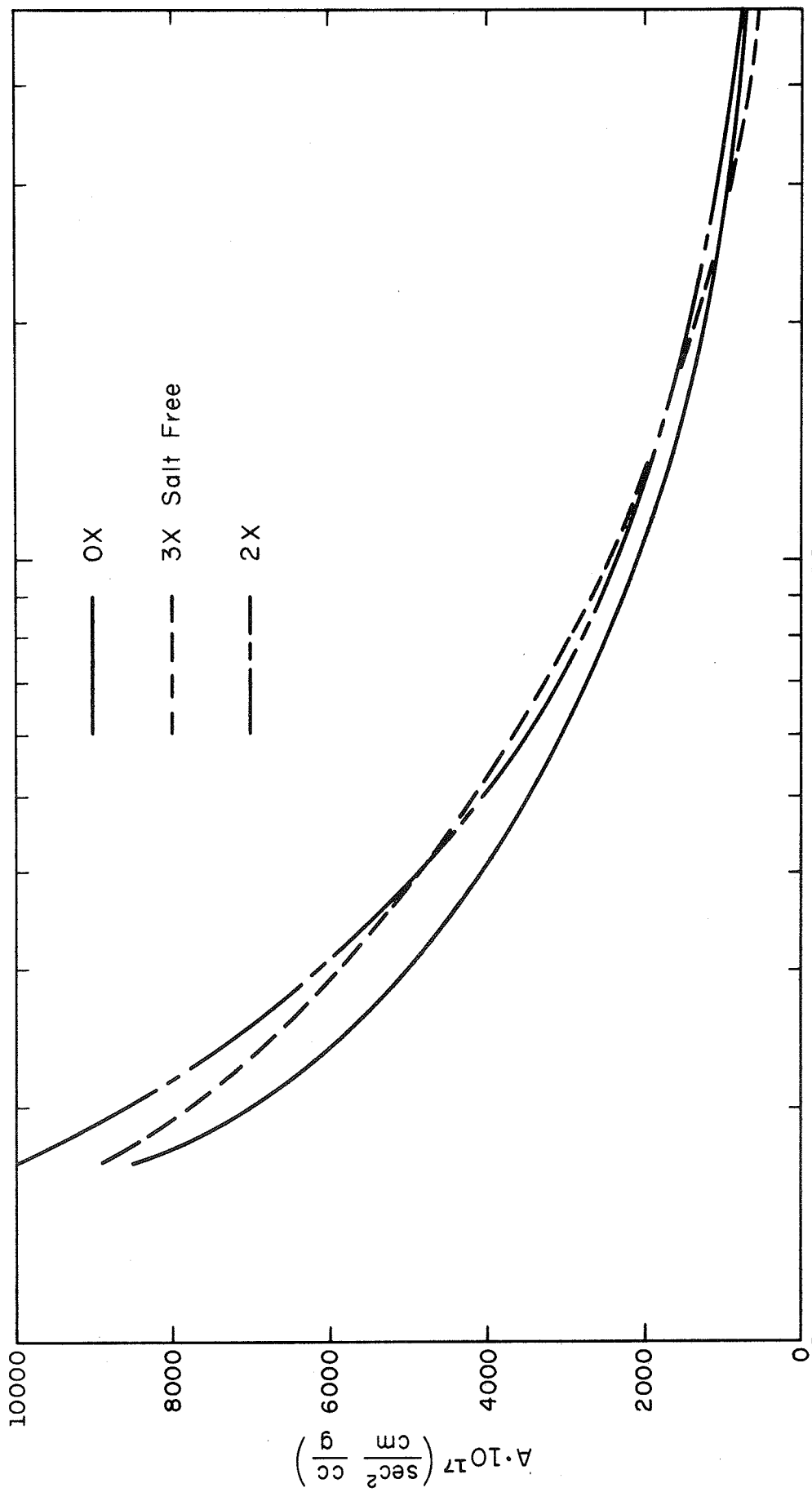

FIGURE 4-18

COMPOSITE ULTRASONIC SPECTROGRAM
OVALBUMIN (T = 10.0°C)

Ov-3X material exhibits an interesting spectrum in that it crosses the Ov-0X and Ov-2X spectra at least once, and this possesses a different frequency dependence. The manufacturer of the ovalbumin reported the Ov-2X (control #9343) and Ov-3X (control #9326) both originated from the same material, the latter being a continuation of the purification process in that it is once more crystallized and then dialyzed against distilled water. Thus the Ov-3X spectrum cannot be explained as being the result of different material. An experiment testing the effect of minute salt concentration changes will be discussed and interpreted following the discussion of BSA.

Finally, an ultraviolet spectrogram was obtained for the Ov-2X and Ov-3X to detect possibly any differences in the spectrum, but none were so detected. The two plots fell identically one upon the other.

Another globular protein, bovine serum albumin (BSA), was investigated to determine the importance of molecular weight on the magnitude and frequency dependence of the ultrasonic absorption of albumins (BSA - M = 68,000 and Ov - M = 46,000). The ultrasonic spectrogram in Fig. 4-15 results, in this study, from an aqueous solution of BSA-0X investigated at 10.0°C from 1.680-50.50 MHz at its isoelectric point. Comparison between the two albumins in Fig. 4-17 reveals no significant difference in the spectra, considering a difference of about 3:2 in their respective molecular weights. Thus it is concluded that molecular weight is not an important parameter in determining biopolymer absorption spectra. Further evidence of this is seen by noting that between BSA and Hb at 10.0°C in Fig. 4-17 there is roughly a 10-50% difference in the excess ultrasonic absorption magnitude and both of these molecules have approximately the same molecular weight.

Further, in Fig. 4-15, the difference in excess frequency-free absorption per unit concentration between the 10.0°C and 20.0°C (Kessler, 1968a) data becomes negligible at the higher frequencies of the spectrogram indicating that the excess absorption is independent of temperature, within this temperature range, at frequencies greater than 50 MHz. This result is quite possible since, at high frequencies, for a relaxing media, the absorption magnitude approaches asymptotically either the solvent value, if all energy exchange processes are relaxed, or, more likely, the magnitude of the unrelaxed higher frequency mechanisms. Owing to the method of data presentation, the former would result in a zero magnitude for the A parameter.

Also, according to the Hb plots at 10°C and 25°C in Fig. 4-17, the two approach each other at the higher frequencies, similar to the BSA case already discussed.

Crystallized BSA in aqueous solution showed a lesser excess absorption magnitude than the uncrystallized material used in this study at 20.0°C (Kessler, 1968b). This result is in agreement with the Hb data of Fig. 4-11 but in conflict with the Ov data shown in Fig. 4-18. This point is significant as it shows the importance of the polymer solution purity and the contaminant's effect upon the excess absorption magnitude. As differences in molecular weight can be ignored when comparing the same polymers, an experiment was performed to determine the effect upon the excess ultrasonic absorption due to slight variations in salt concentration. Two stock solutions of two liter volumes each, one BSA-0X and the other Ov-2X, were prepared to concentrations of approximately 0.025 gm/cc. Half of each (1 liter) was dialyzed three times for eleven hours each at

5-10°C against 100 liters of singly dionized and distilled water. In order to test for the amount of salt remaining after the dialysis procedure, a water sample of the third dialyzing medium was analyzed by the Illinois State Water Survey. Their result, via resistance measurement, indicated at most 0.90 parts per million (ppm). A sample from the distiller tested to, at most, 0.15 ppm. The ultrasonic spectrograms, Figs. 4-19 and 4-20, indicated up to a 20% decrease in excess absorption magnitude for the dialyzed protein solution compared to the stock solution. For ovalbumin, Fig. 4-19, the excess absorption magnitude always remains less for the dialyzed solution over the entire frequency range 1.68-19.70 MHz whereas for BSA, Fig. 4-20, the differences become negligible at the higher frequency limit. In both cases, the dialysis process removed some material which was contributing to the absorption spectra, as is evident in Fig. 4-21 where the difference between the non-dialyzed and dialyzed ultrasonic absorption parameters, $A_{ND} - A_D$, is plotted. Considering the kinds of small ion(s) or molecule(s) removed in the dialysis process which can exhibit similar relaxation behavior as that shown in Fig. 4-21, the 1-1 electrolytes must be ruled out as their magnitude and frequency spectra have shown to not correlate with Fig. 4-21 (Stuehr and Yeager, 1965). For example, NaCl solutions have negligible excess absorption relative to pure water (Leonard, 1950). Though it is possible that some amino acids such as glycine were dialyzed out, the excess ultrasonic absorption per unit concentration to be expected is approximately $100 \times 10^{-17} \frac{sec^2}{cm} \cdot \frac{cc}{gm}$ for glycine and one-third that for triglycine, both at 4°C and below 10 MHz (Hammes and Pace, 1968). This is also much less in magnitude than depicted in Fig. 4-21. Finally, it should be noted that for the Ov-2X,

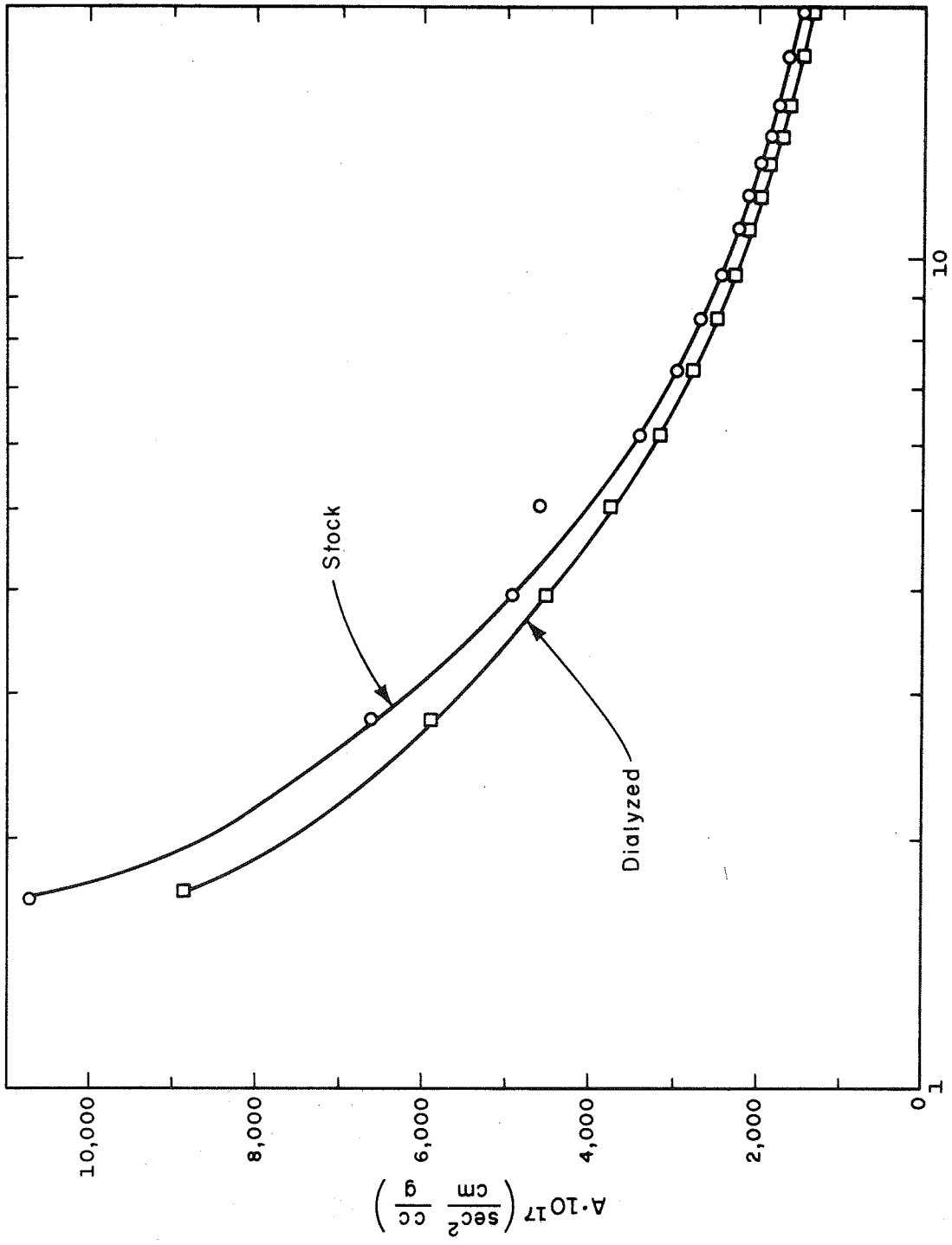

FIGURE 4-19
ULTRASONIC SPECTROGRAM
OVALBUMIN-2X (T = 10.0°C)

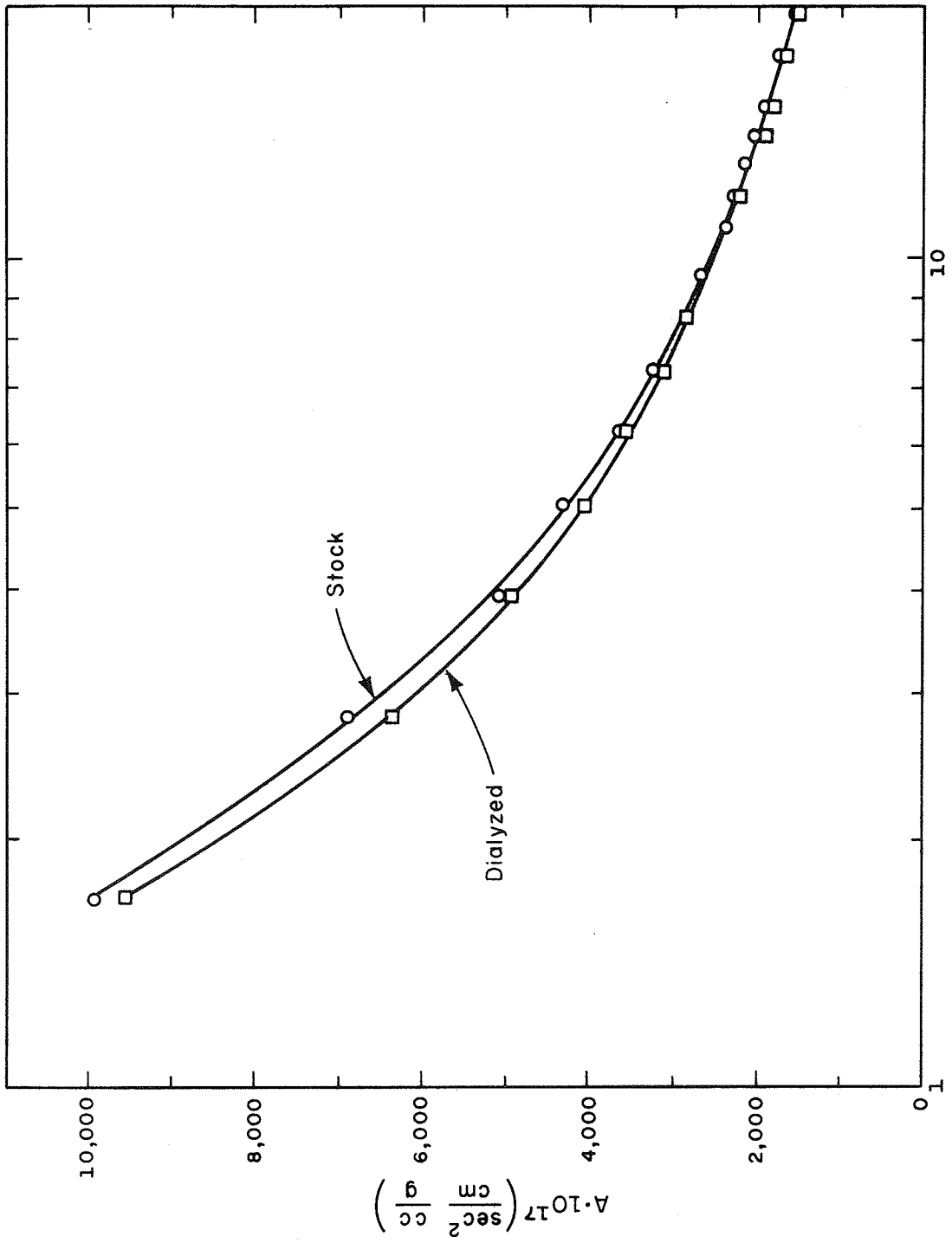

FIGURE 4-20
ULTRASONIC SPECTROGRAM
BOVINE SERUM ALBUMIN (T = 10.0°C)

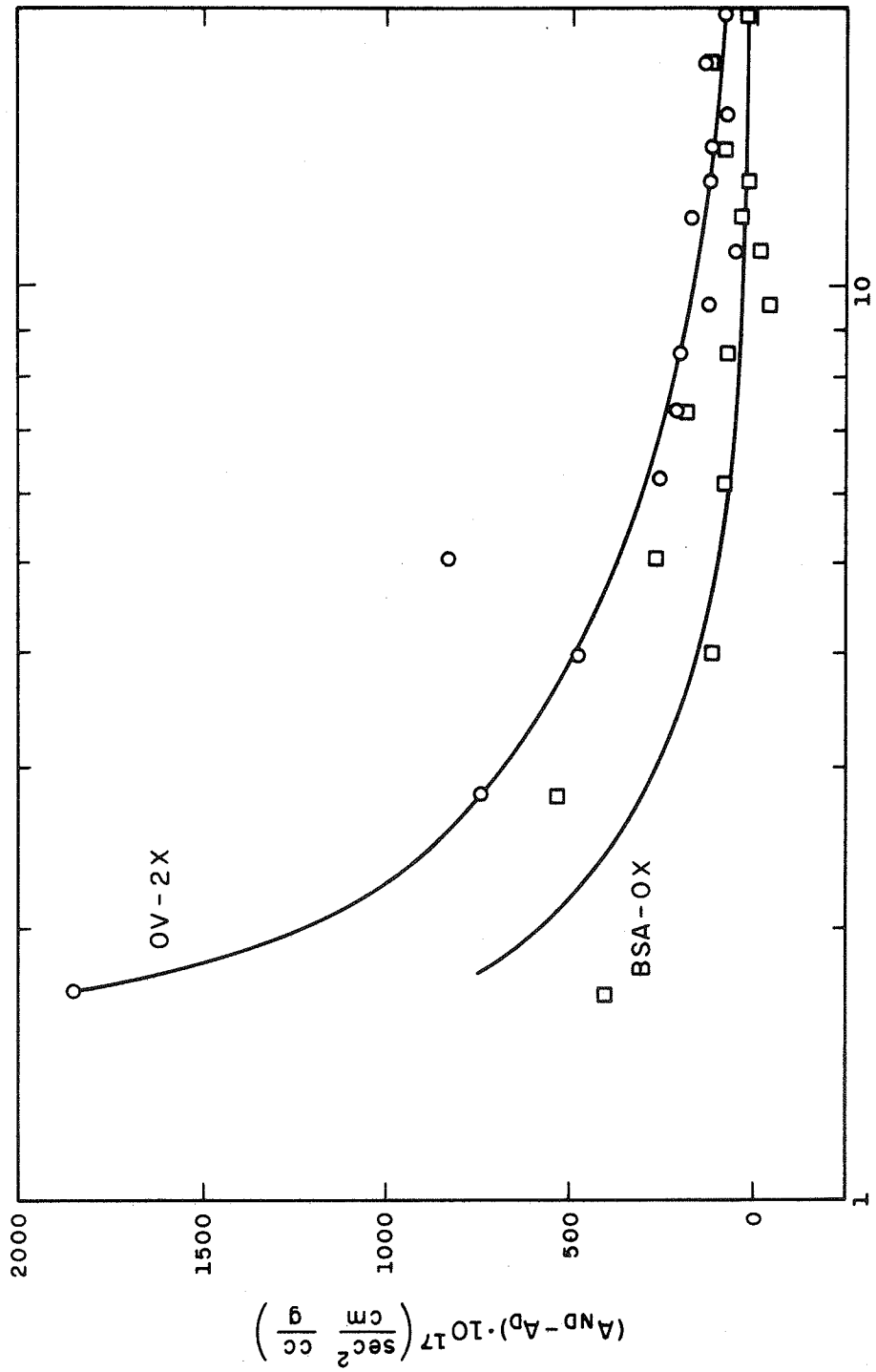

FIGURE 4-21
ULTRASONIC SPECTROGRAM
(See Text for Explanation)

$A_{ND} - A_D$ is much greater than that for the BSA-OX. Comparing the two stock solutions, the Ov-2X should be of a much purer quality than the BSA-OX, resulting in less contaminants being removed during the dialyzing procedure.

The three biopolymers discussed so far, viz., hemoglobin, ovalbumin and serum albumin, are all globular proteins. Another biological molecule of considerable importance which has a much different structure than the globular proteins is deoxyribonucleic acid (DNA). This molecule has a rod-like structure composed of two polynucleotide chains in the form of a double helix with a diameter between 12 and 22 Å and a length linearly dependent upon molecular weight. According to the Watson-Crick (1953) model, the mass per unit length ratio is 185 daltons/Å, a dalton being the molecular weight unit of mass. Thus for a double stranded DNA molecule of molecular weight around 10^6, the length of this biopolymer is 5400 Å. The ultrasonic spectrogram shown in Fig. 4-16 was obtained at 10.0°C with an aqueous solution of Deoxyribonucleic Acid Sodium Salt (calf thymus) of molecular weight about 10^5, yielding a length of the order of 540 Å. The solute concentration was around 0.025 gm/cc. Also plotted on Fig. 4-16 are three data points for a 10.0°C aqueous solution of highly polymerized salmon sperm DNA (around 10^6), at a concentration of 0.00358 gm/cc. The solvent for the calf thymus DNA is water whereas for the salmon sperm DNA it is SSC (0.15 M NaCl + 0.015 M $Na_3C_6H_5O_7$), and the ultrasonic absorption of both being plotted as a function of temperature in Fig. 4-1. The citrate ion functions as a chelating agent, that is, it binds the metal ion necessary in the enzymatic degradation of the DNA molecule.

Comparison of the aqueous solutions of calf thymus DNA and the globular proteins shows (Fig. 4-17) a lesser ultrasonic absorption

magnitude for the DNA by 8-15%. The DNA frequency dependence is similar to that of Hb but not to that of Ov, the latter slope being greater than the calf thymus DNA or Hb. In addition, for equivalent solute concentrations of 0.00358 gm/cc at 10.0°C, the ultrasonic velocity in salmon sperm DNA solutions is 1460.5 m/s whereas the extrapolated values (see Figs. 4-4, 4-5 and 4-7) for Hb is 1449.6 m/s and for Ov is 1450.0 m/s.

The calf thymus DNA is not of the highest quality and it is suspected that approximately 1-2% of the dry extractant is protein. This is deduced from the extinction coefficient, $E\Big|_{1\ cm}^{1\%}$ versus ultraviolet wavelength, λ, curve of Fig. 4-22 where the ratio $E_{280}/E_{260} = 0.61$. For very pure nucleic acids this ratio is 0.5 while for very pure protein it is 1.75, where variations in the latter ratio result as the number of protein aromatic groups vary (Clark, 1964).

Thus far the discussion of the aqueous solutions of biopolymers has been concerned with the observed ultrasonic absorption spectra near their isoelectric point, pI. Altering the pH from the pI by the addition of either HCl or KOH results in changes of the molecular charge distribution and consequently its conformation. Thus buried amino acid side chains of globular proteins, as a result, are exposed to the surrounding environment, which, as will be discussed, can alter the acoustical properties of the solution. As the pH is decreased from the pI, the globular proteins acquire a positive charge, whereas a net negative charge accumulates for a base titration at pH's greater than the isoelectric point. As a result of the net charge due to titrating an acid or base, most proteins have a tendency to expand, due to the repulsive electrostatic forces between similarly charged side chains (Martin, 1964).

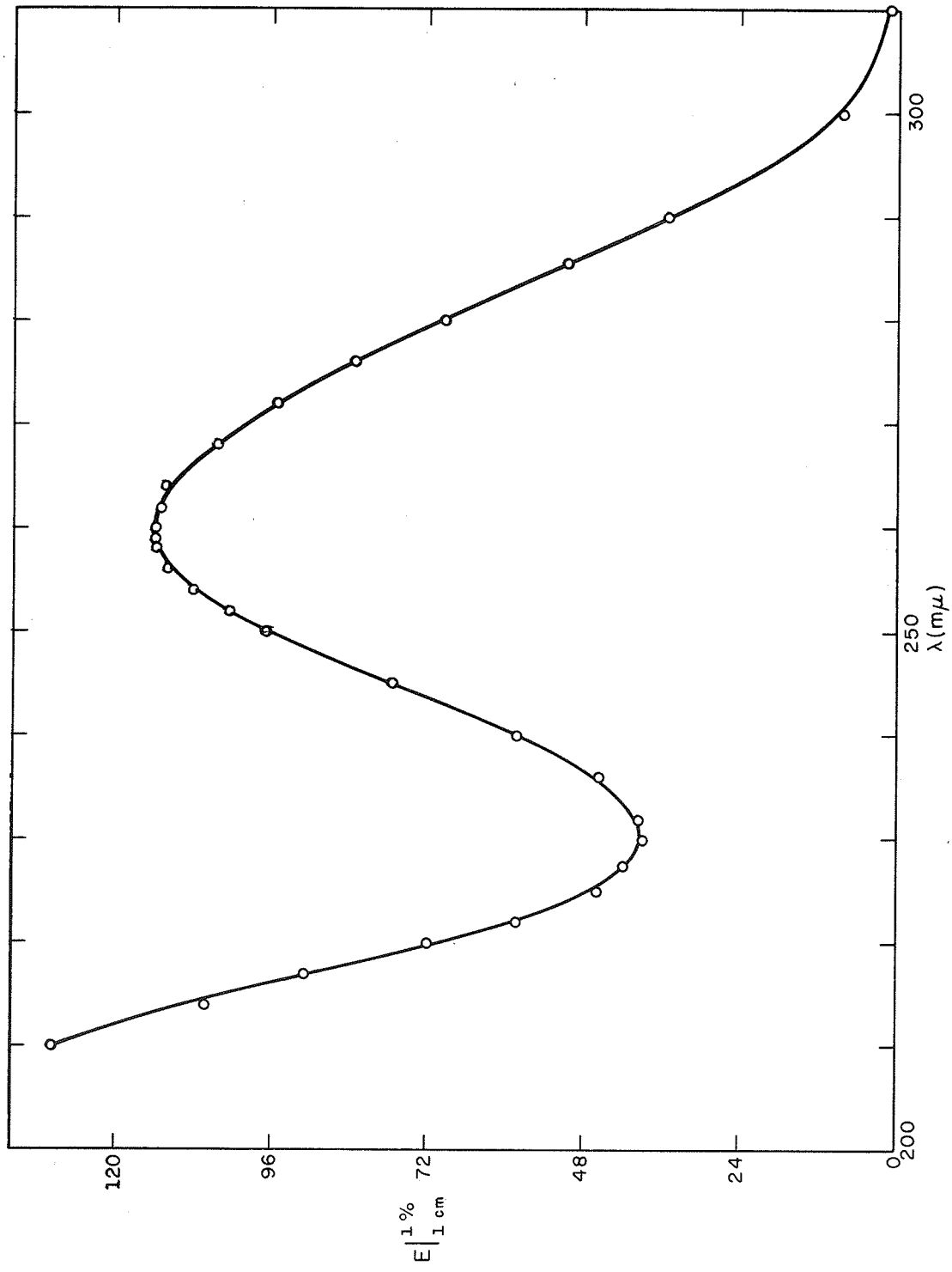

FIGURE 4-22
EXTINCTION COEFFICIENT VS WAVELENGTH
CALF THYMUS DNA

The ultrasonic titration of hemoglobin has been examined extensively in this study. Figures 4-23 and 4-24 represent the ultrasonic absorption titration curves, i.e., A vs pH at constant frequency and temperature for Hb-OX at 10.0°C over the frequency range 2.390-50.50 MHz. These two figures represented preliminary titration data for hemoglobin. The general shape of these titration curves resembled quite closely the titration curves for BSA, see Fig. 4-25, (Kessler, 1968a; Kessler and Dunn, 1969), the increase in excess absorption below pH 4.3 in BSA being correlated with the intermediate N-F' transition (Foster, 1960). The N form of the BSA molecule represents its compact, rigid conformation which results in aqueous solutions at $4.3 < pH < 10.5$. The F' state corresponds to the molecule expanding, as the pH is reduced to between 4.3-3.6, into two subunits linked together by a flexible polypeptide chain. However, Hb does not exhibit this form of transition yet the increased excess absorption occurs within the same pH range. Similarly, in the alkaline pH region, both BSA and Hb show excess absorption increases beyond pH 9.5. Thus it is tempting to conclude that the cause for such similar titration behavior is attributable to similar processes occurring in both Hb and BSA.

The ultrasonic absorption titration curves were repeated for a purer preparation of bovine hemoglobin and these results are shown in Figs. 4-26 and 4-27. The alkaline pH measurements were extended beyond 12.2 and show an excess absorption peak around pH 12.2. The composite curve, Fig. 4-28, which includes both grades of Hb indicate that the uncrystallized hemoglobin did not indicate the peak since the absorption measurements were not extend beyond pH 12.2. The composite ultrasonic absorption titration curve also shows the similar trends between the two Hb grades. The differences in the

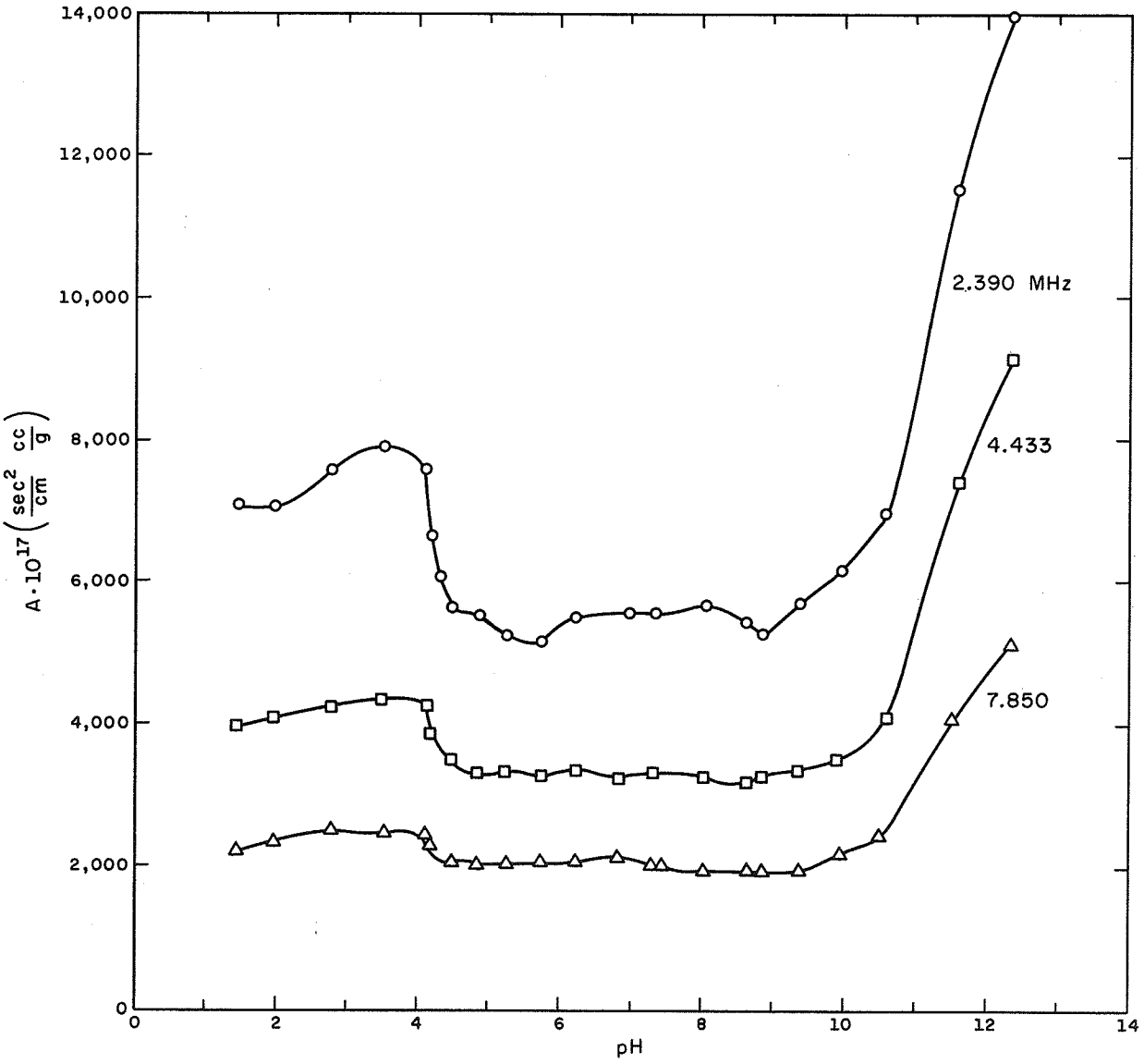

FIGURE 4-23

ULTRASONIC ABSORPTION TITRATION CURVE
BOVINE HEMOGLOBIN-OX (T = 10.0°C)

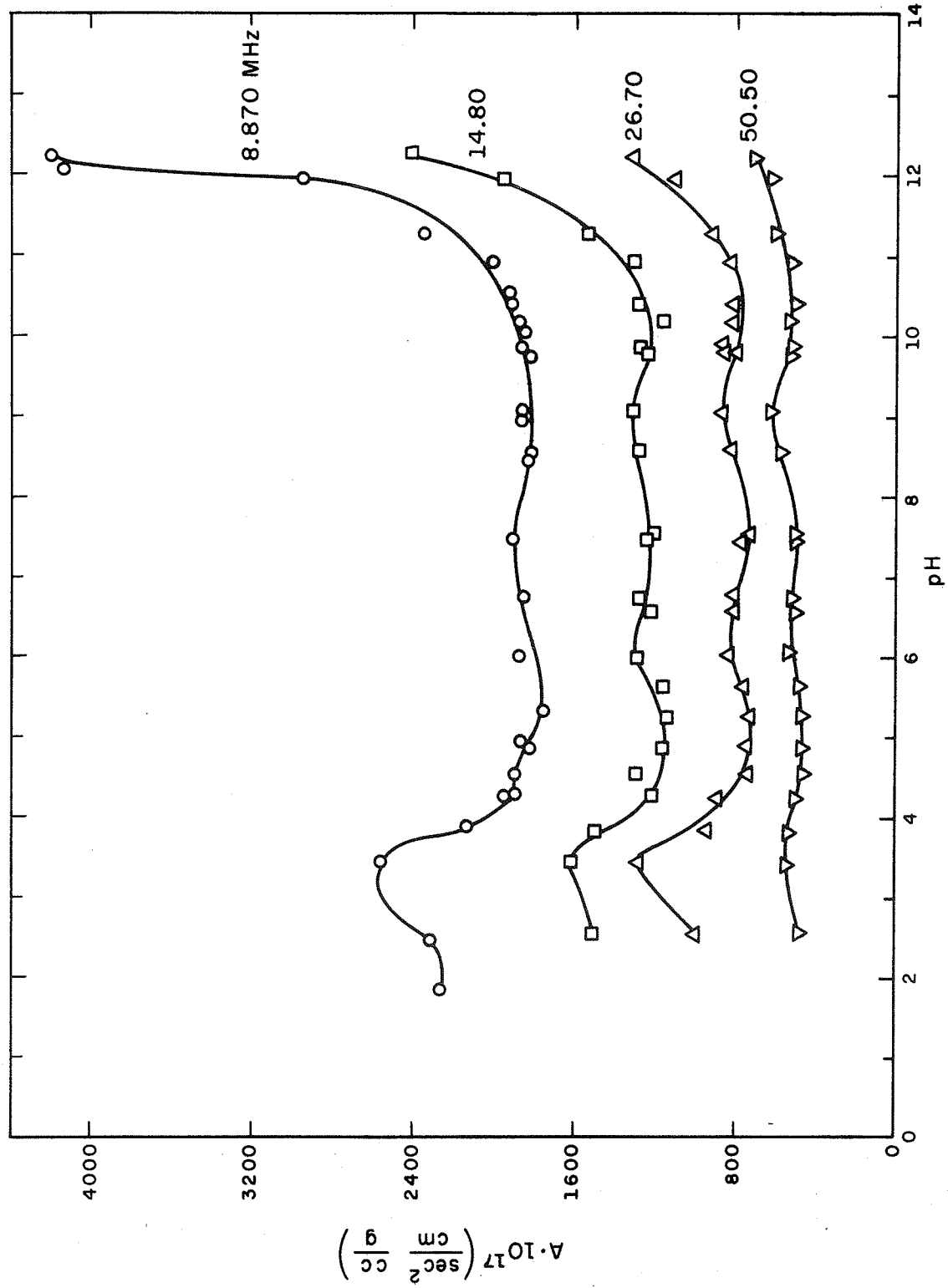

FIGURE 4-24

ULTRASONIC ABSORPTION TITRATION CURVE
BOVINE HEMOGLOBIN-OX (T = 10.0°C)

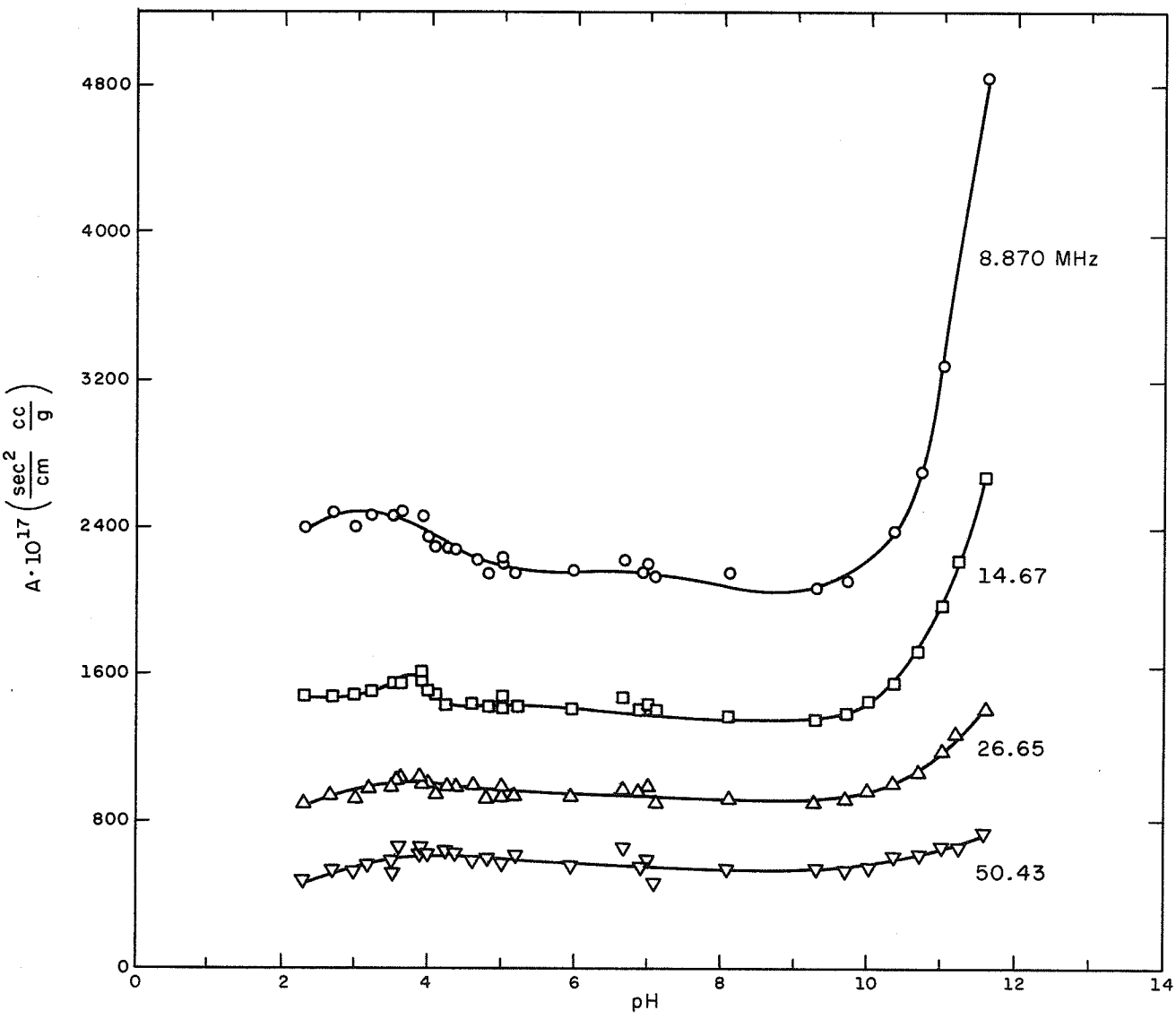

FIGURE 4-25

ULTRASONIC ABSORPTION TITRATION CURVE
BOVINE SERUM ALBUMIN (T = 20.0°C)
(Kessler, 1968a)

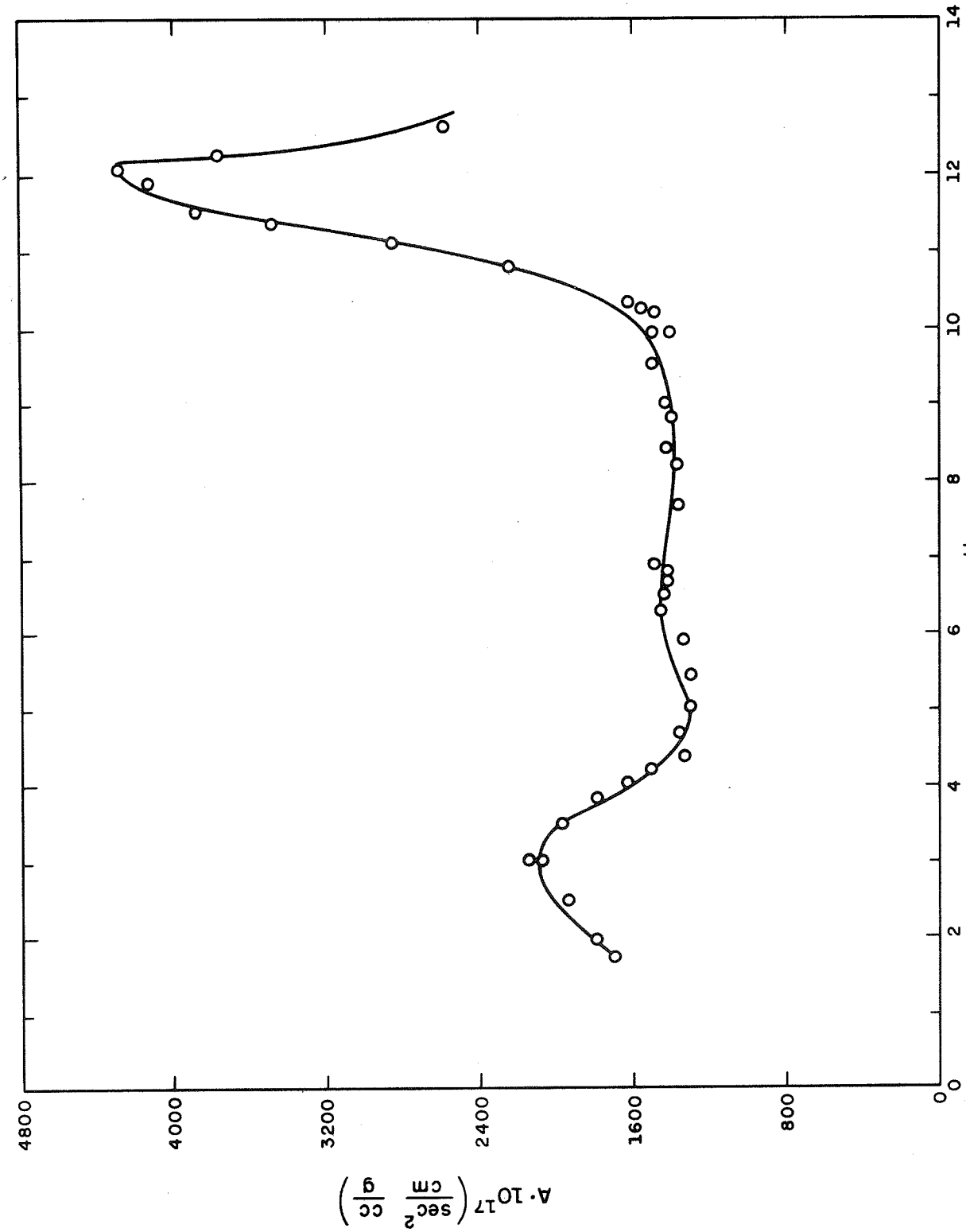

FIGURE 4-26

ULTRASONIC ABSORPTION TITRATION CURVE
BOVINE HEMOGLOBIN-2X (T = 10.0°C; f = 10.22 MHz)

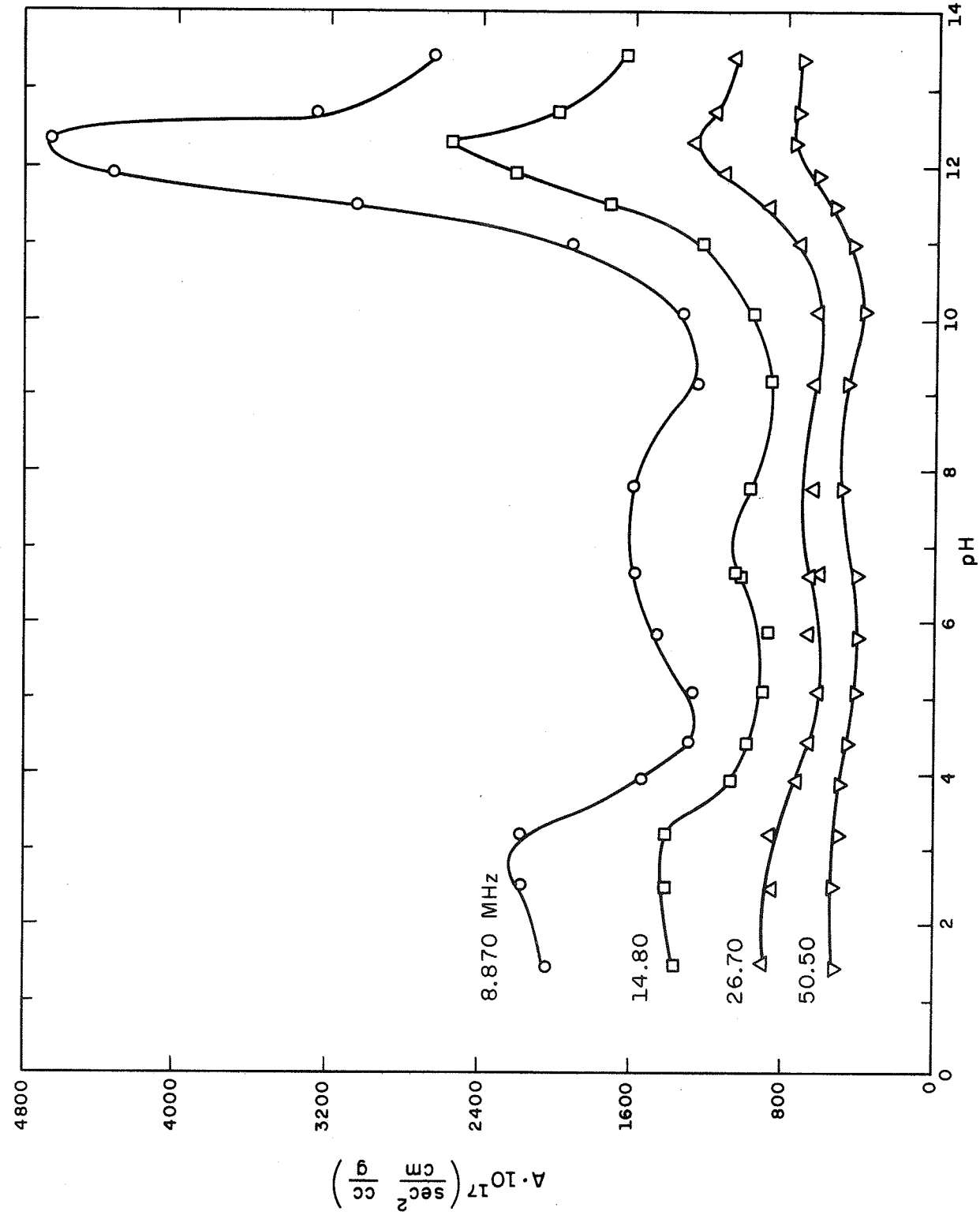

FIGURE 4-27

ULTRASONIC ABSORPTION TITRATION CURVE
BOVINE HEMOGLOBIN-2X (T = 10.0°C)

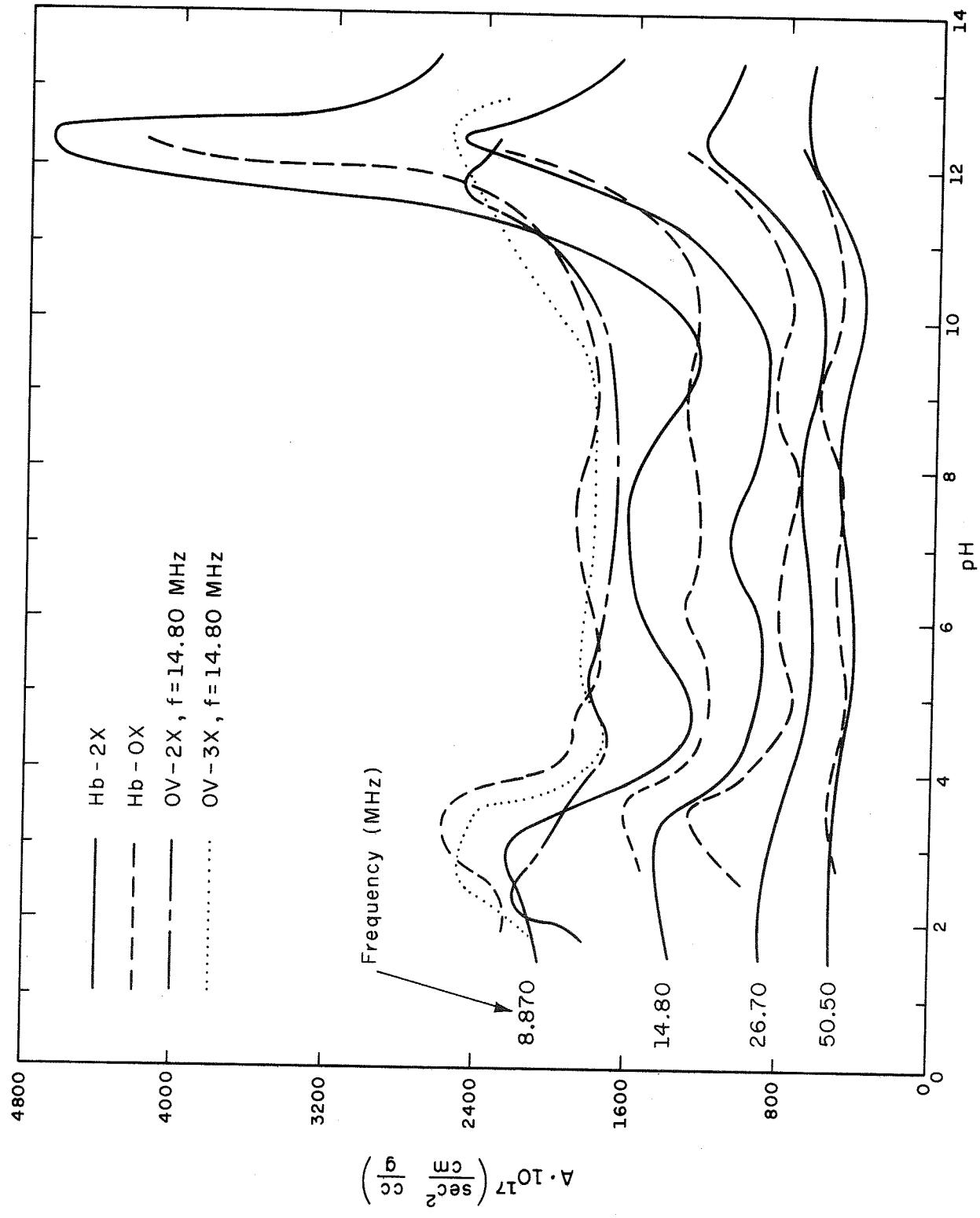

FIGURE 4-28
COMPOSITE ULTRASONIC ABSORPTION
TITRATION CURVE (T = 10.0°C)

absorption magnitude peaks will be discussed below when the mechanism responsible for these peaks in the absorption curve for Hb, BSA and Ov in the neighborhoods pH 2-4 and 11-13 is discussed.

The temperature dependence of the aqueous solution of Hb-2X in the alkaline pH range of 9-13.5 is shown in Fig. 4-29. The general trend from the 10.0°C to 35.4°C curves is a decrease in the excess ultrasonic absorption and a reduction in the pH value at which the curve peaks.

Finally, the effect on the ultrasonic velocity in aqueous solutions of Hb-2X at 10.0°C as a function of pH is shown in Fig. 4-30, the ordinate parameter being defined as

$$\frac{\Delta v}{c} = \frac{v_{Hb} - v_{H_2O}}{c} \qquad (4\text{-}7)$$

where v_{Hb} is the speed of sound in the hemoglobin solution at concentration, c, and v_{H_2O} is that of the solvent (Greenspan and Tschiegg, 1959) at the stated temperature. The excess velocity curve is constant within the pH range 4-10 and increase outside these limits, with these increases corresponding to the absorption increases of Figs. 4-26 and 4-27.

The ultrasonic absorption titration curve for aqueous solutions of Ov-2X and Ov-3X are shown in Fig. 4-31 for only one frequency, viz., 14.80 MHz, at 10.0°C, where it is seen that they behave very much like those of Hb and BSA. Figure 4-31 curves are superimposed on the composite titration curve of Fig. 4-28 for comparison with Hb.

Figure 4-32 is the ultrasonic absorption titration curve in the acid pH region at 10.0°C and 25.0°C over the frequency range 5.690-19.30 MHz for aqueous solutions of highly polymerized DNA. It is seen that an absorption maximum also occurs for this biopolymer in the pH region 2.5-2.7.

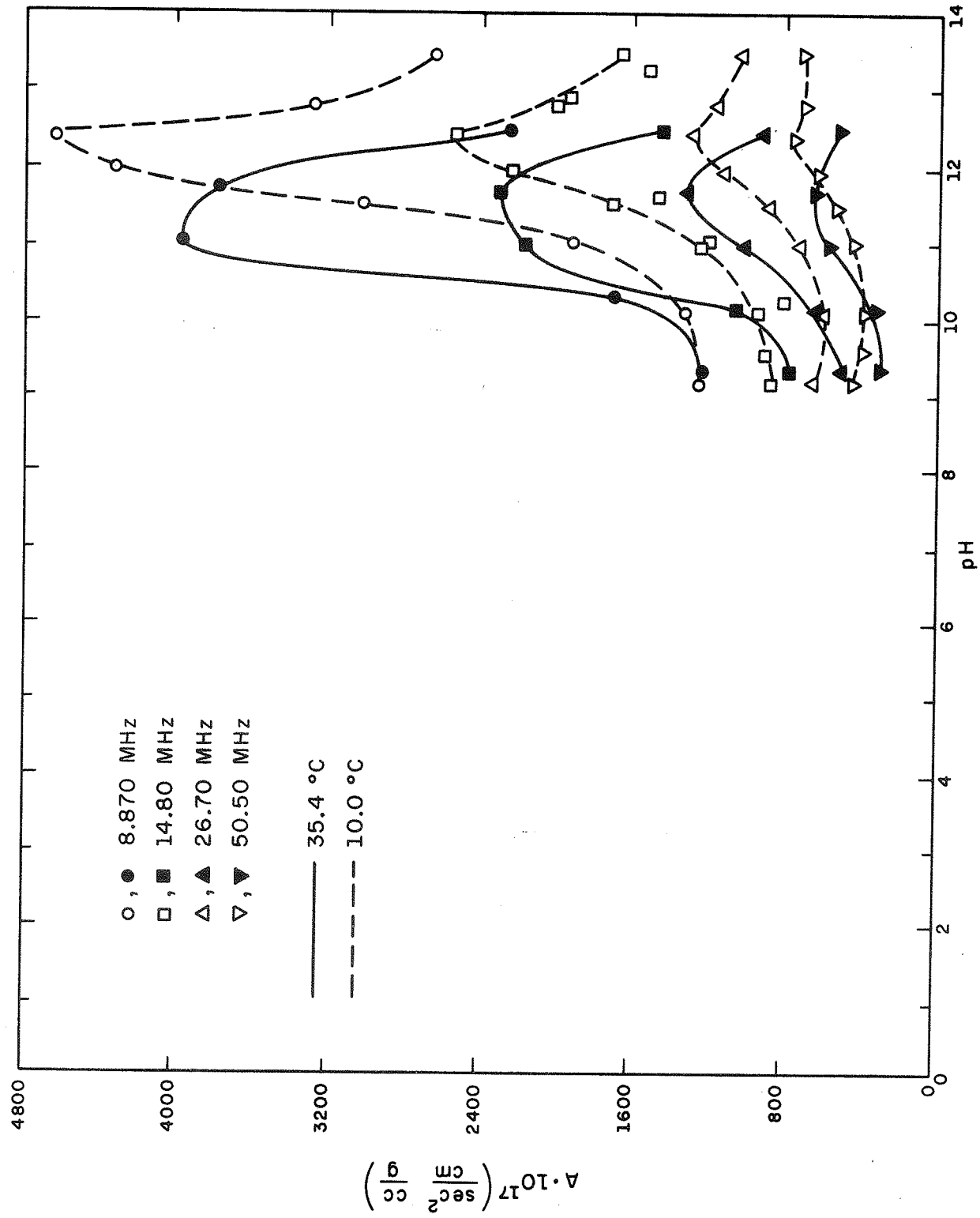

FIGURE 4-29

ULTRASONIC ABSORPTION TITRATION CURVE
BOVINE HEMOGLOBIN-2X

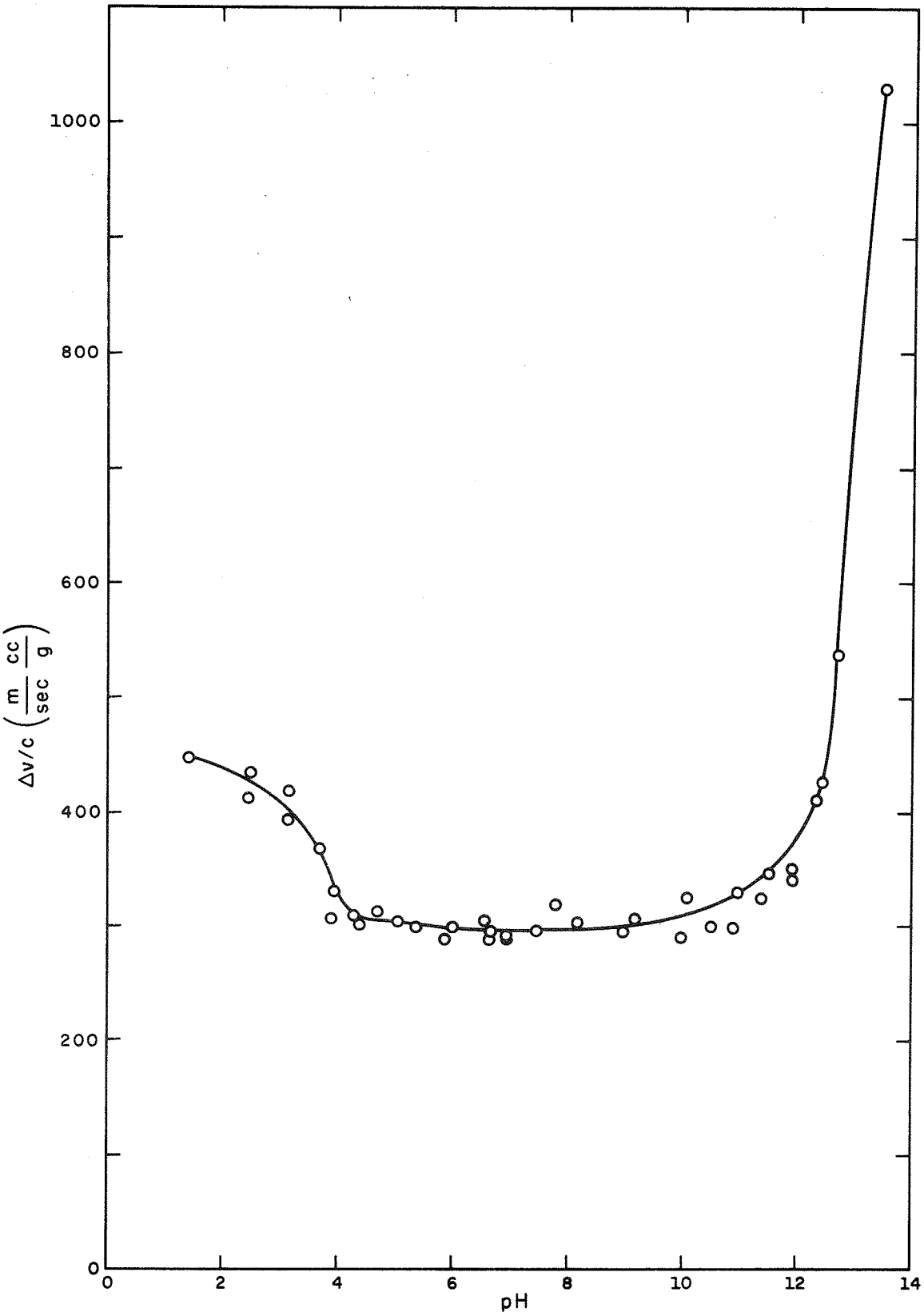

FIGURE 4-30

ULTRASONIC VELOCITY TITRATION CURVE
BOVINE HEMOGLOBIN-2X (T = 10.0°C; f = 8.870 MHz)

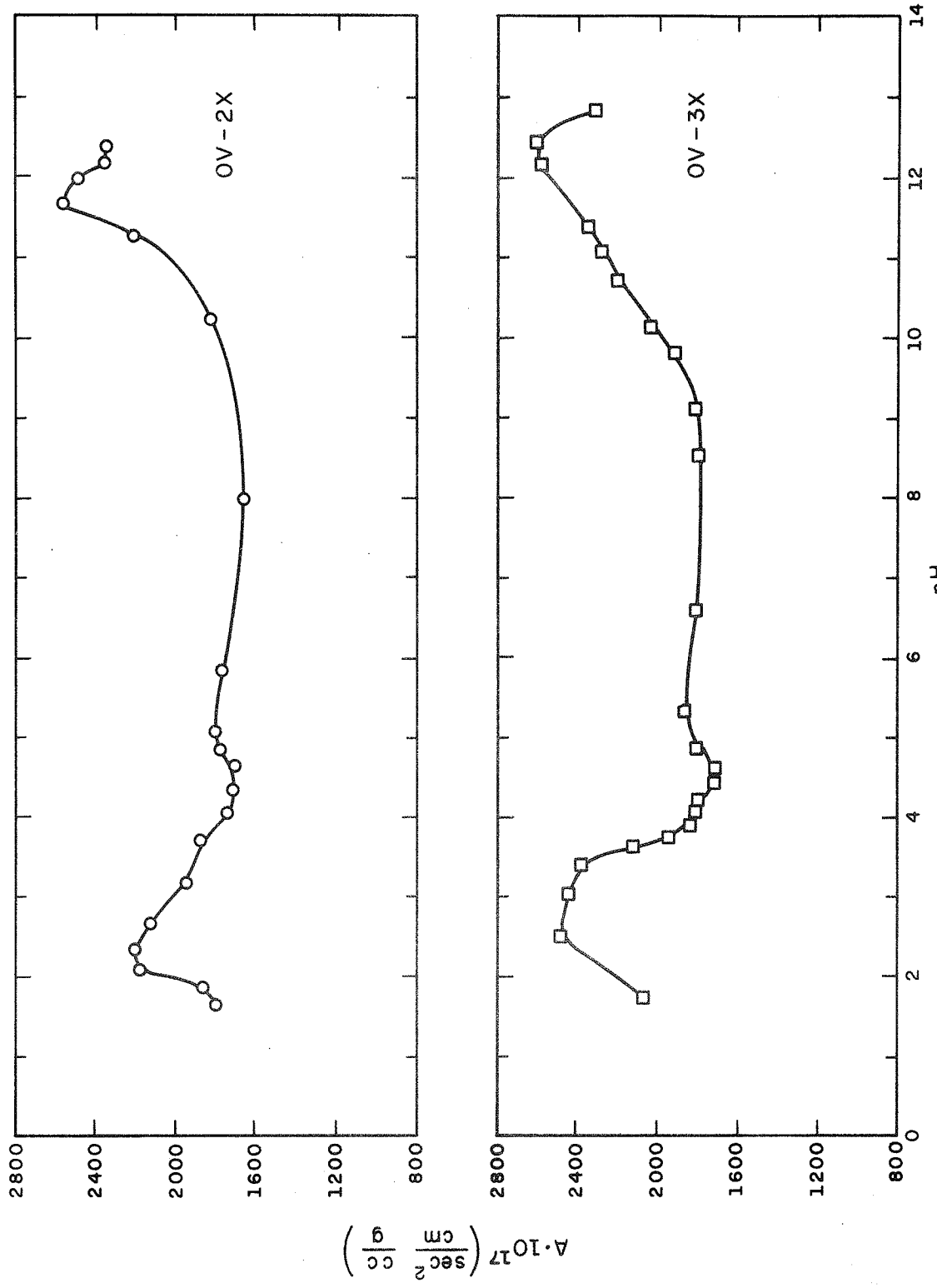

FIGURE 4-31

ULTRASONIC ABSORPTION TITRATION CURVE
OVALBUMIN-2X AND 3X (T = 10.0°C; f = 14.80 MHz)

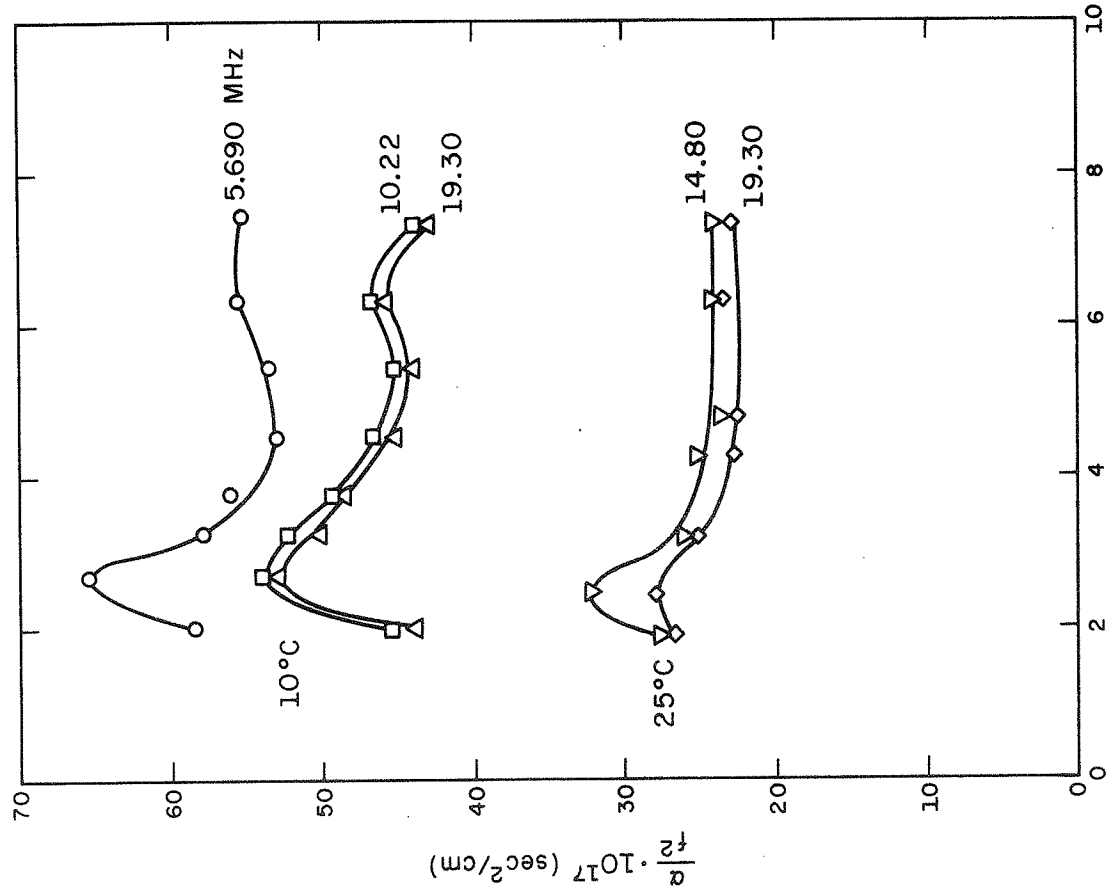

FIGURE 4-32

ULTRASONIC ABSORPTION TITRATION CURVE
SALMON SPERM DNA (T = 10.0°C AND 25°C)
(T = 25°C, Christman, 1970)

No detectable velocity dependence on pH was observed at either temperature within the accuracy of the measuring system ± 0.5 m/s.

The conformal changes in hemoglobin which result from guanidine hydrochloride (GuHCl) solutions have been characterized by a number of investigators (Kurihara and Shibata, 1960; Kawahara et al., 1965). Thus, in order to correlate the excess ultrasonic absorption of hemoglobin solutions to the known conformal changes which this biopolymer experiences as the GuHCl concentration is varied, it is necessary to investigate first the solvent (aqueous solutions of GuHCl) as a function of concentration, temperature and frequency. Figure 4-33 shows the frequency-free (total) ultrasonic absorption as a function of molar concentration at 10.0, 22.2 and 37.1°C. No relaxation processes were observed, though the absorption is always less than that of the solvent, at the same temperature. The minimum in α_{OBS}/f^2 appears to occur at lesser concentrations as the temperature increases.

Figure 4-34 shows the ultrasonic velocity, at 8.870 MHz, of the aqueous solutions of GuHCl as a function of concentration. The most interesting detail of this figure, which includes the three temperatures 10.0, 22.2 and 37.1°C, is its anomolus behavior at 6.5 M GuHCl where the three curves intersect, indicating temperature independence within this thermal range.

The observed ultrasonic absorption of GuHCl can be divided into two parts, one due to the shear viscosity of Stokes and the other due to structural effects. The former can be calculated from Stokes' equation for frequency-free absorption due to shear viscosity by using the values of viscosity and density calculated from the empirical equations (Kawahara and Tanford, 1966)

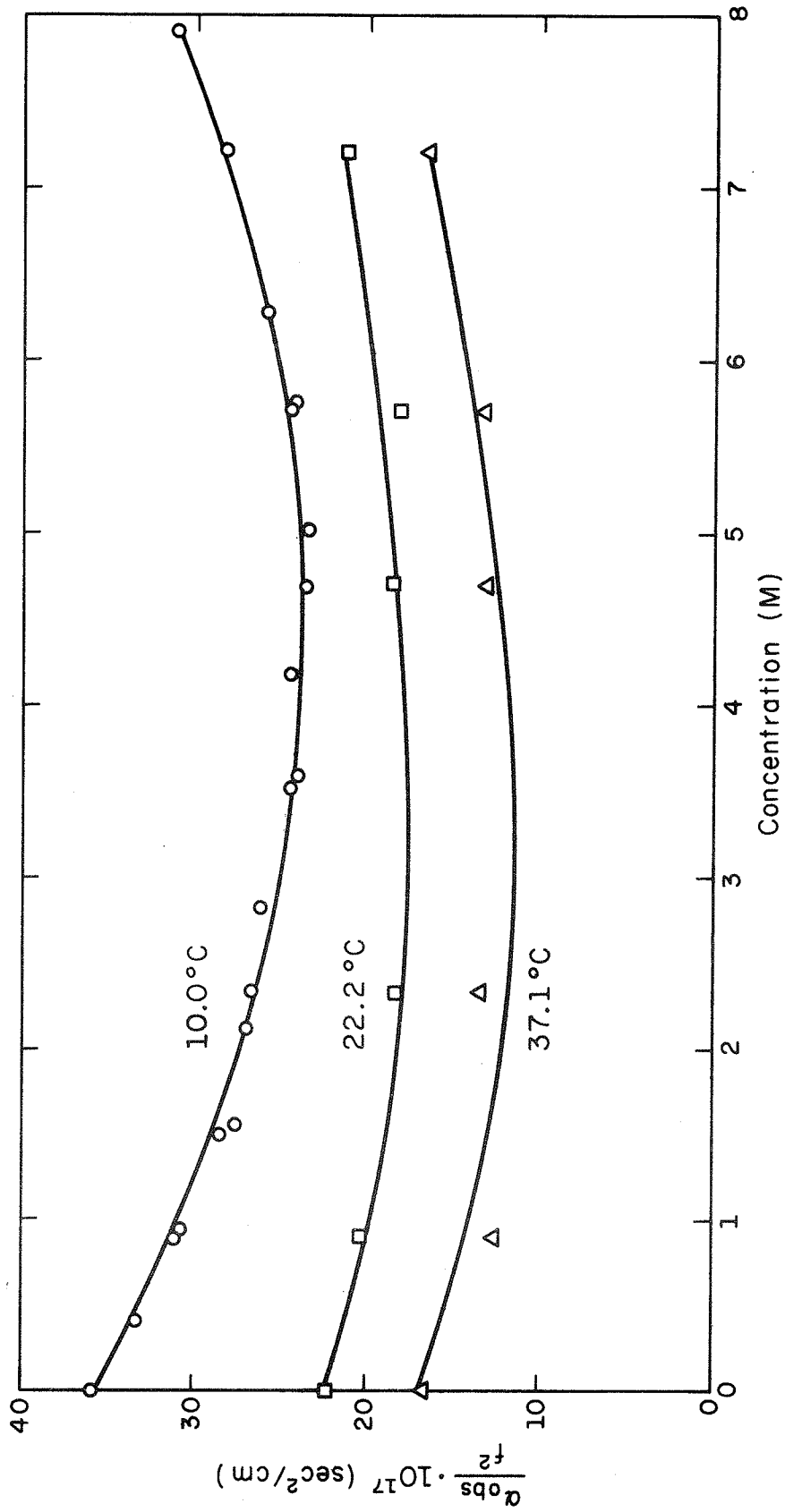

FIGURE 4-33

CONCENTRATION DEPENDENCE ON OBSERVED ABSORPTION
GUANIDINE HYDROCHLORIDE (f = 8.870-50.50 MHz)

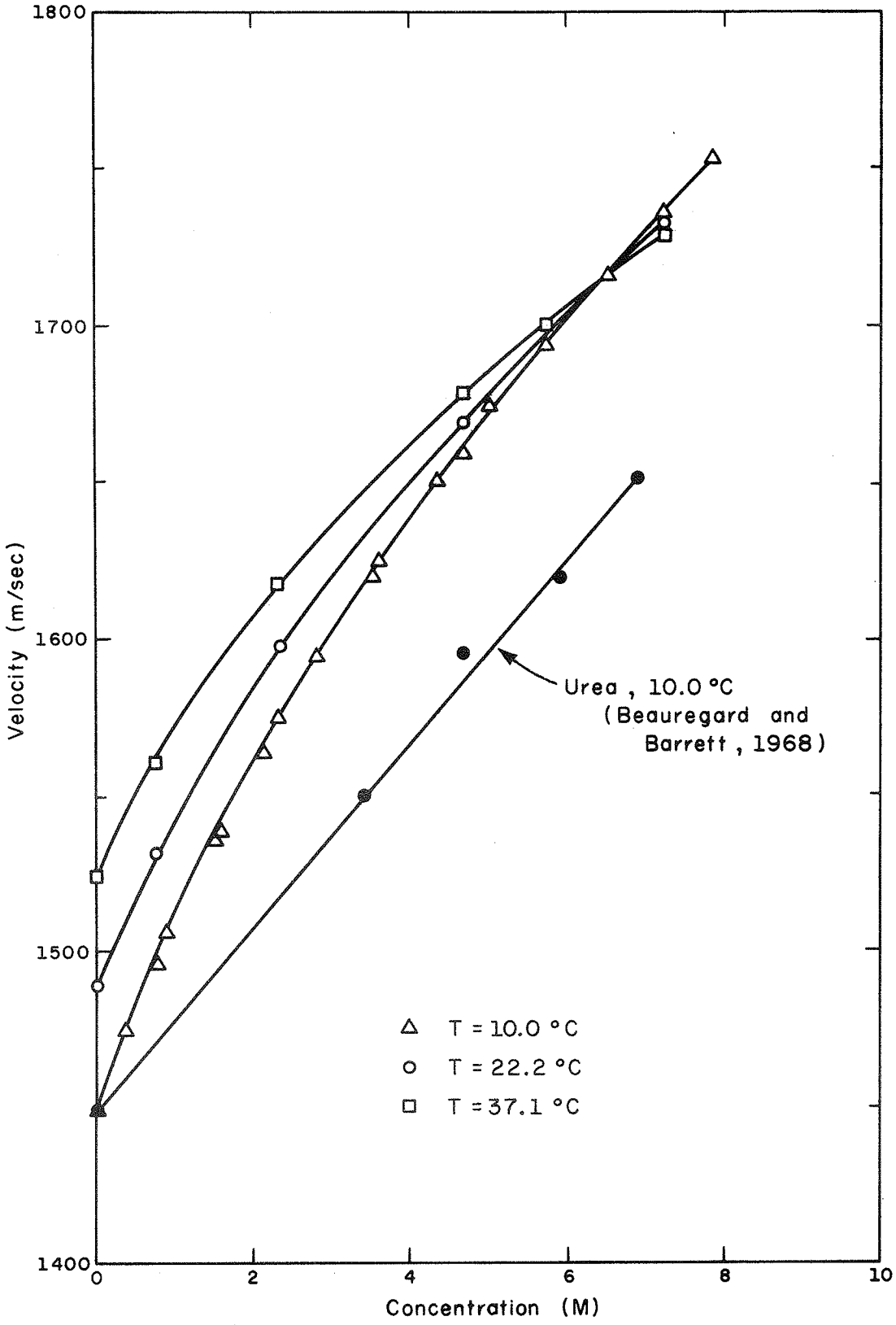

FIGURE 4-34

CONCENTRATION DEPENDENCE ON VELOCITY
GUANIDINE HYDROCHLORIDE (f = 8.870 MHz)

$$\eta = \eta_o[1 + 0.005m^{1/2} + 0.0180m + 0.01213m^{3/2}] \qquad (4\text{-}8)$$

$$\rho = \rho_o[1 + 0.271W + 0.0330W^2] \qquad (4\text{-}9)$$

where η_o and ρ_o are the values for water at the appropriate temperature for viscosity and density, m is the molal concentration and W represents the weight fraction of GuHCl in the solution. Although these two equations are applicable within the temperature range 15-35°C, the extention to 10.0°C and 37.1°C should not introduce appreciable error. Therefore substituting (4-8) and (4-9) into

$$\frac{\alpha_{SHEAR}}{f^2} = \frac{8\pi^2}{3c_o^3}\frac{\eta}{\rho} \qquad (4\text{-}10)$$

and using the velocity values in Fig. 4-34 and η_o and ρ_o values in Table 4-5, yields Fig. 4-35a. Taking the difference between the observed absorption and that due to shear viscosity to obtain the absorption due to structural effects, i.e.,

$$\frac{\alpha_{STRUCTURAL}}{f^2} = \frac{\alpha_{OBS}}{f^2} - \frac{\alpha_{SHEAR}}{f^2} \qquad (4\text{-}11)$$

yields Fig. 4-35b.

Table 4-5

Viscosity and Density Values for Water

T (°C)	ρ_o(gm/cc)[a]	η_o(cp)[b]
10.0	0.99973	1.310
22.2	0.99772	0.9554
37.1	0.99332	0.6907

[a] Weast and Selby (1966-67) page F-4

[b] Dorsey (1940) page 183

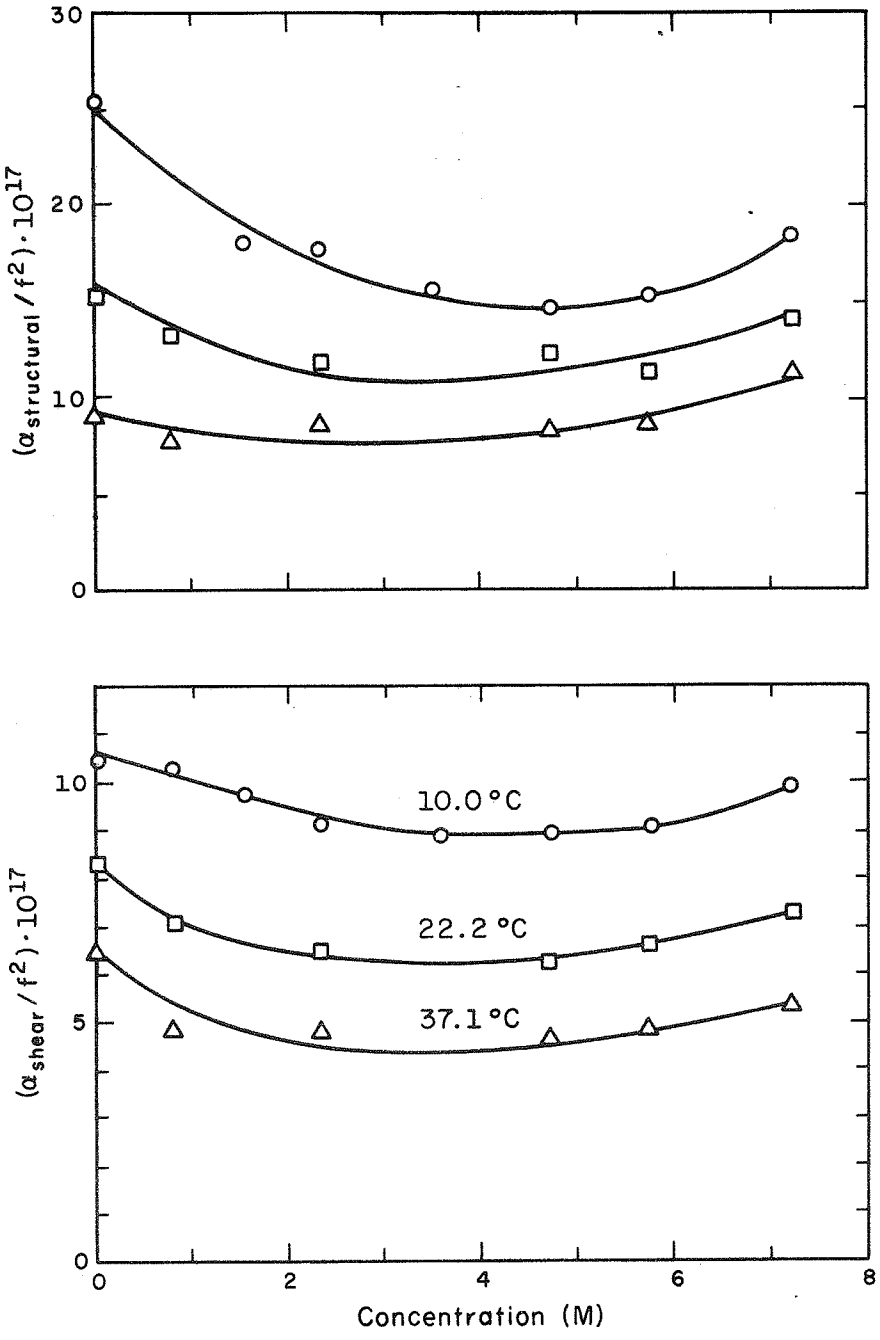

FIGURE 4-35

CONCENTRATION DEPENDENCE ON SHEAR
AND STRUCTURAL COMPONENTS OF ABSORPTION
GUANIDINE HYDROCHLORIDE (f = 8.870-50.50 MHz)

Now to investigate the effect of aqueous solutions of GuHCl on hemoglobin, the GuHCl concentration was increased to 5.4 M for Hb-0X and to 6.8 M for Hb-2X as is indicated in Figs. 4-36 and 4-37, respectively, where the ordinate parameter is defined as

$$A = \frac{\alpha_{OBS} - \alpha_{GuHCl}}{c_{Hb} \quad f^2} \tag{4-12}$$

where α_{OBS} is the measured absorption at frequency f and hemoglobin concentration, c_{Hb}, and α_{GuHCl} is the absorption of the solvent (the aqueous solution of GuHCl) taken from Fig. 4-33. Whether or not this is a valid method of presenting this data is not known since it has not been determined whether the absorption is a linear function of hemoglobin concentration for each of the solvents. In any case, the trend seems to be that initially the absorption parameter increases to a maxima, around 1.8 M GuHCl for Hb-0X and 2.1 M GuHCl for Hb-2X, and then decreases, finally leveling off for GuHCl concentrations greater than 4-5 M, the higher frequencies leveling off at lower concentrations.

If the assumption is valid that the ultrasonic absorption in aqueous solutions of biopolymers is a result of a viscous process, either shear or bulk, then the temperature dependence of this viscous process can be described by (Eyring, 1936; Hirai and Eyring, 1958)

$$\eta = \eta_o e^{\Delta F'/RT} \tag{4-13}$$

where F' represents the apparent activation energy of the particular viscous process concerned, R is the gas constant and T is the absolute temperature. Substituting (4-13) into the frequency-free (total) absorption equation (Herzfeld and Litovitz, 1959)

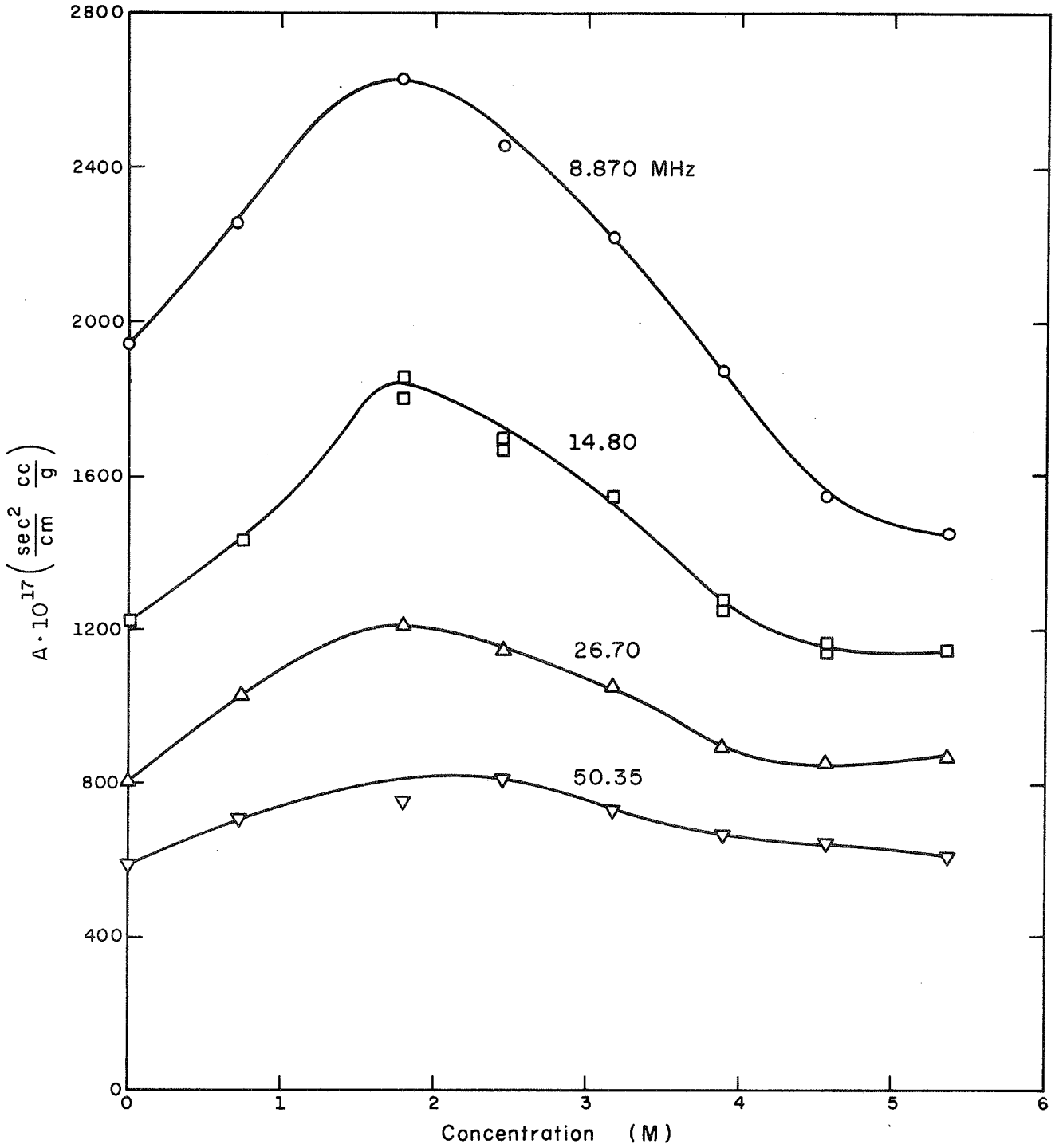

FIGURE 4-36

GuHCl CONCENTRATION TITRATION
BOVINE HEMOGLOBIN-OX (T = 10.0°C)

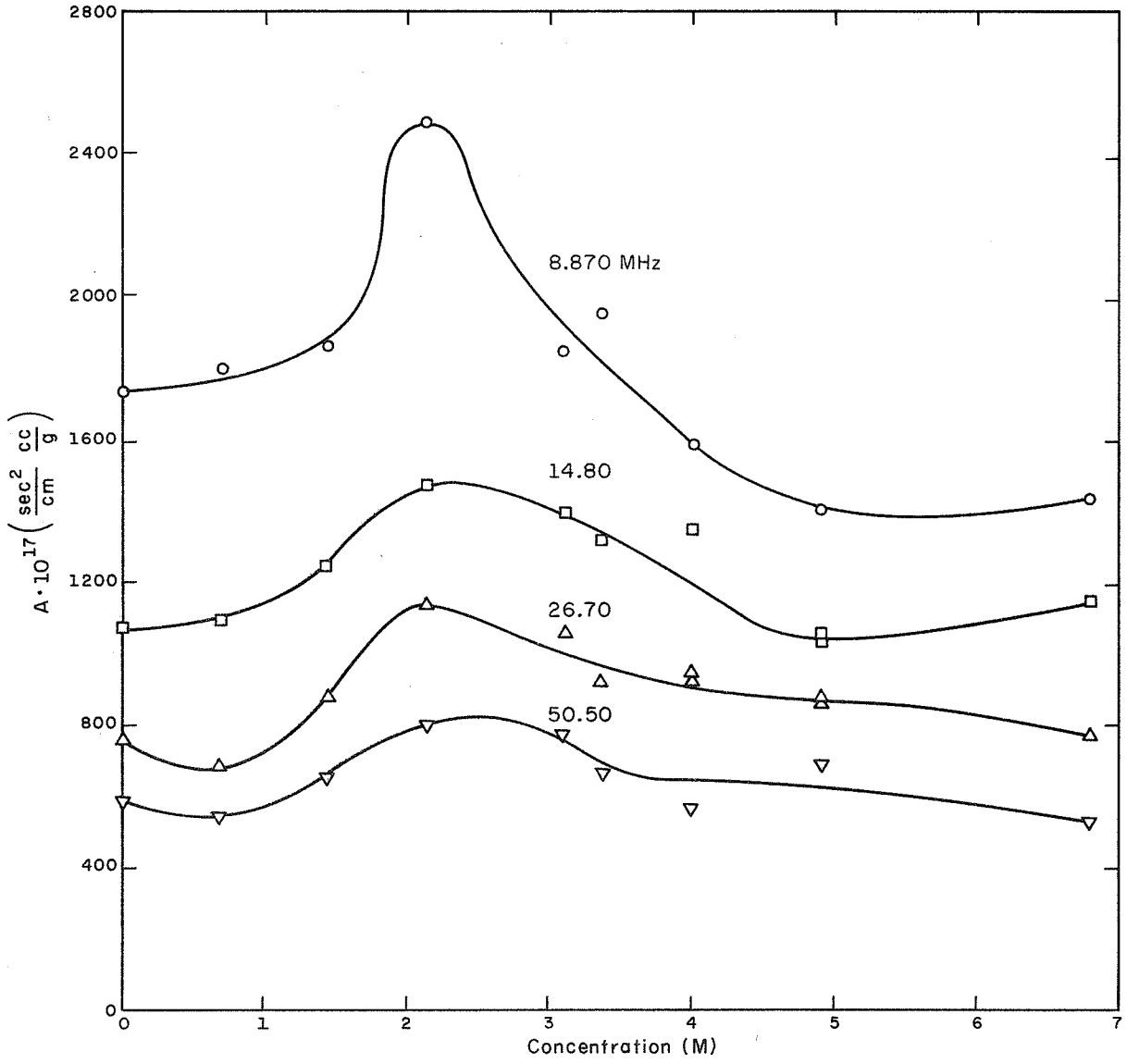

FIGURE 4-37

GuHCl CONCENTRATION TITRATION
BOVINE HEMOGLOBIN-2X (T = 10.0°C)

$$\alpha/f^2 = \frac{2\pi^2}{\rho_o c_o^3}\left(\eta_v + \frac{4}{3}\eta_s\right) \tag{4-14}$$

yields

$$\alpha/f^2 = \frac{2\pi^2}{\rho_o c_o^3}\left(\eta_{ov} + \frac{4}{3}\eta_{os}\right)e^{\Delta F/RT} \tag{4-15}$$

where $\Delta F = \Delta F'_v + \Delta F'_s$. Rearranging (4-15) so that all temperature dependent parameters are on the left hand side gives

$$\frac{\alpha}{f^2} c_o^3 = \frac{2\pi^2}{\rho_o}\left(\eta_{ov} + \frac{4}{3}\eta_{os}\right)e^{\Delta F/RT}. \tag{4-16}$$

The temperature dependence of ρ_o, the solvent density, is ignored as it is shown in Table 4-5, to be relatively insignificant, and thus the exponential coefficient is then considered a constant. To determine ΔF, an Arrhenius plot is drawn, that is, $\log_{10} \alpha c_o^3/f^2$ versus $1/T$ is plotted, the slope being proportional to the activation energy.

Data for α/f^2, here being the total absorption, and velocity, c_o, were obtained over the temperature range 10-37°C at four frequencies in an aqueous solution of twice crystallized hemoglobin at a concentration 0.0349 gm/cc. Velocity was measured only at 8.870 MHz since dispersion is negligible at this concentration (Carstensen and Schwan, 1959b). These data are plotted in Fig. 4-38, along with that of water, the latter being calculated from Pinkerton's (1949a) values of α/f^2, see Fig. 4-1, and Greenspan and Tschiegg's (1959) values of velocity. Table 4-6 lists the activation energies calculated from the slope of the Arrhenius plot. In all cases ΔF is less than that of water but with a definite frequency

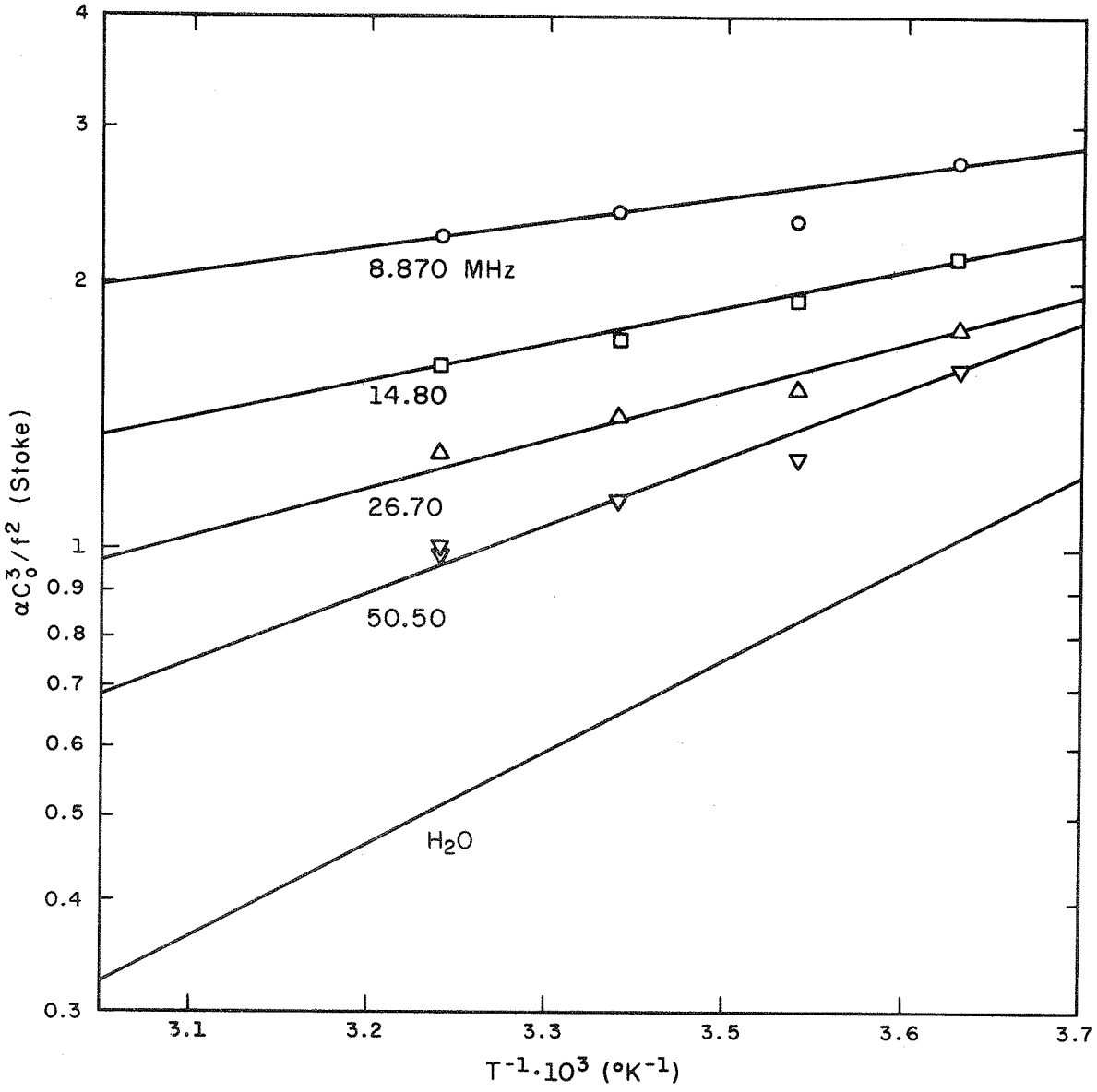

FIGURE 4-38

ARRHENIUS PLOT OF AN AQUEOUS SOLUTION OF
BOVINE HEMOGLOBIN-2X (0.0349 gm/cc)

dependence of increasing energy with increasing frequency. Similar activation energy calculations for BSA (Kessler, 1968a; Kessler and Dunn, 1969) in neutral aqueous solutions at a concentration of 0.05 gm/cc revealed no frequency dependence between 8.87-26.66 MHz, within their experimental error.

Table 4-6
Activation Energies
Aqueous Hb-2X - Conc = 0.0349 gm/cc

pH	f (MHz)	F (kcal/mole)
6.9	8.870	1.18
6.9	14.80	1.95
6.9	26.70	2.63
6.9	50.50	3.44
Water	All	4.48

An Arrhenius plot is shown in Fig. 4-39 for varying concentrations of GuHCl and the values obtained for ΔF are tabulated in Table 4-7. Fig. 4-40 is a plot of the calculated ΔF as a function of GuHCl concentration. Interestingly, ΔF peaks around 2.0 M concentration, similar to the maxima of Figs. 4-36 and 4-37, and appears to level off as concentration is increased.

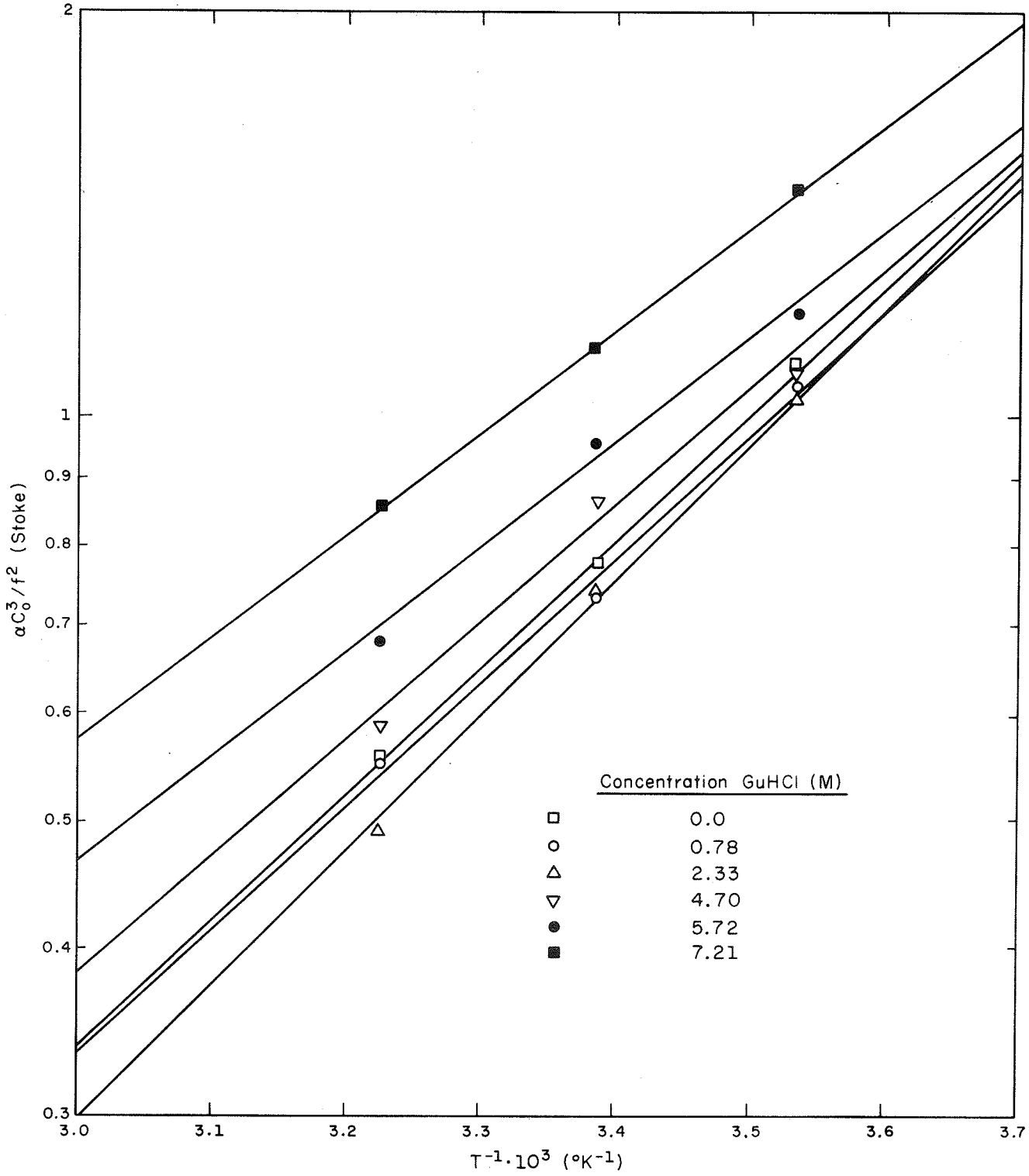

FIGURE 4-39

ARRHENIUS PLOT OF AQUEOUS SOLUTIONS OF
GUANIDINE HYDROCHLORIDE

Table 4-7

Activation Energies

Aqueous GuHCl

Conc	(kcal/mole)
0	4.48
0.50*	4.16
0.78	4.10
1.00*	4.09
1.50*	4.62
2.00*	4.60
2.33	4.86
3.00*	4.27
4.70	3.89
5.72	3.63
7.21	3.52

*Extrapolated values

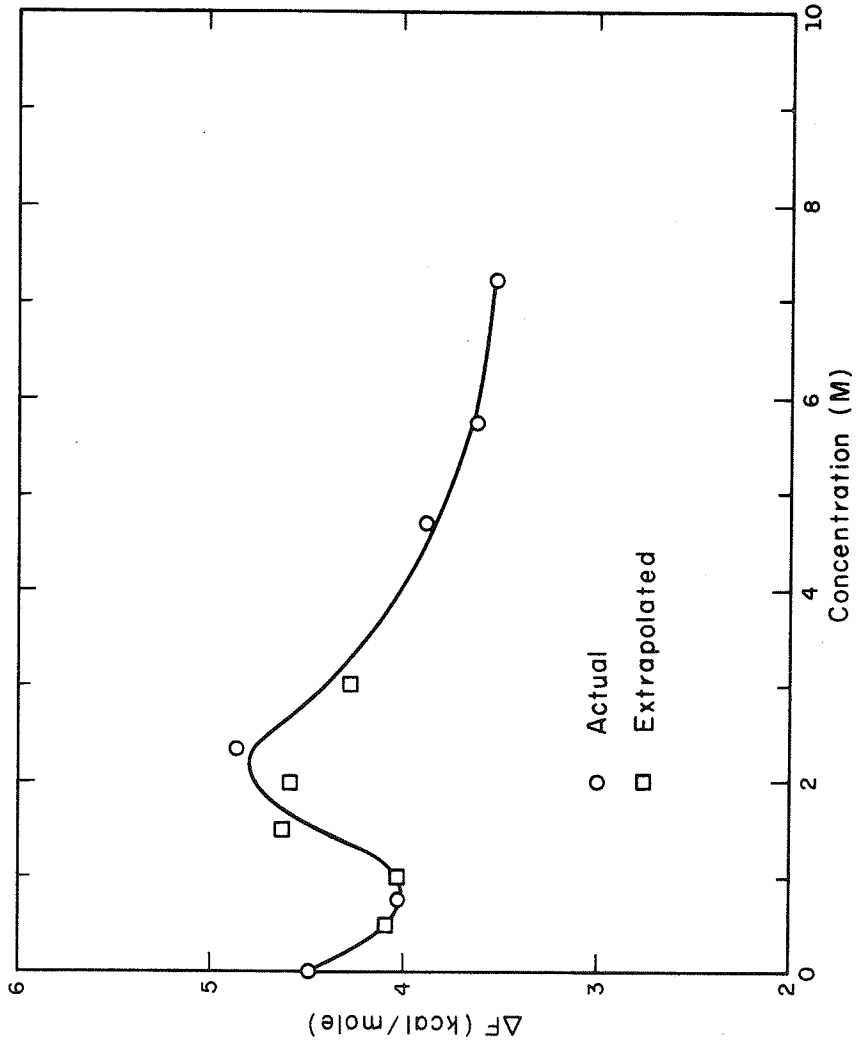

FIGURE 4-40
ACTIVATION ENERGY VS GuHCl CONCENTRATION

CHAPTER 5 DISCUSSION

In order to correlate the ultrasonic data presented in the previous chapter with absorption mechanism, it is necessary to have available details of the structure and function of the biological macromolecules in aqueous solution. The manner in which the structure of water is modified within the immediate vicinity of these molecules is essential to the understanding of the thermodynamic properties of their stability (Lumry and Biltonen, 1969). Two basic types of biopolymers have been considered in this study, viz., globular proteins and nucleic acids. The former consist of one or more polypeptide chains, each made up of from the twenty more common amino acids (including imino acids). These monomeric units are connected through the formation of secondary amide linkages between the α-carboxyl and α-amino groups of adjacent amino acids, such connections being termed peptide bonds. The order in which the amino acids are connected by peptide bonds in the chain is called the primary structure of the protein. The secondary structure of the protein results from hydrogen bond formation between polypeptide components, and these bonds produce the helical and sheet structure of the chain. The twisting of the polypeptide chain into layers, crystals or fibers is attributed mainly to non-covalent bonds which include interpeptide and side-chain hydrogen bonds, ionic bonds and apolar (hydrophobic) bonds (Schachman, 1963). Of these, the hydrophobic bonds are probably most important in determining the folded, tertiary structure in addition to the secondary protein structure (Kauzmann, 1959; Klotz, 1960; Tanford, 1962; Nemethy and Scheraga, 1962c; Richards, 1963; Schachman, 1963; Brandts, 1969). Finally the quaternary structure is determined by the intermolecular interaction among the independent polypeptide chains,

independent in the sense that the chains are not covalently linked to one another (save for disulfide links) (Mahler and Cordes, 1966).

Nucleic acids are among the largest macromolecules known, some ranging in molecular weight up to 10^9 or more (Mahler and Cordes, 1966). The primary structure of nucleic acids is a polyester chain (called a polynucleotide chain) consisting of alternating phosphoric acid and pentose sugar with a base connected to the sugar. The nucleotide monomer consists of a phosphoric acid, sugar and base. The bases found in nucleic acids are either pyrimidines or purines. In deoxyribose nucleic acid (the sugar is D-2-deoxyribose) the common bases are the pyrimidines thymine (T) and cytosine (C) and the purines adenine (A) and guanine (G).

The secondary structure of DNA consists of two righthanded helical polynucleotide chains of opposite polarity (the internucleotide linkages of one chain is opposite that of the other chain) and coiled around the same axis to form a double helix. In addition, the bases are on the inside of the helix in pairs arranged in such a fashion that a pyrimidine (T or C) of one chain always pairs (through hydrogen bonding) with a purine (A or G) of the opposite chain (Watson and Crick, 1953). As a result of spacial requirements A pairs only with T and G only with C. Even though hydrogen bonds are important in controlling the form and specificity of the helix, they do not appear to be particularly important in maintaining the stability of the helix, i.e., the holding together the strands of the DNA double helix. The main contributions to the helix stability are attributed to the stacking forces which are the electrostatic and hydrophobic interactions between the parallel stacked bases (Mahler and Corder, 1966; Bloomfield, 1968).

The excess ultrasonic absorption in aqueous solutions of biological

molecules has been attributed to the solvent structure around the macromolecules (Kessler, 1968a; Kessler and Dunn, 1969; Lewis, 1965). Thus it appears profitable to consider the interaction between solvent (water) and solute, however, first much smaller molecules will be dealt with. Frank and Evans (1945) postulate that an apolar molecule in water modifies the water structure, in its immediate vicinity, to that of greater structuring, i.e., increasing the hydrogen bonding among water molecules. These regions of greater structure, due to the apolar molecules have been termed "icebergs" which may represent several different structures, none of which are necessarily the same as ordinary ice. Némethy and Scheraga (1962b, c) have treated the iceberg formations around apolar molecules statistically, based upon the "flickering cluster" theory of water (Némethy and Scheraga, 1962a; Frank and Wen, 1957; Frank, 1958). Their basic assumption is the "somewhat greater" probability of finding a cluster around an apolar molecule than in pure water. Némethy and Scheraga (1962c), initially agreeing with Kauzmann's (1959) proposal that association of apolar side chains would occur within the interior of the protein, verified theoretically that extended regions of ice-like water on the protein surface are thermodynamically unfavorable. However, this does not preclude short ordered ice-like structures occurring around exposed apolar sections of the protein.

Bloomfield (1968) reports that two types of hydration occur with DNA molecules in aqueous solutions, short-range "thermodynamic" hydration and long-range hydrodynamic hydration. Hearst and Vinogard (1961) and Hearst (1965) found that there is a dependence upon the thickness of the water hydration shell as a result of differing water activities. The activity of species i, a_i, is equal to an activity coefficient, y_i, times the concentration of species i, c_i, viz., $a_i = y_i c_i$. For an ideal solution